

Rochester Institute of Technology

RIT Digital Institutional Repository

Theses

2004

Development of a human visual system with the ability to detect inconsistent events

Jeremiah D. Brazeau

Follow this and additional works at: <https://repository.rit.edu/theses>

Recommended Citation

Brazeau, Jeremiah D., "Development of a human visual system with the ability to detect inconsistent events" (2004). Thesis. Rochester Institute of Technology. Accessed from

This Thesis is brought to you for free and open access by the RIT Libraries. For more information, please contact repository@rit.edu.

Development of a Human Visual System with the Ability to Detect Inconsistent Events

Jeremiah D. Brazeau

Department of Computer Science
Rochester Institute of Technology

A thesis, submitted to the Faculty of the Golisano College of Computing
and Information Sciences in partial fulfillment of the requirement for the
degree of Master of Science in Computer Science.

Approved by:

Advisor: Dr. Roger Gaborski

Roger Gaborski 4/19/2004

Reader: Dr. Michael Van Wie

Michael Van Wie 4/19/04

Observer: Dr. Edith Hemaspaandra

Edith Hemaspaandra 4/19/04

April 2004

Thesis/Dissertation Author Permission Statement

Title of thesis or dissertation: Development of a Human Visual System
with the Ability to Detect Inconsistent Events

Name of author: Jeremiah D. Brazeau
Degree: Master of Science
Program: Computer Science
College: Golisano College of Computing and Information Sciences

I understand that I must submit a print copy of my thesis or dissertation to the RIT Archives, per current RIT guidelines for the completion of my degree. I hereby grant to the Rochester Institute of Technology and its agents the non-exclusive license to archive and make accessible my thesis or dissertation in whole or in part in all forms of media in perpetuity. I retain all other ownership rights to the copyright of the thesis or dissertation. I also retain the right to use in future works (such as articles or books) all or part of this thesis or dissertation.

Print Reproduction Permission Granted:

I, Jeremiah D. Brazeau, hereby **grant permission** to the Rochester Institute of Technology to reproduce my print thesis or dissertation in whole or in part. Any reproduction will not be for commercial use or profit.

Signature of Author: Jeremiah D. Brazeau Date: 4/19/04

Print Reproduction Permission Denied:

I, _____, hereby **deny permission** to the RIT Library of the Rochester Institute of Technology to reproduce my print thesis or dissertation in whole or in part.

Signature of Author: _____ Date: _____

Abstract

Current research has shown that it is possible to create a general purpose learning system that models the first few layers of the human visual system. The goal of this thesis is to build upon that idea and produce a computational model capable of learning different aspects of visual information. Simulations show that the system is capable of learning and distinguishing different types of motion. Results also give one explanation, consistent with current experiments, explaining how the human visual system learns information and as such may produce the capability to predict behavior in future experiments.

Acknowledgements

I would like to take the opportunity to thank the people who have supported me through my Masters experience.

Contents

Abstract	i
Acknowledgements	ii
Contents	iii
List of Figures	vii
List of Tables	xiv
1 Introduction	1
1.1 Approach	3
2 Background	5
2.1 Processing Visual Information	5
2.1.1 The Layout of the Human Visual System	6
2.1.2 Motion Processing	11
2.2 Models of Self Learning	12
2.2.1 Self Organizing Maps	13
2.2.2 Hebbian Learning	15
2.3 Early Development of the Visual System	16

2.3.1	Genetic Influences	16
2.3.2	Environmental Influences	17
2.3.3	Activity Before Sight	19
2.4	Conclusion	20
3	Discussion of Related Work	21
3.1	Computation Models for Learning Orientation	21
3.1.1	von Malsburg's Method: Hebbian Learning	22
3.1.2	Linsker's Method: Information Maximization	22
3.1.3	SOM Models	24
3.1.4	Correlation-based learning models	25
3.1.5	RF-LISSOM	25
3.1.6	HLISSOM	26
3.1.7	Conclusion	26
3.2	Computation Models for Learning Motion	27
3.2.1	Complete Motion Processing Models	27
3.2.2	One Extention of HLISSOM	28
3.2.3	Layer Specific Models	28
3.3	Conclusion	29
4	A Model of Motion Processing: DS-LISSOM	30
4.1	Overview	31
4.2	Modeling Retinal Activations	34
4.3	Processing from the Retina to LGN	36
4.4	Modeling V1	39
4.5	Modeling MT	40

4.6	Training the System	43
4.7	Inconsistency Detection	44
4.8	Conclusion	46
5	Development of Visual Preferences	47
5.1	Formation of Selective Neurons	47
5.1.1	Orientation Selectivity	49
5.1.2	Motion Selectivity	49
5.2	Finding Inconsistencies	51
5.2.1	Finding Changes in Orientation	54
5.2.2	Finding Changes in Motion	56
5.2.3	Long Term Memory	56
5.2.4	Working with Natural Images	64
5.3	Conclusion	66
6	DS-LISSOM: A Users Guide	67
6.1	Explanation of the GUI	67
6.2	A simple example	69
6.3	Using Different Data	70
7	Conclusion and Future Work	72
7.1	Modeling More of the Visual System	72
7.1.1	More about V1	73
7.1.2	Modeling MT	73
7.1.3	Modeling MST	73
7.2	Finding Inconsistent Events	74

A Source Code	75
A.1 Vision System	75
A.2 GUI Creation	75
A.3 DS-LISSOM	81
A.4 Helper Functions	117
A.5 Rainbow Colormaps	119
 List of Abbreviations	 123
 Bibliography	 124

List of Figures

2.1	The above images are examples of ON-center and OFF-center cells which are types of retinal ganglion cells. These cells exist between the back of the retina and the lateral geniculate nucleus (LGN).	6
2.2	(a) and (b) are examples of neurons in V1 that act as edge detectors. (c) and (d) are examples of neurons in V1 what will respond most strongly to vertical dark and light bars. The pictures above describe the receptive fields of these neurons. In other words a neuron in V1 will respond when the particular pattern exists within its receptive field in the previous layer (in this case the LGN).	9

- 2.3 This figure represents the layout as discussed so far. Information travels in through the eye to the retina. From there information moves down the retinal ganglion cells and onto the LGN. From the LGN information continues on to V1. V1 is the first area to show orientation selectivity which is possible because of the structure of its receptive fields. There is also evidence that V1 is directionally selective in humans, as it is in other species. From V1 information moves to the MT region where motion processing is started. From here information travels to a number of regions including the MST, FSA and MT+ subregions. 10
- 3.1 Linsker organized his system as a number of layers. The connections between layers are linear so it would be possible to perform all steps at once. Only 4 layers are shown here but more are possible. By the sixth layer the responses resemble those found in V1's simple cells although neighbors do not show similar orientation preferences. 24
- 4.1 Each of the major areas of DS-LISSOM are labeled. This is a pictorial view of DS-LISSOM. 32
- 4.2 These images are examples of the oriented Gaussians which are used as the afferent weights from the input image to the LGN. These act as simple edge detectors as it is thought the Retinal Ganglion cells do. 35

- 4.3 The circle represents the receptive field of a cell - for example a cell in MT. This represents the fact that the preceeding layer, in this example V1, must be both longer and wider. 36
- 4.4 Each of the top images represent a receptive field of a single cell in MT. An MT's receptive field will draw data from multiple points in time. In the above example, an MT is looking at 5 different points in time. As an object moves the developing MT cell will adjust its weights such that it will respond most strongly when, in this example, a bright object moves to the right through its receptive field. 42
- 5.1 These are two examples of cells that are formed when a strong edge and bar are present in an image. The result is the formation of edge and bar detectors that activate most strongly when an edge or bar is present in the appropriate part of its receptive field. 48
- 5.2 The first row shows the input image, the response in V1 after only a 10 iterations, the response after 10,000 iterations. The second row shows a number of cells after 10 iterations and after 10,000 iterations. 50

- 5.3 The lines represent connections between a cell in V1 and cells in the LGN that are within its receptive field. The lighter lines represent connections with strong weights while darker lines represent connections with weak weights. This particular cell will initially become active if there are a large number of bright cells on its left side and little activity on its right side (indicating the presence of an edge). 51
- 5.4 The first row gives an example of a simple edge cell formed by DS-LISSOM when trained on 10,000 random ellipsoids. The second row gives an example of a simple bar cell, again formed by training the system on random ellipsoids. The first two columns give different views of a cell's afferent weights, which are used to describe its receptive field and when it will become active. The third column shows the equivalent simple cell as it was described in previous chapters. This example helps to show that DS-LISSOM is in fact capable of learning and forming cells that are sensitive to orientation, as are those observed in biological experiments. 52
- 5.5 This orientation map was formed after training the system for 10,000 iterations on random ellipsoid patterns. The darker colors are preferences for horizontal orientations while light colors are more selective of vertical orientations. The result is a map that shows that system has a wide variety of orientation preferences. Similar maps can be formed to show the directional preferences of MT. 53

- 5.6 Each of the above images represent one period in time and the weights between cells in a particular time period in a cells receptive field to a cell in MT. An MT's receptive field, in other words, not only contains an area at the current time step, but that same area in previous time steps. As shown by the images this allows an MT cell to be most active when and an object appears in the appropriate regions of its receptive field in each time period. The above sequence shows a preference for movement in the rightward direction. 54
- 5.7 This figure demonstrates the weight changes that occur when the input to the system changes. The first large spike in the plot occurs when DS-LISSOM first sees the horizontal lines. Since at this moment the map is completely random, there are large changes in weight. The second large spike occurs when vertical lines are introduced for the first time to the system. The top two figures show examples of the vertical and horizontal lines that are sent to the system. 55
- 5.8 Unlike 5.7 this experiment was performed on DS-LISSOM after it had been prenatally trained on random ellipsoids. Although learning again occurs, it is important to realize that the relative amount of change in the maps is significantly reduced. Learning still must occur since the system has never seen horizontal and vertical lines presented in this way. 57

- 5.9 In this example, no pretraining occurred. In this way, the system became oriented to seeing only a few specific orientations. The top row shows the type of input images that were sent to the system. The first 900 iterations were input of a circle moving from the left to the right. After that the circle changed direction, moving from the right to the left. With this change in direction came a change in the amount the inhibitory weights were being adjusted. 58
- 5.10 Like 5.9, this example was performed on DS-LISSOM with no pretraining. The top row shows the types of input images that were sent to the system. Images of a circle moving from the left to the right were displayed for the first 900 iterations. Next, images of a circle moving up and to the right were shown. The increase in weight change coincides with the change in direction. 59
- 5.11 The detection of movement occurs not only with circles, but in the plot, with boxes as well. 60
- 5.12 DS-LISSOM is also able to distinguish complex backgrounds from the moving objects. The above plot shows the detection of an ellipse's change of direction, even when a complex background exists. 61
- 5.13 Once DS-LISSOM has seen an image, it is capable of retaining that knowledge. In the above sequence DS-LISSOM was shown horizontal lines 20 times in a row, followed by vertical and horizontal lines being displayed one after the other. As the plot shows DS-LISSOM reacts less strongly. 62

- 5.14 The above plot shows that once DS-LISSOM is trained it is already capable of perceiving a number of different directional motions. The amount of weight change is minimal, since many parts of the map are already tuned to this directional motion. 63
- 5.15 The input image is of two roads. The top road is the only one where motion from cars occurs. At first, cars will only pass from the right to the left. After some time a bus moves from the left to the right. The plot shows the change in learning that occurs when the bus enters. Because the system was first trained on random ellipsoids, much of the other movement, such as the movement in the trees, does not effect the results. 65
- 6.1 A screenshot of DS-LISSOM's graphical user interface 71

List of Tables

Missing Page

Chapter 1

Introduction

Although much is known about the human visual system, few models have been produced that are capable of processing information under circumstances as diverse as those encountered by the human eye. One problem that computers face is that they simply are not yet capable of processing so much information so quickly, perhaps because the human brain is more complex, having an estimated 10^{15} synapses compared to the Pentium 4's 42 million transistors (Kandel *et al.*, 1991; Bednar, 2002).

Although computers are not as complex, many models have been proposed that are capable of learning different aspects of the human visual system. Some of these models look for predefined patterns that occur within images (for example, edges are often found using a difference of gaussians approach). Although these approaches are good at finding specific patterns within images, they are unable to adapt to or to find novel patterns. Other models try to make use of neural networks to look for more general patterns within image data. These approaches generally have a better chance of finding patterns that were not predetermined; however, they may require training before they

begin to give meaningful results.

From a biological point of view, the approach of neural networks allows for the ability to adapt to different environments. One question still remains: how is the human visual system able to learn so quickly, given that it has never been presented any visual stimulus? Recent experiments show that the visual sensory system in mammals has gotten around this problem by specifying, in the genome, a method of training (Bednar, 2002). The advantage of specifying a form of training instead of actual capabilities seems to be that it allows for the system to see many features early on while also allowing for a system that is able to adapt to a number of different environments. Such training occurs before birth and can prepare the visual system for what it will encounter later in life. Given that training occurs within the visual system before it is introduced to an open environment, some level of proficiency in sight can be gained before birth. Research also suggests that in many mammals a special directionally selective set of cells exist. These cells, combined with learning that occurs prenatally, could lay the foundation for all that humans see in terms of motion.

Experiments have shown that when information into the visual system is disrupted, the resulting system is not capable of perceiving all forms of visual stimulus. Of particular interest is the ability to use this fact to detect novel events that occur within a series of images. As simulations will show, it is possible to train a system in one environment with the intention of later placing the system in a similar environment, such that the amount of activity that occurs within different parts of the simulated visual system can be used to determine the novelty of the new environment.

This thesis looks at one model of the visual system, which accounts for

such prenatal activity, and furthermore is capable of becoming orientation selective. An attempt is made to expand that model, proposing a system that is capable of distinguishing different types of directional motion. Finally, the amount of activity in the system is investigated to see whether or not it is possible to determine the occurrence of novelty within images.

1.1 Approach

A system that models the different areas of the human visual system including the retina, LGN, V1 and MT areas is constructed and compared to what is already known about the human visual system, with a hope that such a system will be able to make predictions about the outcomes of future experiments. The visual system was chosen because it is a well studied sensory system, and because many models of visual detection currently exist.

The system will be based on work published by James Bednar, which describes a system named HLISSOM (Bednar, 2002). This system was created to study the pattern generation hypothesis, which states that learning occurs prenatally in such a way that the visual system comes prewired, and yet contains the ability to adapt to the environment in which it is later placed. HLISSOM models only parts of the retina, LGN and V1 layers of the visual system, and only looks at orientation processing (Bednar, 2002). The system created for this thesis expands upon this model in order to process motion. In particular, this thesis looks at directional processing since it is well studied in a number of different species.

The simulations focus on the ability of the system to learn different aspects of its environment and use that knowledge to guide future decisions. Of

particular interest is the system's ability to distinguish between what it has seen in the past and what it has not yet seen. This will be the main method of testing the systems success and/or failure. Further comparisons will be made to visual detection systems that do not rely on learning.

Chapter 2

Background

Two topics are most relevant to this work. The first is a strong understanding of the human visual system. This includes understanding the different areas of the human visual system, how they are connected and what each of the areas function is (Blake *et al.*, 2003; Kandel *et al.*, 1991; Rosenzweig *et al.*, 1999). The second is Self Organization. Self Organization is a machine learning technique that requires no user input in order for the system to learn useful information. The main form of self organization that will be used in this system is modified Kahonen Maps and Hebbian Learning (Kohonen, 1997; Hebb, 1949).

2.1 Processing Visual Information

The human visual system consists of a number of independent layers that communicate with one another. Each of these layers is thought to be made up of cells specific to the functioning of that layer. Each layer is also connected to a number of other layers providing for information to be combined and allowing for a system of feedback.

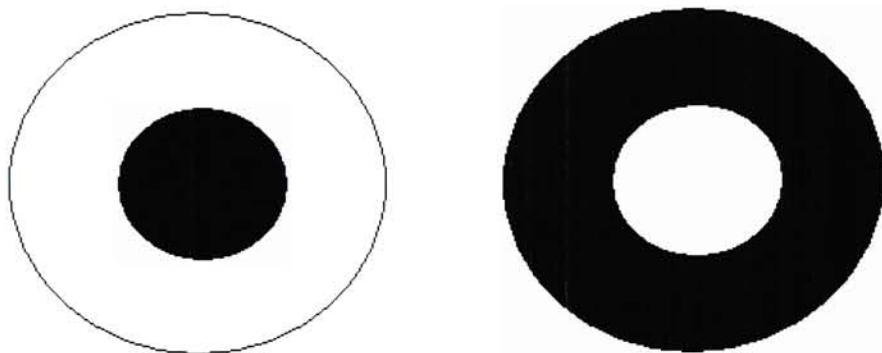


Figure 2.1: The above images are examples of ON-center and OFF-center cells which are types of retinal ganglion cells. These cells exist between the back of the retina and the lateral geniculate nucleus (LGN).

In order to simplify the model, only monochrome information is kept. As such, this section focuses on parts of the visual system that make use of monochrome information and ignore the parts of the visual system required for color processing.

2.1.1 The Layout of the Human Visual System

The first layer in the visual system is the retina. The retina is responsible for taking light, varying by wavelength and intensity, and producing an internal response. The retina is composed of 2 different types of cells that respond to different light information: the rods and the cones. The rods are responsible for seeing light whose wavelength is around 500nm. The rods are much more sensitive to intensity and as such allow us to see even when little light is available. The cones come in three types: those that peak around 445 (blue),

those that peak around 540 (green) and those that peak around 570 (red). Activity that these cells detect is encoded, and patterns of electrical activity are generated in neurons called the retinal ganglion cells (Rosenzweig *et al.*, 1999).

Retinal ganglion cells respond most strongly to edges between light and dark areas and as such perform a type of edge detection. Two specific retinal ganglion cells that are known to exist are ON-center and OFF-center cells shown in Figure 2.1. ON-center retinal ganglion cells respond most strongly when there is a light area surrounded by a darker region. This entire region is known as the retinal ganglion cell's receptive field (RF). The OFF-center retinal ganglion cells by contrast have the strongest response when there is a dark spot that is surrounded by a light region.

As information passes through the retina it then moves up the optic nerve to the lateral geniculate nucleus (LGN), located in the thalamus. As with the retinal ganglion cells of the retina, there are two specific types of response cells in the LGN (ON and OFF). The ON-center retinal ganglion cells connect to the ON cells of the LGN and OFF-center retinal ganglion cells connect with the OFF cells of the LGN. Each of the cells in the LGN is connected to a region of cells, its receptive field, such that when a response is generated in that region, the specific LGN cell will also respond.

From the LGN, information travels to the primary visual cortex (V1). The V1 layer is the first layer that is orientation selective. Just as the LGN layer is connected to the retina, the V1 layer is connected to the LGN layer such that each cell of the V1 layer is connected to a region within the LGN. The types of cells in V1 differ from those found in previous layers. There are two types of cells commonly found in V1: simple and complex. Simple cells can

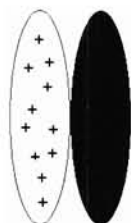
be thought of as edge and bar detectors. Figure 2.2 shows 4 different simple cells. The first two are selective of edges while the second two are selective of bars, or lines, that run through their receptive field. Complex cells still respond to orientations; however, these cells may only respond when an edge exists moving in a particular direction. This said, V1 is also one of the layers in the human visual system that is sensitive to direction. Cells, such as some complex cells, that are selective of direction are generally termed DS cells (Directionally Selective) (Blake *et al.*, 2003).

From the primary visual cortex, information branches to a number of other areas along two main pathways. This first pathway leads to the temporal cortex. The temporal cortex is responsible for our understanding and recognition of objects. The second pathway leads to the parietal cortex. The parietal cortex is responsible for processing and understanding motion.

The first stop in the parietal cortex is MT (Rosenzweig *et al.*, 1999). MT is most responsive to edges that move in a specific direction. The receptive fields in MT tend to be much larger than those in V1 (in fact they can be up to 10 times as large). In order to account for such selectivity, MT must be given information from more than one time period. Such information is provided through feedback loops and delayed responses.

Once through MT, information moves to a number of other regions. At each step the information is reprocessed in a more refined manner than in the area that proceeds it. In this way, more complex patterns of motion can be observed as one proceeds farther along the motion pathway (Grzywacz & Merwine, 2002).

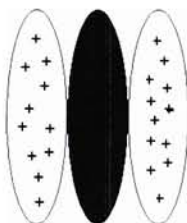
At this point the visual system can be laid out as shown in 6.2.



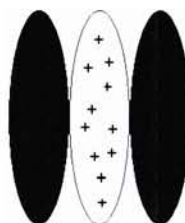
(a) Vertical Edge Detector



(b) Horizontal Edge Detector



(c) Dark Bar Detector



(d) Light Bar Detector

Figure 2.2: (a) and (b) are examples of neurons in V1 that act as edge detectors. (c) and (d) are examples of neurons in V1 that will respond most strongly to vertical dark and light bars. The pictures above describe the receptive fields of these neurons. In other words a neuron in V1 will respond when the particular pattern exists within its receptive field in the previous layer (in this case the LGN).

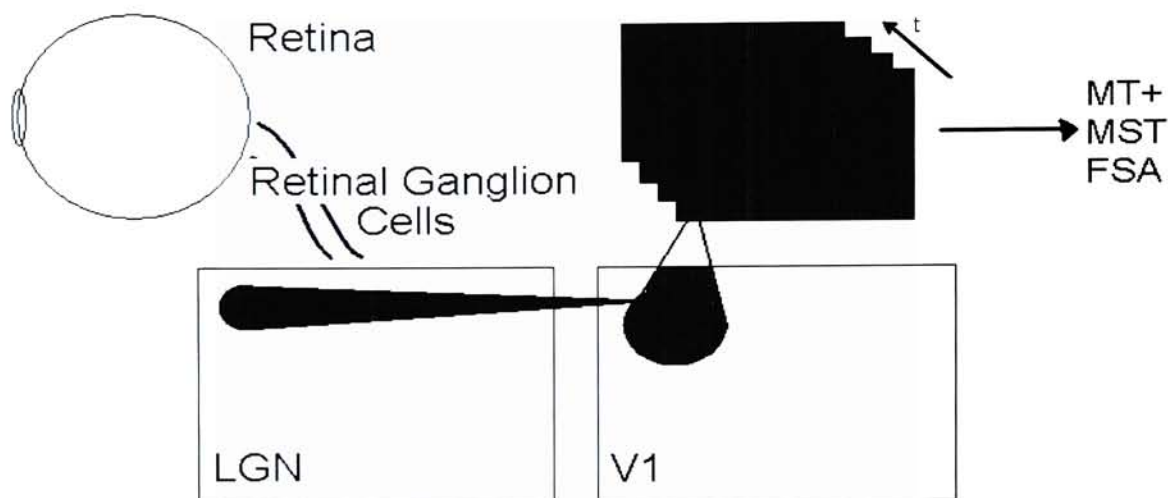


Figure 2.3: This figure represents the layout as discussed so far. Information travels in through the eye to the retina. From there information moves down the retinal ganglion cells and onto the LGN. From the LGN information continues on to V1. V1 is the first area to show orientation selectivity which is possible because of the structure of its receptive fields. There is also evidence that V1 is directionally selective in humans, as it is in other species. From V1 information moves to the MT region where motion processing is started. From here information travels to a number of regions including the MST, FSA and MT+ subregions.

2.1.2 Motion Processing

Newton once said that in order to understand motion one needs to know direction, speed and acceleration. As humans we are able to distinguish motion. We are also capable of differentiating speeds of objects. When it comes to acceleration however, we are not as capable.

Newton was describing motion in a scientific sense; however, his ideas also relate to a human's perception of motion. A number of different things need to happen in order for the brain to get a picture of motion. Seeing motion is not as simple as noticing an object move across a screen. For example, consider what happens if you watch a car driving down the street as you move your head. You have a sense that the car is still moving, even if it remains within your sight. Another example would be if you were sitting in the car. Even if you pass someone who is standing, you are able to tell that they are not moving, even though they move across your visual field. In order to accomplish all of this a number of areas of the brain play a role. Two of the major players are the MT and MST areas.

William T. Newsome performed experiments on monkeys to help show the function of MT (Newsome & Pare, 1998). Prior to the experiment, monkeys were trained to report their perception of direction while watching dots move in specific directions. During the experiment the same patterns of dots moving were shown to the monkeys and brain activity was recorded. The results showed a direct correlation with the activity with the cells in MT. Further experiments showed that a monkey's responses could be altered by injecting MT cells with low levels of current (Grzywacz & Merwine, 2002).

The MT area is one of the first areas that shows preference for motion in

one direction or another independent of the orientation of the object that is moving. Such a result may indicate that the MT uses information from the output of V1, and other areas, from different times. In this way it would be possible for the directionally selective cells in MT to become active when objects form the appropriate orientation through time.

The MST region of the brain is also very important in our understanding of motion. This area seems to be responsible for understanding motion by using information that is not visually available. It is this area that helps us to understand that when we turn our head everything in a room remains still even though it is crossing our visual field. In terms of understanding motion, this is vital.

2.2 Models of Self Learning

A number of different models have been produced for learning information about arbitrary systems. Many of these models require some form of interaction to take place. For the visual system this is not desirable since we as humans do not require any interaction with our environment to initially see. Nor do outside forces tell us whether or not what we are seeing is correct or incorrect. Therefore, these other forms of computer learning must be investigated. Two such systems are Self Organizing Maps and Hebbian Learning. Both are capable of recognizing patterns that exist when given input, and both attempt to form different categories based on these patterns, such that when new input is given to the system, it can be placed in the appropriate category.

2.2.1 Self Organizing Maps

The previous sections have briefly outlined the layout of different components of the human visual system. Each of these different areas plays an important role when looking at developing a model that is capable of processing visual information. What still needs to be explained is how all of these different areas will contribute to learning in a computer simulated model. It is clear that as humans we do not have to be told how to see; rather, over time we simply learn that ability on our own. In fact we are able to recognize some things when we are first born. In order to accomplish this within a computational environment, some form of self organization must be present.

Self Organizing Maps (SOM), also known as Kohonen maps, were first developed by Teuvo Kohonen around 1989. Kohonen maps are capable, without any previous knowledge, of associating concepts with categories. In particular, each concept becomes associated, over time, with a location on the map. Concepts that are similar are located near each other on the map, while dissimilar concepts are further apart on the map.

The obvious question that remains is how does the map update itself in such a way that no interaction is required? This has to do with the setup of the map. You can think of the map as a 2 dimensional matrix. In this matrix each cell has a vector of weights. There is one weight for each of the attributes associated with an input vector. The weights of each cell are initially random.

Like most neural networks, a Kohonen map learns over a series of rounds. During each round all input vectors are read in some arbitrary order. Once read, an input vector is processed by first selecting a winner from the Kohonen

map and then updating the surrounding cells of the winner. In order to pick the winner, the input vector is compared with all weight vectors in the map. The winner is that vector in the map which is most like the input. To determine how close two vectors are a distance measure is defined. Some well-known measures of distance are the Euclidean distance and Manhattan distance. During the update phase of this process, each of the vectors that surround the winner is updated to more closely resemble the winner. The size of this surrounding area, and the amount by which these surround vectors, are changed is slowly reduced during each round such that well-defined groups can be formed.

Self Organizing Maps can be described by the following algorithm:

1. Read an input vector.
2. Determine which of the cells in the Kohonen map is the winner.

$$\|input - node_{winner}\| = \min_i \|input - node_i\|$$

Here distance for a single node can be defined as:

$$d_{out} = \sum_{in} (input_{in} - node_{in})^2$$

3. Modify the weights w_i of the winning node and its neighbors so that they more closely resemble the input.

Input vector = p_i

$$h(r,t) = a(t)v(r)$$

$a(t)$ is the learning coefficient

$v(t)$ is the neighborhood function

$$w_i(t+1) = w(t) + h(r,t)(p_i - w_i(t)) \text{ if } i \in \text{neighborhood}$$

$$w_I(t + 1) = w(t) \text{ if } i \notin \text{neighborhood}$$

4. Decrease the size of the neighborhood of the winning nodes
5. Decrease the learning coefficient, $a(t)$, which controls the amount of change of each of the neighbors in the winning neighborhood.
6. Learning finishes when the learning coefficient is zero.

2.2.2 Hebbian Learning

Hebbian Learning is based on the principles of a work published by the Canadian neuropsychologist Donald O. Hebb. Hebb states:

When an axon of cell A is near enough to a cell B and repeatedly or persistently takes part in firing it, some growth process or metabolic change takes place in one or both cells such that A's efficiency, as one of the cells firing B, is increased (Hebb, 1949).

In other words, Hebb felt that if receptors are subject to repeated stimulation, they will learn to act together as a closed system, even after that stimulation is no longer present.

This idea of learning has carried over into computer science and is termed Hebbian Learning. Hebbian Learning is described as an unsupervised learning algorithm in which the weight between two neurons will increase if both the source and target neurons are active at the same time (Medler, 1998). A simple formula for this would be:

$$\Delta W_{ij}(t) = \gamma * x_i * x_j$$

where W_{ij} is the weight from neuron x_i to neuron x_j . A more general model might also take into consideration time and learning thresholds.

2.3 Early Development of the Visual System

Although the structure of the visual system is well studied, there is still much debate over how this structure is defined within the genome. There are two major encampments, those that feel that genetics act as a blueprint for the structure of the visual system and those that feel environmental influences are responsible for its structure. These two sides are found throughout psychology and has become known as the Nature vs. Nurture debate.

As most occurrences of this debate, there is no clear evidence for either side; rather, it is more likely that some of the human visual system follows a blueprint that is predefined in our genetic code while other parts of our visual system adapt and are formed based on environmental influences. The following sections describe how both genetics and the environment are able to work together to form a system capable of perceiving visual information.

2.3.1 Genetic Influences

In building a strong case for the role genetic influences play on the production of a visual system, it can be useful to acknowledge trends that occur within cultures or families. For example, if twins are separated at birth, what are the chances that both are near sighted, or both are color blind? These questions have long been studied by psychologists as a way to determine the significance of genetic factors in making us who we are. As a result there are a number of important experimental results that show the importance of genetic factors in defining the visual system. For example, studies have been able to show that myopia (near-sightedness), hyperopia (far-sightedness) and color blindness all are linked to genetic influences (Coon, 2000).

Physical structure is also clearly defined, and it is known that the visual system amongst different species is not the same. For example, turtles have far more directionally selective cells than humans. Such distinctions exist long before birth and thus before any visual environmental influences are present. There is very little difference in structure within a single species.

Receptivity to orientation and motion may also in part be defined genetically. For example, humans are not very good at learning to correctly perceive objects if there is a time delay. If you watch a poorly made movie you may notice that there is a delay between the sound you hear and the visual movement of the mouth. No matter how long you watch the show, you will never be able to correctly perceive the movie.

In terms of orientations, a few experiments have been able to show the role that genetics plays in the development of the visual system. Advances in medical imaging have allowed for full orientation preferences to be measured in animals. Such studies have been able to show that orientation preferences exist before there is any visual experience (and thus any environmental influences). Furthermore, these studies have shown that such orientation preferences closely mirror those found in adults (Crair & Stryker, 1998).

2.3.2 Environmental Influences

Chalupa and Rhoades found that visual deprivation significantly changed directional selectivity, speed preference, and receptor field organization. When they looked at hamsters raised in stroboscopic illumination there were signs of visual deprivation, showing that an environment can influence the visual system (Chalupa & Rhoades, 1988).

Perhaps more well known is the work of Nobel Prize winner Torsten Wiesel. In one of his lectures he describes experiments that he performed with David Hubel while investigating the response properties of cortical cells in cats during postnatal development. The experiments, performed on kittens, required that the eyelids of a subject be fused shut. He found that if only one eye was kept shut during the first three months after birth, and then allowed to open, the kitten was blind in the eye that was initially closed. If the same experiment was performed on an adult cat, blindness did not occur. Such work provides evidence that environmental influences are important for proper development of the visual system (Wiesel, 1982).

More recent experiments on kittens raised without sight in one eye have shown the development of non-specific lateral interactions for that eye. If, on the other hand, strabismus, more commonly known as crossed-eyes (a condition in which a both eyes can not be aligned simultaneously), was present in kittens, then the lateral connections were found to become patchier (Kasamatsu *et al.*, 1998; Gilbert *et al.*, 1990; Lowel & Singer, 1992).

Blakemore and Cooper were able to show that kittens raised in environments with only vertical stripes developed in such a way that they were good at seeing vertical stripes but bad at seeing horizontal stripes. In other words it is possible that edge detectors in V1 only developed for vertical lines (Blakemore & Cooper, 1970).

Finally, Stratton was able to show that the entire visual system can be affected by environmental influences. In his experiments, goggles were used to invert an incoming image. The question was whether or not an observer would be able to perceive visual information appropriately, and the answer is yes. After several days of wearing the goggles, a subject perceived his/her

environment in the same way he/she had before the goggles were introduced (Stratton, 1897).

2.3.3 Activity Before Sight

It is important to understand the connection that genetics plays in the development of visual perception both through genetically defined structures and genetically defined activity. Up to this point we have seen that the structure of the visual system can be defined by genetics, and that the environment can have long lasting effects on visual perception; still, newborn babies are capable of perceiving some objects as soon as they open their eyes. The question then is how perception is defined genetically before birth.

Experiments have shown that spontaneous neural activity occurs in many different cortical and subcortical areas. Recent experiments have shown that such activity, if disrupted, can have long lasting developmental effects.

One example of spontaneous neural activity is retinal waves. A number of experiments have been able to link retinal waves with the development of the visual system. One such experiment disrupted all retinal waves. As a result the LGN failed to develop as it should, and neurons in V1 were found to be less selective of orientation (Chapman, 2000; Chapman & Stryker, 1993). Other recent experiments have been able to show that retinal waves can also be instructive. For example, one experiment involved artificially activating a large number of axons in the optic nerve of ferrets, so that activity in these areas still existed although the activity was not the same as naturally occurring retinal waves. The result was that neurons in V1 were less selective of orientation, which shows that it is not only activity that is important, but

also the type of activity. (Katz & Shatz, 1996).

Another example of spontaneous neural activity is ponto-geniculo-occipital (PGO) waves that occur during rapid-eye-movement (REM) sleep. These waves travel from the brainstem to the LGN, visual cortex, and a number of subcortical areas. In human adults, these waves are strongly correlated with dreams and their associated imagery (Marks *et al.*, 1995). Experiments on kittens have shown that when visual stimulation is only allowed in one eye, by fusing the other eye shut, the LGN and V1 are affected (as described previously). When combined with the disruption of REM sleep the effects on the LGN and V1 areas have been found to be stronger indicating that PGO waves may help visual development even when visual impairments exist for a short while (Marks *et al.*, 1995).

Bednar has spent a great deal of time looking into the effects of spontaneous neural activity within the visual system. His work stems from research showing that such activity occurs within many developing cortical and subcortical areas, including the visual cortex and retina. His development of a computer simulated visual system has been able to further show that such stimulation, when it occurs prenatally, can ready a system for interacting with its environment (Bednar, 2002).

2.4 Conclusion

This chapter has looked at the layout of the visual system and at a number of computer algorithms that are useful in modeling such a system including Self Organizing Maps and Hebbian Learning. Finally, we discussed how the human visual system is thought to develop, including conflicting views

regarding the roles that genetics and the environment play.

Chapter 3

Discussion of Related Work

The focus of this thesis is the development of a computational model for the perception of orientation and motion. To date a large number of models have been produced, some more biologically oriented than others. Most of these systems store information in maps, which support the belief that many of the lower-level areas in the human visual system are organized retinotopically. That is, each of these areas is stored as a map which is capable of preserving the topography of the retina. In this section a number of the models that currently exist are presented. How well they model the different aspects of the human visual system, described in the previous chapter, is also discussed.

3.1 Computation Models for Learning Orientation

A large number of computational models of the human visual system exist, and as computers have been capable of performing calculations more quickly these models have evolved to take advantage of the increase in computational power. What follows is a discussion of these systems, their abilities in generating orientation maps, and how closely each system models a biological

representation of the human visual system.

3.1.1 von Malsburg's Method: Hebbian Learning

In 1973 von Malsburg was able to show that columns of orientation-selective neurons could develop, without supervision, from oriented binary bitmap patterns. Like most models that follow, von Malsburg's model was based on Hebbian Learning.

This model formed a strong basis for most of the following models and contained many of the characteristics found in later models, including the acknowledgement of lateral connections (in this case they are fixed strength), the treatment of the retina and cortical areas as two-dimensional arrays, and a method of assigning a value between connections which describes that connections strength (Bednar, 2002; von der Malsburg, 1973; Rochester *et al.*, 1956).

Like many of the models based on von Malsburg's, most of the problems stem from the fact that lateral connections are of fixed strength. On the other hand, this particular model is capable of creating a map whereby neighboring cells share orientation preference, and as described by Bednar has the capability to produce pinwheels within the orientation maps, which had not previously been accomplished (Bednar, 2002).

3.1.2 Linsker's Method: Information Maximization

Linsker created a model based on local Hebb-like synaptic modification rules. The modified rule used is

$$\delta w_j = k(yx_j + bx_j + cy + d)$$

where $y x_j$ is the Hebbian term and k is the learning rate. Each of the three remaining terms modify the network to follow some set of constraints where b , c and d are different constants (Linsker, 1986; Rolls & Deco, 2002).

The network is put together as a multi-layer system as shown in Figure 3.1. Each layer, except for the first, looks at an area of the previous layer forming Receptive Fields. The first layer acts as input similar to the cones and rods in the retina of the eye.

In order to train the network, random firing takes place. Over time each of the layers starts to form preferences. Rolls and Deco have observed that by the third layer, the formation of receptive fields that resemble center-surround cells could be found, and by the sixth layer, the receptive fields had become elongated and responded best to oriented edges or bars.

Although the system was capable of developing receptive fields that were orientation selective, the overall map was disorganized. This was due to the lack of lateral connections. As a result cells in the sixth layer did not share similar orientation preferences when neighboring each other. This leads to redundancy within each layer. Another problem also exists because of the way in which the system was randomly trained. When the system is first placed in a real environment there is no guarantee that it will be capable of perceiving anything in this new environment (Rolls & Deco, 2002).

A more fundamental problem with this system is that it does not address higher order features such as a correlation between multiple edges. As such, this system is only capable of learning simple orientations.

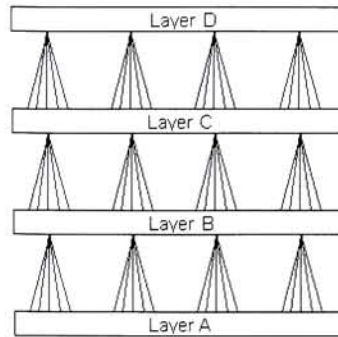


Figure 3.1: Linsker organized his system as a number of layers. The connections between layers are linear so it would be possible to perform all steps at once. Only 4 layers are shown here but more are possible. By the sixth layer the responses resemble those found in V1's simple cells although neighbors do not show similar orientation preferences.

3.1.3 SOM Models

Neither of the previous two models were capable of storing data retinotopically. This is in part because the two previous models generally modeled only a small number of neurons. Specifically, because of computational constraints, the von Malsburg model was only capable of expressing a few neurons, all with overlapping receptive fields. By the late 1980's and early 1990's, the amount of computational power available had grown immensely. As a result, new models were produced, and many of these made use of a more abstract network known as the Self Organizing Map (SOM) produced by Kohonen.

Work by Durbin and Mitchison (along with others) used SOM's and modified them to work within the orientation domain. The results were promising, capable of producing orientation maps that were comparable to those found in the visual system and included properties such as pinwheels, fractures and linear zones (Bednar, 2002).

3.1.4 Correlation-based learning models

Correlation-based learning stems from the observation that the visual system may be linear. If this observation were true, then a function could replace sequences of input patterns. Such a system would greatly improve the speed of calculations when compared to the two previous models, which involve incremental Hebbian learning. This approach was first suggested by Miller in 1994.

This model made a number of improvements in terms of what parts of the visual system were modeled. For one, on and off center cells in the LGN were modeled, and as a result multi-lobed receptive fields formed (no previous model accomplished this). Although a step in the right direction, the maps produced by this model were not as realistic. The receptive fields were close to binary whereas receptive fields observed in animals have smooth edge transitions. As a result the responses achieved by the more computationally intensive Hebbian learning method proved more realistic and biologically plausible (Bednar, 2002; Piepenbrock *et al.*, 1996).

3.1.5 RF-LISSOM

SOM models, although more computationally expensive, have produced more realistic results. One thing that these models have lacked in is an explanation of lateral connections. SOM models use a fixed neighborhood, but some suspect that lateral connections formed prenatally help form orientation maps (Bednar, 2002). As a result a new model is needed that accounts for the patchy lateral connections that are formed prenatally.

RF-LISSOM (the Receptive-Field Laterally Interconnected Synergetically

Self-Organizing Map) was the first model to accomplish this (Sirosh, 1995). This model was based on previous SOM models but no longer approximated lateral connections via a fixed neighborhood. Instead, incremental Hebbian learning was used to develop both lateral and afferent connections. As a result, redundancy within maps, produced by previous models, was reduced.

The major drawback to this system is that responses on real images are less realistic, since it does not account for both ON and OFF cell layers. Bednar has shown that this limitation must be overcome when working with natural images (Bednar, 2002). As a result the system has been modified and is discussed in the next section.

3.1.6 HLISSOM

HLISSOM was produced as an extension to the LISSOM model. It includes not only the ability to learn lateral connections, but also the ON and OFF center channels first introduced in the Correlation-based learning models. The resulting model has been shown to work with real images, an ability that previous models have lacked. It is also capable of sending information to higher cortical areas. In particular, it models face-selectivity (Bednar, 2002).

3.1.7 Conclusion

Although this and all previously discussed models are capable of modeling orientation selectivity, none of these models extend to the perception of motion. In particular, although orientation selectivity exists within V1, direction selectivity also exists and therefore should be accounted for in these models.

The next chapter is based on the HLISSOM model and looks at expanding that model to account for directional selectivity in the V1 and MT areas.

3.2 Computation Models for Learning Motion

A number of people have also investigated motion perception. Many of these models are based on simplifications of the human visual system and do not as closely follow a biological approach. Discussed below are a number of these systems.

3.2.1 Complete Motion Processing Models

A few models have been developed that encompass the entire motion processing pathway of the visual system. These models have shown to be capable of responding to motion in much the way we as humans respond to motion. Many of these systems directly specify the layout of the visual system. As a result, these systems do not internally learn responses, and are only an estimation of what occurs naturally.

Experiments on these systems have shown that it is possible to produce a system that can determine not only simple but complex motions such as rotations, contractions and expansions. These systems can also determine simple motion such as speed and direction (Pomplum *et al.*, 2002; Grossberg *et al.*, 2001). As a result these systems are useful in explaining human behavior in terms of motion as a whole, and some interesting results in terms of attention have been found (Pomplum *et al.*, 2002).

What these systems lack is the ability to learn motion. They are preprogrammed and therefore do not help to explain how motion perception is

learned. For example, if this system were only told about horizontal motion, it would never be capable of learning vertical motion.

3.2.2 One Extension of HLISSOM

Bednar has discussed a possible expansion to the HLISSOM model which would provide it with some sense of direction. The extension involves spatio-temporal effects at the LGN and V1 layers. As proposed, the model could be expanded to include 4 separate LGN layers each responding to a different point in time.

This model has shown the formation of long range lateral connections between neurons that share similar direction preference. Clearly this is a step in the right direction, but the model only goes as far as explaining interactions between neurons at the V1 layer. As such, more work is needed to expand this model to account for directional and speed selectivity at the MT layer.

It is not clear at this time whether or not this model is capable of working on real images, as no data has yet been published using real images as input (Bednar & Miikkulainen, 2003).

3.2.3 Layer Specific Models

Although looking at the entire visual system is ideal in understanding its overall function, some research has focused on just one layer of motion processing. These models are ideal when wanting to gain insight into the functioning of a specific layer. For example, researchers at Boston University have developed a model capable of describing optic flow selectivity in the MST layer of the

visual system. Their model uses a back-propagation network to investigate the different interactions that take place in MST, specifically looking at the interaction between locally complex motions with global motion. A major drawback is that the system requires supervised learning (Beardsley & Vaina, 1998). Similar models have also been produced for other specific areas of the visual system (Simoncelli & Heeger, 1998).

3.3 Conclusion

Previous models have shown the ability to model the beginning stages of the visual cortex in a generic way. Other models have shown that it is also possible to model higher cortical areas of the visual system using linear models. What these models have not yet shown is the ability to generalize past the V1 layer in order to process motion. Nor have they been used to aid in novelty detection within image sequences. The next chapter will discuss a model that will attempt to overcome these shortcomings and show that Hebbian learning can account for both orientation and direction selectivity within the visual system.

Chapter 4

A Model of Motion Processing: DS-LISSOM

This thesis presents a modified version of HLISSOM (Bednar, 2002). HLISSOM is a biologically inspired model of the human visual system focusing on the information pathway from the retina to V1. The new model presented here attempts to expand HLISSOM to model directional selectivity as it is found at the MT layer. The expanded model also attempts to detect novelty by looking at the amount the system must change in order to incorporate the new information. This chapter focuses on presenting the structure of the model, and discusses how each step is biologically inspired.

HLISSOM was chosen as the model to follow because of its strict adherence to emulating biological processes and its ability to work with real images. Also, few parts of the HLISSOM system are specified beforehand, and therefore it is possible to make connections between the way the model learns and experiments performed on animals. In later sections we will demonstrate this connection.

One major omission in this model is the lack of chromatic information.

Experiments have shown that the chromatic properties of an object have little influence on MT neurons' motion processing when there is sufficient luminance contrast (Thiele *et al.*, 1999). As such, in order to simplify the model, chromatic information is not processed.

4.1 Overview

In this section DS-LISSOM (Directionally Selective LISSOM) is laid out in its entirety. Later sections will focus on how each of the layers are developed. A pictorial representation of the layout of DS-LISSOM can be seen in Figure 4.1. Information is first processed by the retina. There are two such sources of information: real images which represent sight and synthetically generated images which represent spontaneous activity within the visual system (as discussed in previous chapters). Spontaneous activity will later be shown to train the system in a way that is biologically similar to the visual stimulation that occurs prenatally. From the retina, information travels toward the LGN. The LGN layer is designed to be most responsive to bright and dark spots within a given receptive field. To more accurately account for this information, the LGN layer is made up of two separate channels. One of the channels is most responsive to light spots, while the other is most responsive to dark spots. From the LGN, information will travel to V1. For this to occur, each neuron in V1 looks at a region within the LGN layer (its receptive field). As learning occurs, it will not only become sensitive to a particular orientation, but lateral connections will also be updated such that neighboring neurons will share similar orientation preferences. In this system, lateral connections to nearby neurons will be excitatory, while longer lateral

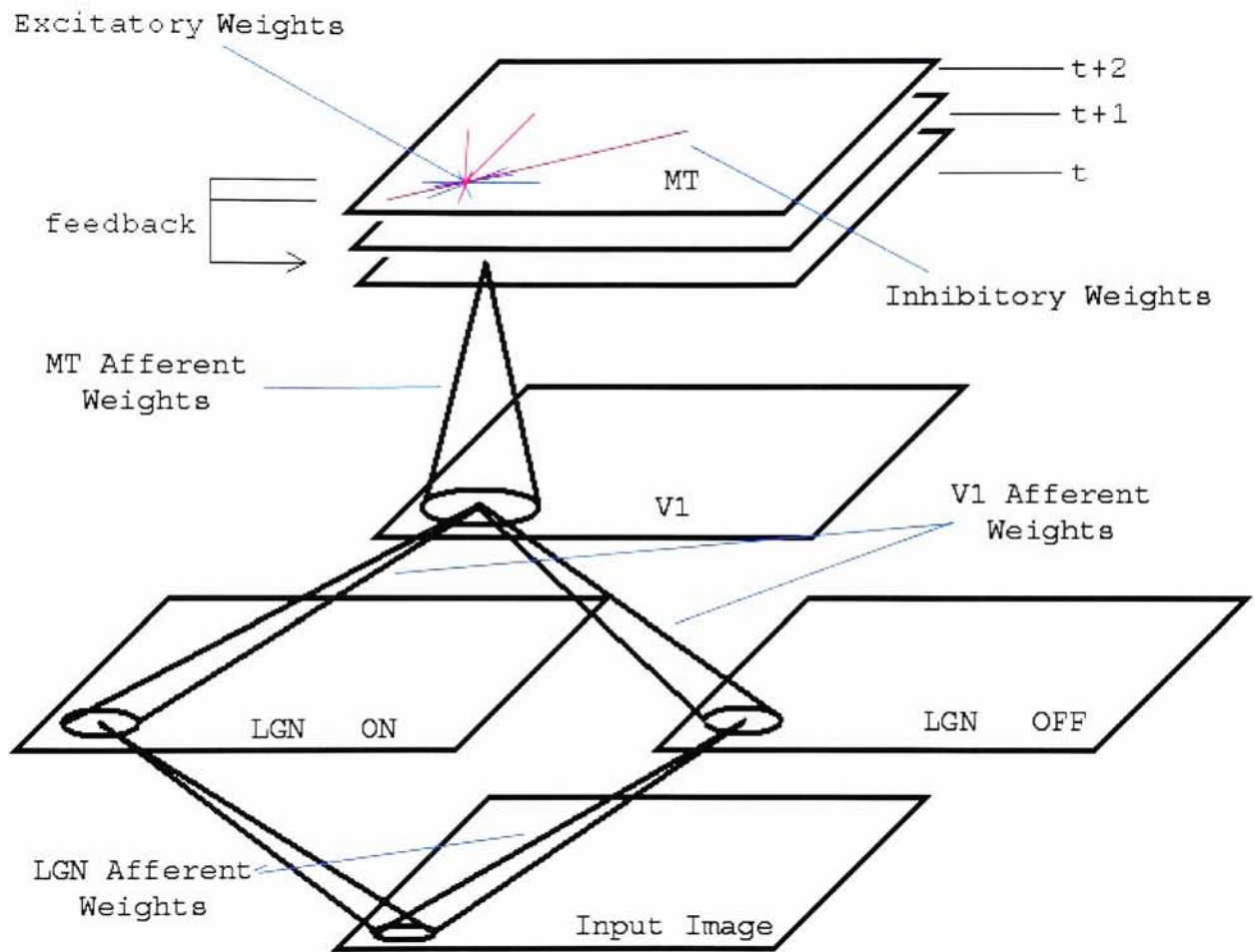


Figure 4.1: Each of the major areas of DS-LISSOM are labeled. This is a pictorial view of DS-LISSOM.

connections will be inhibitory. To move to the MT layer, a similar process takes place. Each neuron in MT pulls input from its receptive field in the previous layer. In order to account for directional selectivity within the V1 layer, an approximation is made by looking at the different responses V1 has at predetermined time steps. In this way, only edges which are thought to be moving are passed onto MT. Generally speaking, the receptive field of an MT neuron is larger than the receptive field of a V1 neuron. Lateral connections within the MT layer act similar to those in the V1 layer such that neurons with similar direction sensitivity tend to be close to one another. In order to account for directional information, MT must process information from a series of time steps. To accomplish this, MT feeds back information from the previous steps to itself.

The following sections will look at how each of the layers is constructed. In each section the following symbols are used

- η is the final activation of a particular layer.
- ζ is the afferent response of a neuron.
- ξ is the activation of a cell in the receptive field of another cell.

4.2 Modeling Retinal Activations

Information, or activation, in the retina comes from one of two places depending on whether or not the system is thought to be in a prenatal or postnatal stage. During the prenatal stage the retinal activation consists of patterns of oriented Gaussians as shown in Figure 4.2. These patterns can be generated by the following equation:

$$\xi_{xy} = \exp\left(-\frac{((x - x_0)\cos(\theta) - (y - y_0)\sin(\theta))^2}{a^2} - \frac{((x - x_0)\sin(\theta) + (y - y_0)\cos(\theta))^2}{b^2}\right) \quad (4.1)$$

where a^2 and b^2 specify the length along the major and minor axes, (x_0, y_0) is the center of the Gaussian, and θ is its orientation. The x and y coordinates are chosen randomly such that the Gaussian occurs within the retinal area of size $R \times R$. θ is also chosen randomly such that $0^\circ \leq \theta < 180^\circ$. A random number of Gaussians occur within each iteration of training. In order that Gaussians do not overlap when multiple Gaussians are present their centers

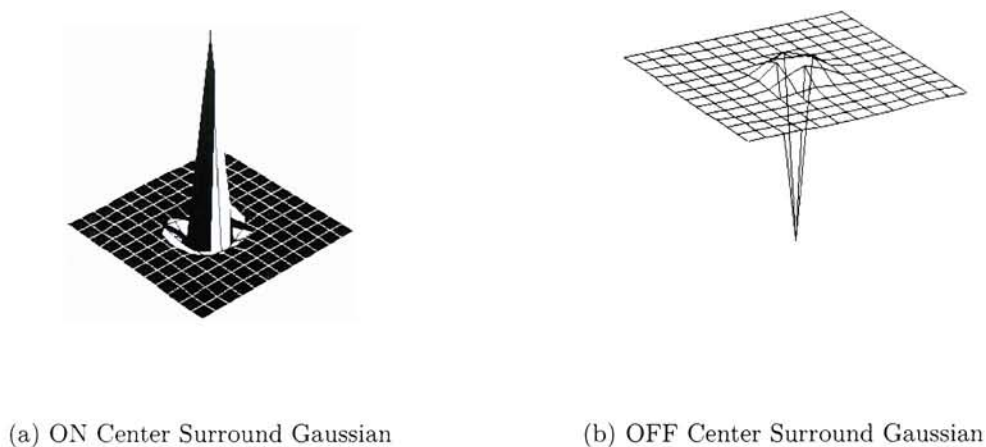


Figure 4.2: These images are examples of the oriented Gaussians which are used as the afferent weights from the input image to the LGN. These act as simple edge detectors as it is thought the Retinal Ganglion cells do.

are specified to be at least d_r units apart. Later chapters will discuss the advantage of training the system on specific images in order to solicit significant responses when looking for novelty.

Once the system is considered to move into the postnatal stage (after approximately 1,000 to 10,000 prenatal iterations for a general learning system) the retinal activation is a response to real input images. These images are converted to grayscale images, which account for intensity contrast information. Experiments have shown that it is the luminance contrast channel which, when present, plays a large role in the detection of motion (Thiele *et al.*, 1999).

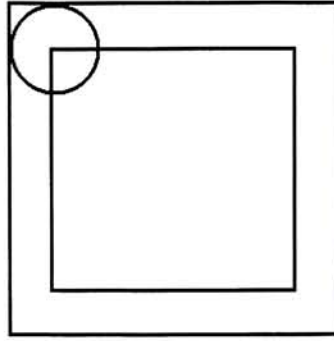


Figure 4.3: The circle represents the receptive field of a cell for example a cell in MT. This represents the fact that the preceeding layer, in this example V1, must be both longer and wider.

4.3 Processing from the Retina to LGN

Like its predecessors, DS-LISSOM is not interested in the learning processes that take place from the retina through the LGN. Therefore the connections to neurons in the ON and OFF channels of the LGN are set to fixed strengths which resemble those found in adult LGN cells. A Difference-of-Gaussians (DoG) model is used to accomplish this. An important design decision is to make sure that information is continuously stored retinotopically. Therefore the way in which each of the two LGN channels is organized is important. The (x, y) position of each neuron in the LGN layer corresponds with the center of each of the receptive fields. A consequence of this is that the LGN layer will be smaller than the retinal layer. The exact size of the LGN layer is the size of the retinal layer minus the diameter of an LGN neuron's receptive field as depicted in Figure 4.3. From the above information, the following equation can be derived for a neuron present in the ON channel of the LGN

$$\mu_{ab,xy} = \frac{\exp(-\frac{(x-x_0)^2+(y-y_0)^2}{\sigma_c^2})}{\sum_{xy} [\exp(-\frac{(x-x_0)^2+(y-y_0)^2}{\sigma_c^2})]} - \frac{\exp(-\frac{(x-x_0)^2+(y-y_0)^2}{\sigma_s^2})}{\sum_{xy} [\exp(-\frac{(x-x_0)^2+(y-y_0)^2}{\sigma_s^2})]} \quad (4.2)$$

In the above equation (a, b) is the position of the neuron, (x, y) is the position of each receptor within the retina with center (x_0, y_0) , σ_c^2 is the width of the central Gaussian, and σ_s^2 is the width of the surround Gaussian. The receptor weights for the OFF channel can similarly be found by subtracting the center Gaussian from the surrounding Gaussian as follows:

$$\mu_{ab,xy} = \frac{\exp(-\frac{(x-x_0)^2+(y-y_0)^2}{\sigma_s^2})}{\sum_{xy} [\exp(-\frac{(x-x_0)^2+(y-y_0)^2}{\sigma_s^2})]} - \frac{\exp(-\frac{(x-x_0)^2+(y-y_0)^2}{\sigma_c^2})}{\sum_{xy} [\exp(-\frac{(x-x_0)^2+(y-y_0)^2}{\sigma_c^2})]} \quad (4.3)$$

A visual representation of the weights for these receptive fields can be seen in Figure 4.2. In order to prevent both ON and OFF cells from being active at the same location at the same time, each cell will be thresholded to have only positive activations. This is consistent with biological systems (Bednar, 2002).

The LGN is divided into two layers: one which represents the ON activation and another which represents the OFF activation from the retinal ganglion cells. Results given by Bednar have shown that when working with

real images this is important, since it will allow the LGN to respond to a wide range of brightness values (Bednar, 2002).

The activation of a single cell in the LGN layer can be calculated by the sum of activations in a cell's receptive field. From this the following is derived:

$$\eta_{ab} = \sigma \left(\gamma_A \sum_{\rho xy} \xi_{\rho xy} \mu_{ab, \rho xy} \right) \quad (4.4)$$

In the above equation, $\mu_{ab, \rho xy}$ is the afferent weight from a cell (x, y) to (a, b) , γ_A is a constant scaling factor, $\xi_{\rho xy}$ is the activation of cell (x, y) , ρ is the location of the receptive field, which can be either the generated input (PGO input) or image input from the photoreceptors, and σ is a piecewise linear approximation of the sigmoid activation function (allowing for faster calculations). The sigmoid activation function can be defined as follows:

$$\sigma(x) = \begin{cases} 0 & x \leq \delta \\ \frac{x-\delta}{\beta-\delta} & \delta < x < \beta \\ 1 & x \geq \beta \end{cases} \quad (4.5)$$

The activation function makes sure that there is at least a minimum amount of activity within the receptive field before the cell becomes active itself. This is extremely useful since many real images are noisy. The sigmoid function also ensures a maximum amount of activity in a particular cell.

4.4 Modeling V1

This is the first area of interest to the learning aspects of DS-LISSOM. It's implementation is identical to that implemented in the previously mentioned HLISSOM model with the exception that statistics are stored in order to determine whether or not a particular orientation has been seen before.

V1 cells are different than cells in the LGN in that their activation is a two-step process. The first step is similar to that of the LGN, and the activation of a cell can be specified by the following equation

$$\zeta_{ij} = \sigma \left(\frac{\gamma_A \sum_{\rho ab} \xi_{\rho ab} \mu_{ij, \rho ab}}{1 + \gamma_N \sum_{\rho ab} \xi_{\rho ab}} \right) \quad (4.6)$$

where ρ specifies the ON or OFF layer from the LGN, (a, b) is a cell within the receptive field of cell (i, j) , $\mu_{ij, \rho ab}$ is the weight from cell (a, b) to (i, j) in the appropriate receptive field ρ , and $\xi_{\rho ab}$ is the activation of the cell (a, b) in the receptive field of cell (i, j) and on either the ON or OFF channel of the LGN specified by ρ .

The constant γ_N is used to make the activation of a cell more selective. This value often starts out near 0 and slowly increases over time such that cells become more selective. As a result of the value of γ_N it is important to keep all of the values spread out across the range from 0 to 1. For this reason the constant γ_A is introduced. Its purpose is to make sure that the afferent responses continuously fall between 0 and 1. If γ_A is not present while γ_N increases, then over time the activation of all cells will move toward

0. rendering the system inactive.

The sigma function is the same as that used when calculating activations in the LGN layer.

Once an initial activation response is calculated, the lateral excitatory and inhibitory weights get their chance to change the response. This is accomplished over a number of rounds using the following equations

$$\eta_{ij}(0) = \zeta_{ij} \quad (4.7)$$

$$\eta_{ij}(t+1) = \sigma \left(\zeta_{ij} + \gamma_E \sigma_{kl} E_{ij,kl} \eta_{kl}(t) - \gamma_I \sigma_{kl} I_{ij,kl} \eta_{kl}(t) \right) \quad (4.8)$$

The excitatory weights are defined as $E_{ij,kl}$, the weight from cell (k, l) in V1 to the cell (i, j) in V1 (and the inhibitory weights) are similarly defined as $I_{ij,kl}$. Each of the settling iterations helps to ensure that responses of nearby neurons will have similar responses, helping reduce the amount of redundancy in the map and aiding in the formation of orientation maps, as previously discussed.

4.5 Modeling MT

At this point things change, because temporal effects need to be considered. This is the first area in this model that is selective of direction. As such some form of feedback needs to be implemented to account for different periods in time. From a psychological point of view, this is thought to be accom-

plished in one of three ways: the Riechardt model, Barlow and Levick model, and the two asymmetrical pathways model. In the Riechardt model, past information acts to further strengthen current activations. The Barlow and Levick model proposes that instead of strengthening current activations, the interaction between past and current information is inhibitory. Finally, the two asymmetrical model combines both an idea of excitation and inhibition (Grzywacz & Merwine, 2002).

DS-LISSOM obtains temporal information using the Riechardt model, which states that the amount of activation at different periods of time have a multiplicative effect on the current activation of the neuron. In DS-LISSOM the amount of activation at a previous time step adds to the total amount of activation. The following equation models this behavior

$$\zeta_{ij} = \sigma \left(\frac{\gamma_A \sum_{\phi ab} \eta_{\phi ab} \mu_{ij, \phi ab}}{1 + \gamma_N \sum_{\phi ab} \eta_{\phi ab}} \right) \quad (4.9)$$

In the above equation, each ϕ is the time in which a cell from V1 (η_{ab}) is measured. For DS-LISSOM, four such layers of information are kept. Because of the changing weights within each layer, the actual activation is not stored; rather, it is recalculated using the current weights for that particular period of time. The following equations describe how each $\eta_{\phi ab}$ is determined:

$$\eta_{0ab} = ((\eta_{ab}(t) - \eta_{ab}(t-1)) > 0) * \eta_{ab} \quad (4.10)$$

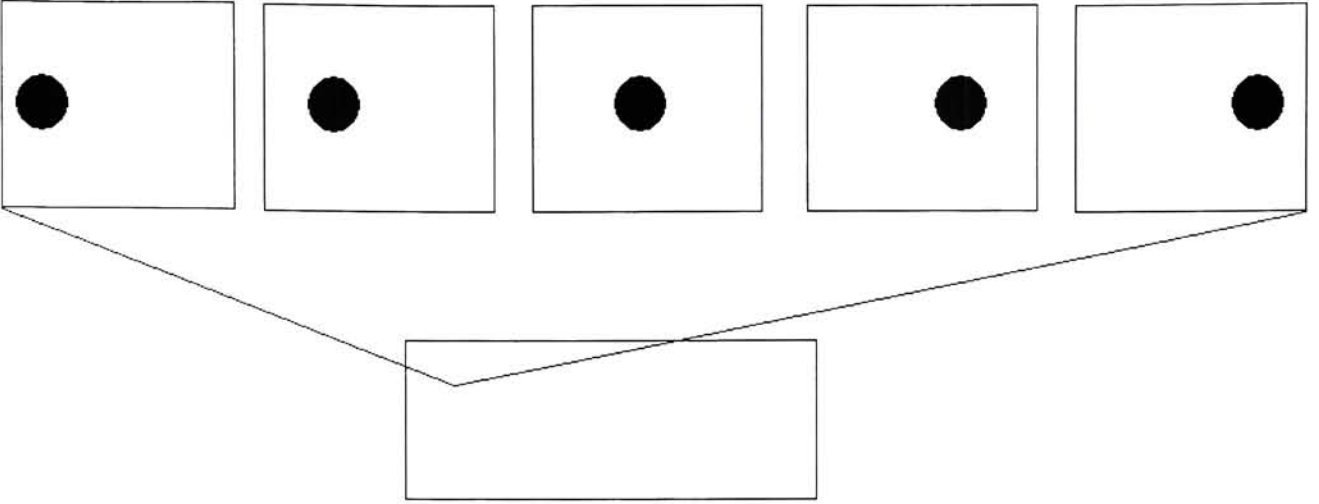


Figure 4.4: Each of the top images represent a receptive field of a single cell in MT. An MT's receptive field will draw data from multiple points in time. In the above example, an MT is looking at 5 different points in time. As an object moves the developing MT cell will adjust its weights such that it will respond most strongly when, in this example, a bright object moves to the right through its receptive field.

$$\eta_{o+1ab} = \eta_{\phi ab} \quad (4.11)$$

In this way ϕ describes how long ago a given activation occurred. Notice the way in which η_{0ab} is produced. The only activations that travel to MT are those activations which have changed from one time step to the next. This is meant as a simple way to model some of the directional selectivity that occurs in V1.

To think about this in a slightly different way, imagine that each of the layers is the actual activation at the current time step of the previous layer. The receptive field of a current cell is the combination of a receptive field in each of these layers, and a connection exists between the cell and each

of the cells in each of these receptive fields. The activation of the cell is the combined total of all of the activation in all receptive fields. Motion is learned because the system will learn where objects exist over time as shown in Figure 4.4.

Just like V1, the MT layer also goes through a number of settling iterations whereby the final response of a cell is formed according to the following equations

$$\eta_{ij}(0) = \zeta_{ij} \quad (4.12)$$

$$\eta_{ij}(t+1) = \sigma \left(\zeta_{ij} + \gamma_E \sigma_{kl} E_{ij,kl} \eta_{kl}(t) - \gamma_I \sigma_{kl} I_{ij,kl} \eta_{kl}(t) \right) \quad (4.13)$$

As in V1 the settling iterations will help reduce redundancy in the map produced by MT. This will also help ensure that nearby neurons have similar patterns of activity, which is a property of cortical responses.

4.6 Training the System

Up to this point it should be clear how cells become active within the system. What is still not clear is how the system is capable of learning in the first place. Learning occurs by recognizing the correlation between input patterns. In the above equations the μ , E and I responses are adjusted over time to adapt to these patterns. This occurs through a form of Hebbian learning using the following equation

$$w_{ij,mn}(t + \delta t) = \frac{w_{ij,mn}(t) + \alpha \eta_{ij} X_{mn}}{\sum_{mn} (w_{ij,mn}(t) + \alpha \eta_{ij} X_{mn})} \quad (4.14)$$

The goal of this equation is to increase the weight, $w_{ij,mn}$, if and only if the activation of a cell in the current level, η_{ij} , and the activation of another cell, X_{mn} , are high at the same time. For afferent connections X_{mn} is the amount of activation of cell mn in the previous layer while lateral connections look at the current level, η_{mn} . α is the learning rate, and it can be helpful to define different learning rates for each layer and for each type of connection. The normalization that takes place keeps connections from growing without bound.

The result of the learning procedure is lateral inhibitory weights that become patchy over time, and excitatory weights, which become strong between close neighbors. As previously mentioned, this means that the maps produced at each layer will form in such a way that neighbors have similar patterns of activity.

4.7 Inconsistency Detection

Inconsistencies are defined as patterns of activity that have not previously been seen. In other words, if only horizontal lines have been seen in the past, vertical lines would be considered inconsistent. This definition lends itself to a natural way to look for inconsistencies: look for large changes in weights throughout the system. In this system it is the inhibitory weights that are watched over time. The change in excitatory weights or afferent weights could

have also been examined (Brazeau *et al.*, 2003). By looking at inhibitory (or excitatory) weights we examine the amount of change within the V1 and MT maps. Looking at the afferent weights then would correspond to examining the amount of change in the previous map(s) as they relate to a cell's receptive field.

A different way to describe this is to look at how much the system is learning. If cells remain active consistently over time, then weight changes will occur fast at first, and slow down over time. This occurs due to the normalization which occurs when calculating the new weights.

Looking for inconsistent events in motion is done in the same way. The amount of weight change is monitored, and jumps in the amount of weight change are indicative of something new being learned.

The most important factor in setting up the system is the way in which it is trained. The next chapter will show that when trained on random input patterns, the system will be prepared to perceive a wide variety of orientations and motions. This is consistent with research which has shown that cats raised with their eyes shut are still able to see when their eyes are later opened. Although a significant result, it is not the desired behavior for a system that is used for determining inconsistencies since it will lead to an inability to see them. Instead, it is important to train DS-LISSOM in the environment that is understood to be the consistent environment. In this way, when changes to that environment (inconsistent events) occur later, the system will respond by adjusting its weights. Again, this is consistent with previously discussed research, which has shown the effects of raising cats in atypical environments.

4.8 Conclusion

The learning system proposed and implemented as DS-LISSOM is a biologically inspired system that is capable of learning both orientation and motion information in a way which is consistent with current knowledge of biological systems. DS-LISSOM further extends previous models by looking at ways to infer that new knowledge is being acquired, and thereby finding inconsistent events. The next section will look at examples of the system at work, and will show that the receptive fields and orientation maps that are formed are biologically accurate.

Chapter 5

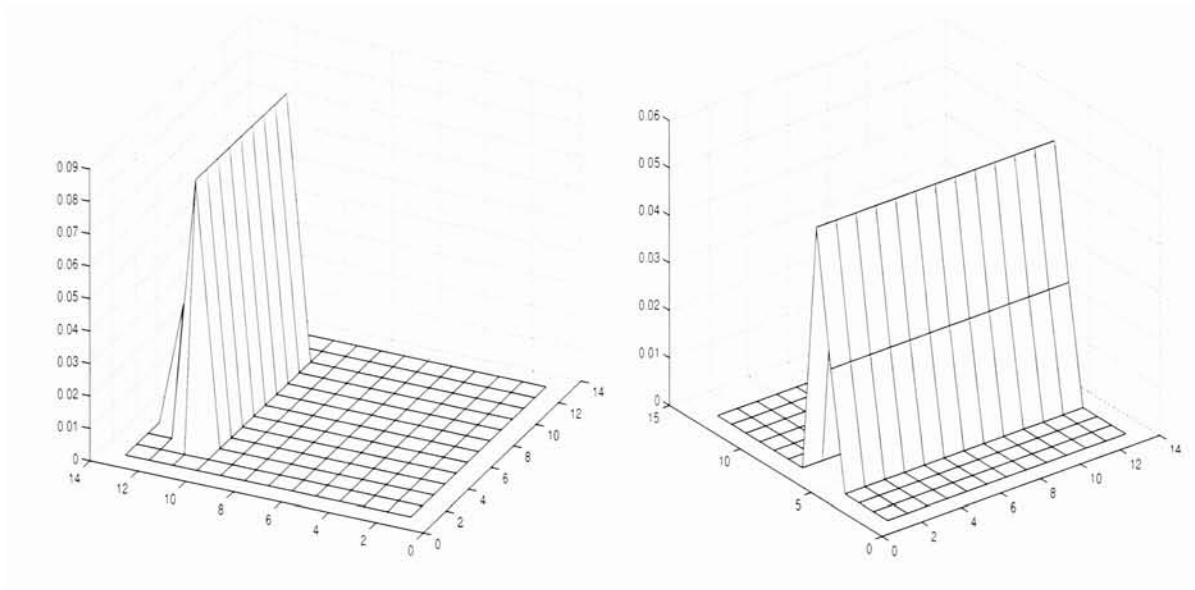
Development of Visual Preferences

This chapter looks at results produced by DS-LISSOM, which was described in the previous section. The results show that it is possible to train the system in such a way that it becomes familiar with both orientation and directions in a general way. Results will further show that when DS-LISSOM is trained on specific input, it will form preferences for only those orientations and directions present within the training set. Finally experiments will show that the system is capable of distinguishing orientations and directions that it has seen before from those it has not seen before.

Each of the experiments were run using the parameter values seen in Appendix B. Using these values DS-LISSOM required 400 megabytes of memory.

5.1 Formation of Selective Neurons

The first, and perhaps most important, result is the formation of cells that are orientation and direction sensitive. Such formation is a direct measure of the capability of the system to learn and retain preferences for visual stimulus.



(a) Edge Selective Cell

(b) Bar Selective Cell

Figure 5.1: These are two examples of cells that are formed when a strong edge and bar are present in an image. The result is the formation of edge and bar detectors that activate most strongly when an edge or bar is present in the appropriate part of its receptive field.

5.1.1 Orientation Selectivity

As previously discussed, orientation selectivity first occurs in the V1 layer of the visual system. If DS-LISSOM learns like its biological equivalents then it too should form preferences for orientation in V1. As Figure 5.1 shows, cells can form such preferences. These images were obtained by training DS-LISSOM on random dark and light bars. The images show the strength of the weights between the cell and each of the cells in its receptive field as shown in Figure 5.3. Additional figures show input images, their resulting activations within V1 and the orientation selectivity of some of the cells of V1.

Recalling what was said about the formation of simple cells, Figure 5.4 shows cells that have formed while training DS-LISSOM, and compares them with their simple cell counterpart.

By looking at each of the cells in V1 and determining their orientation preference, an orientation map can also be formed. Figure 5.5 shows one such map. Notice that there are many features present, which is consistent with current research studies.

5.1.2 Motion Selectivity

Motion is learned by combining V1 responses at different moments in time. The result is the formation of cells in V1 that respond to oriented edges moving in a specific direction. Figure 5.6 gives one example of the selectivity of a cell by looking at its afferent weights into each of the V1 layers from different time steps (recall that there are 4 such layers in DS-LISSOM).

The receptive field for each of the cells in MT is larger than those in V1.

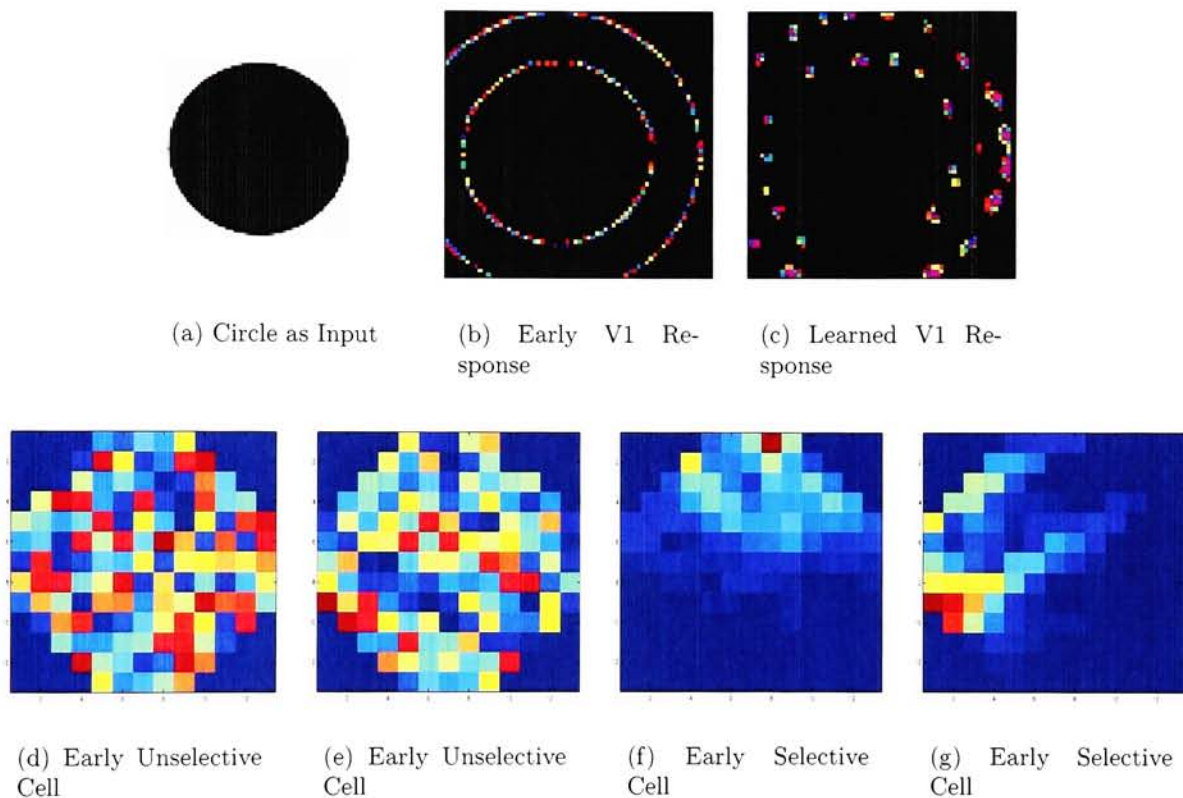


Figure 5.2: The first row shows the input image, the response in V1 after only a 10 iterations, the response after 10,000 iterations. The second row shows a number of cells after 10 iterations and after 10,000 iterations.

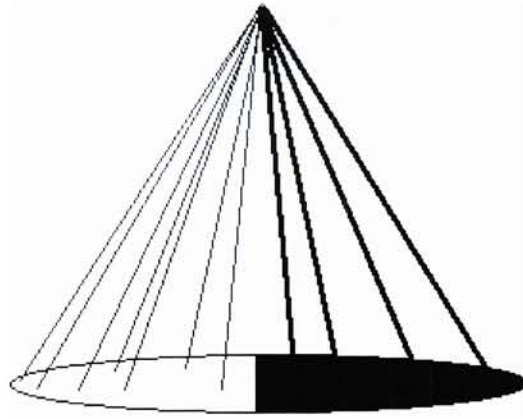


Figure 5.3: The lines represent connections between a cell in V1 and cells in the LGN that are within its receptive field. The lighter lines represent connections with strong weights while darker lines represent connections with weak weights. This particular cell will initially become active if there are a large number of bright cells on its left side and little activity on its right side (indicating the presence of an edge).

As a result the orientation information is not as important; rather, it is the overall movement of an oriented edge as it moves through the receptive field of a particular cell.

5.2 Finding Inconsistencies

Realizing that DS-LISSOM is capable of learning and developing in the same way that current research tells us the visual system learns and develops leads to a question of whether or not certain aspects of DS-LISSOM can be put to use. Recall the findings of Weisel and the experiments he performed on cats. Such experiments have shown that if a visual system is trained in an atypical environment, such as only seeing horizontal lines, then the visual system

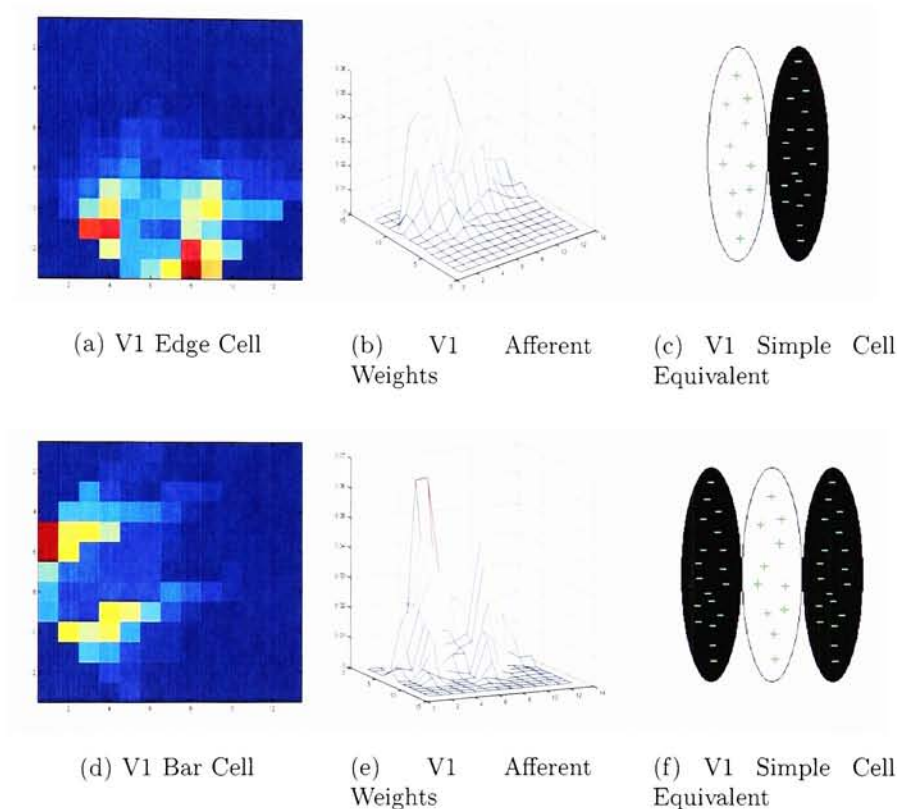


Figure 5.4: The first row gives an example of a simple edge cell formed by DS-LISSOM when trained on 10,000 random ellipsoids. The second row gives an example of a simple bar cell, again formed by training the system on random ellipsoids. The first two columns give different views of a cell's afferent weights, which are used to describe its receptive field and when it will become active. The third column shows the equivalent simple cell as it was described in previous chapters. This example helps to show that DS-LISSOM is in fact capable of learning and forming cells that are sensitive to orientation, as are those observed in biological experiments.

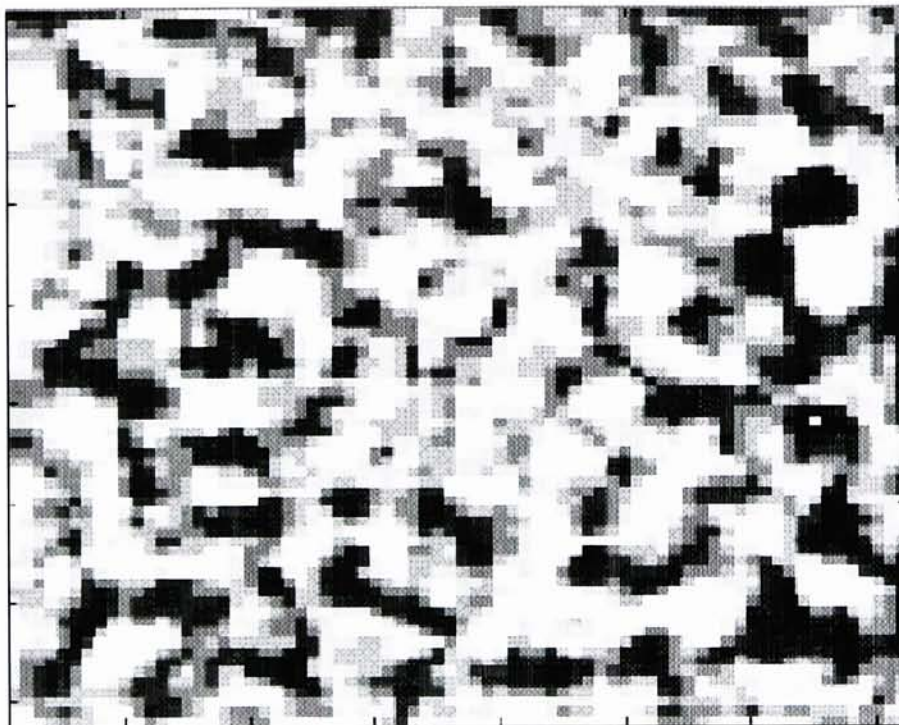


Figure 5.5: This orientation map was formed after training the system for 10,000 iterations on random ellipsoid patterns. The darker colors are preferences for horizontal orientations while light colors are more selective of vertical orientations. The result is a map that shows that system has a wide variety of orientation preferences. Similar maps can be formed to show the directional preferences of MT.

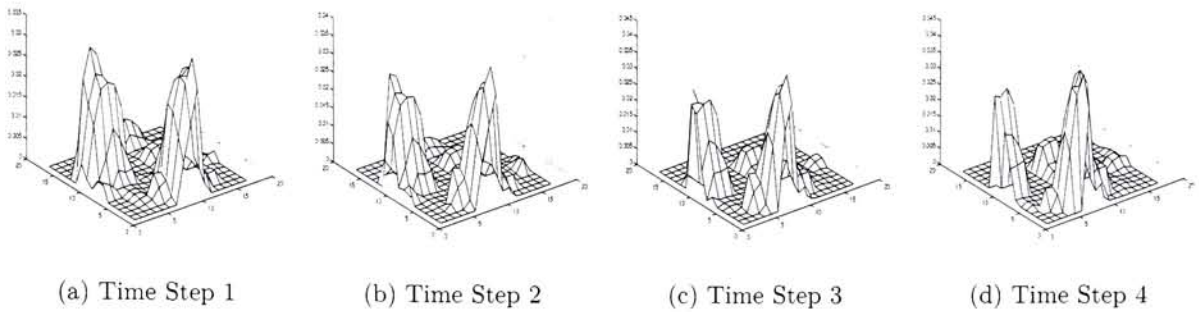


Figure 5.6: Each of the above images represent one period in time and the weights between cells in a particular time period in a cell's receptive field to a cell in MT. An MT's receptive field, in other words, not only contains an area at the current time step, but that same area in previous time steps. As shown by the images this allows an MT cell to be most active when and an object appears in the appropriate regions of its receptive field in each time period. The above sequence shows a preference for movement in the rightward direction.

will develop a strong preference for horizontal orientations, while preferences for vertical orientations are weak. This leads to an extension of DS-LISSOM whereby it is used to look for inconsistencies within a particular environment, as described in the previous chapter.

5.2.1 Finding Changes in Orientation

Figure 5.7 shows one example of DS-LISSOM being trained on only horizontal lines and then being placed in an environment with only vertical lines. The result is a huge jump in the amount of weight change in the inhibitory weights of V1. As suggested in chapter 4, this indicates that there is something inconsistent in this new environment. It is important to note that at this time DS-LISSOM does not have the ability to label the inconsistency, rather it can only indicate that one is present.

Figure 5.8 shows the same experiment: placing the system in an environ-

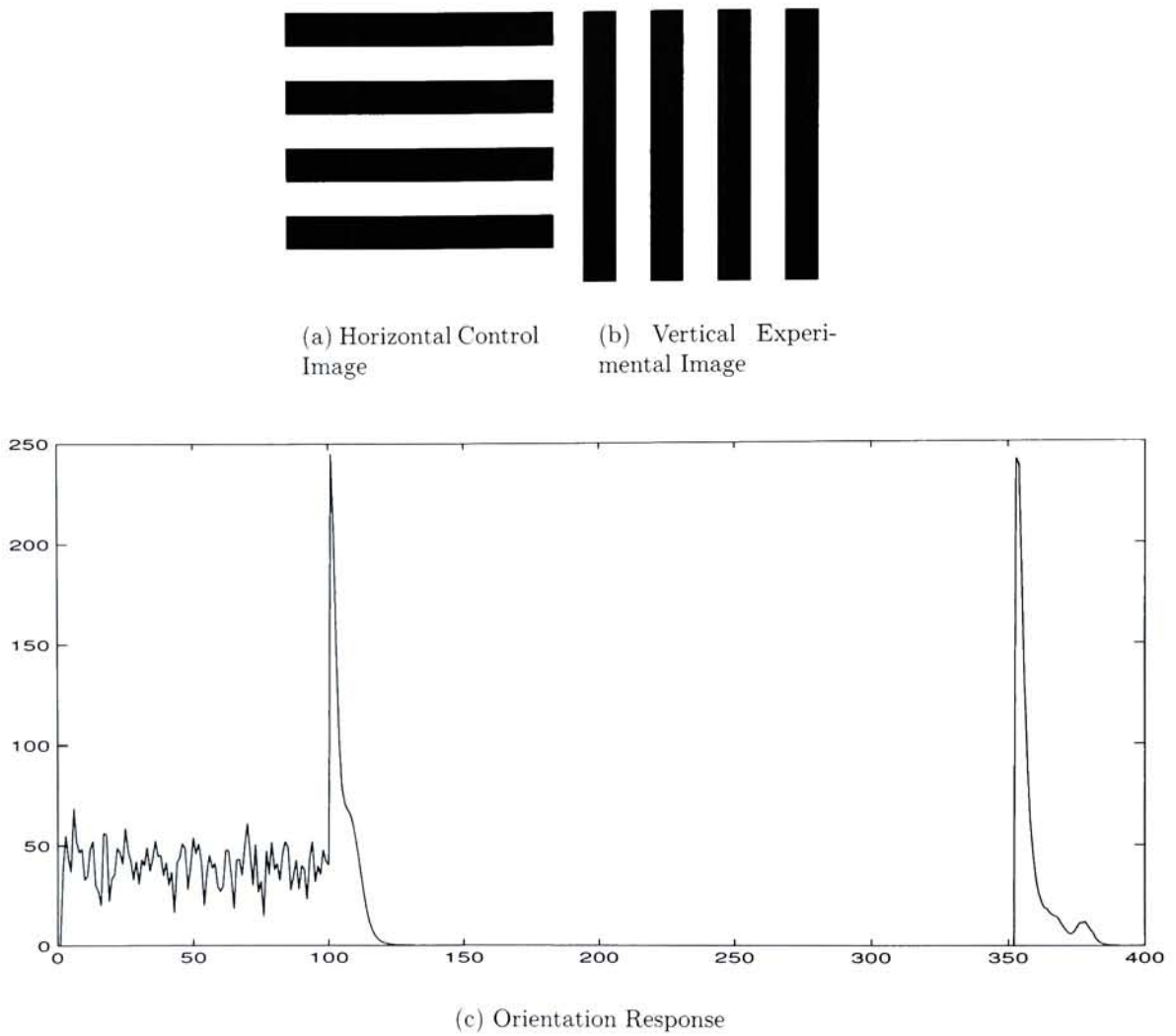


Figure 5.7: This figure demonstrates the weight changes that occur when the input to the system changes. The first large spike in the plot occurs when DS-LISSOM first sees the horizontal lines. Since at this moment the map is completely random, there are large changes in weight. The second large spike occurs when vertical lines are introduced for the first time to the system. The top two figures show examples of the vertical and horizontal lines that are sent to the system.

ment with only horizontal lines and then changing that environment. This time, however, the system is first trained prenatally on a number of random ellipsoids. Although a large change in weights is observed, the overall amount of change is decreased, indicating that the system has already learned some things about both horizontal and vertical lines.

5.2.2 Finding Changes in Motion

Inconsistencies in motion can be found in the same way. Figures 5.10 and 5.11 show some examples of the types of results achieved by using DS-LISSOM.

5.2.3 Long Term Memory

When looking for inconsistencies it is also important to think about what an inconsistency at one period means if that same event occurs in the future. Figure 5.2.3 shows that while DS-LISSOM is still in a mode of learning it can adapt to its new environment, while still remembering some of its old environment. If the new stimulus occurs often enough, it will no longer react to this stimulus as though it were inconsistent. At the same time, the original environment is not forgotten as long as it is still reinforced from time to time.

In some cases, this is not the desired result. Instead, it may be the case that any occurrence of an event that did not occur during training should be marked as inconsistent. In these cases the solution is to stop the learning process completely. In this way weights are no longer adjusted; however, the amount of weight change that would have occurred can be recorded and used to determine if an event has occurred in the past.

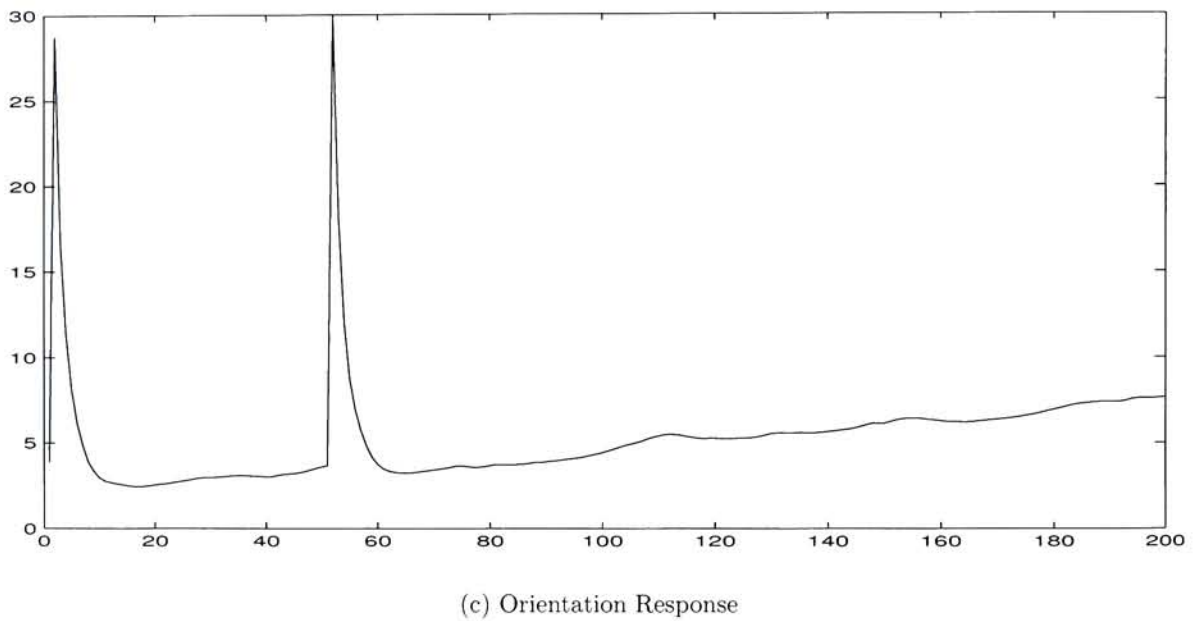
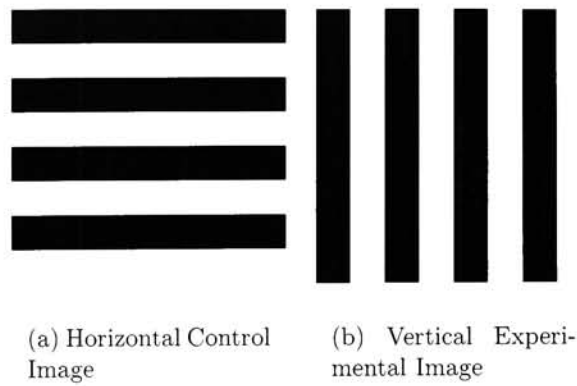
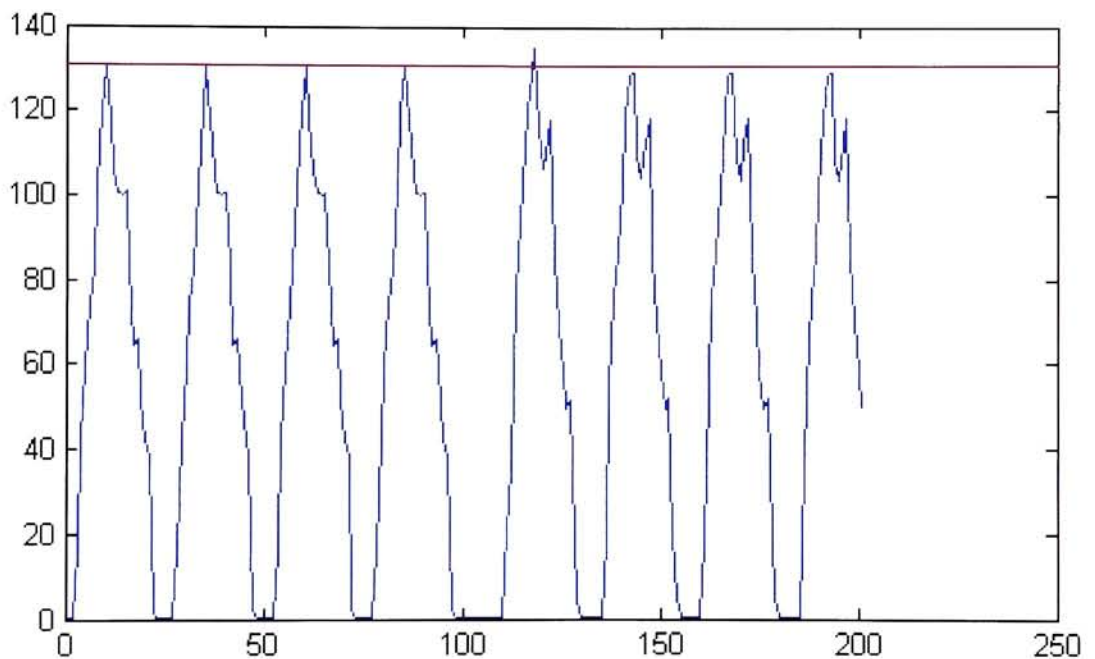
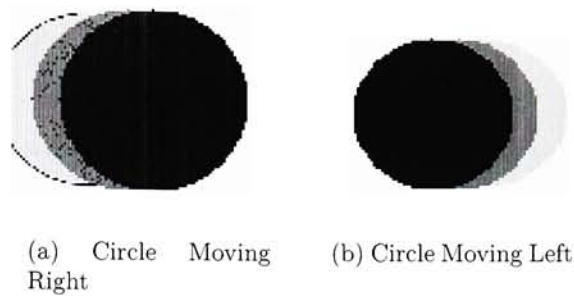
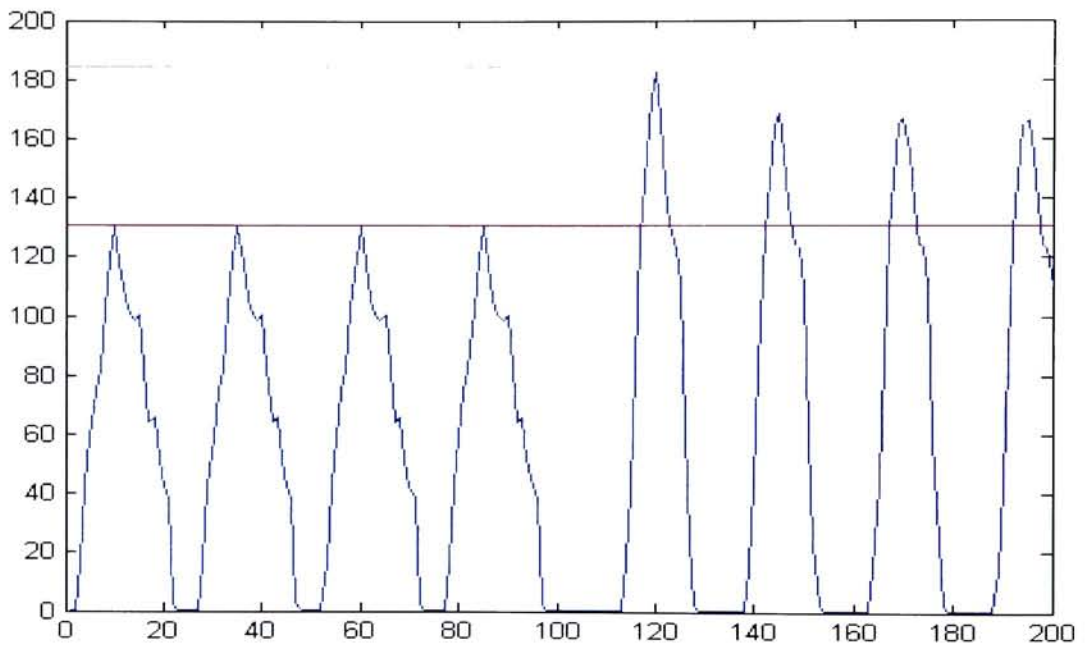
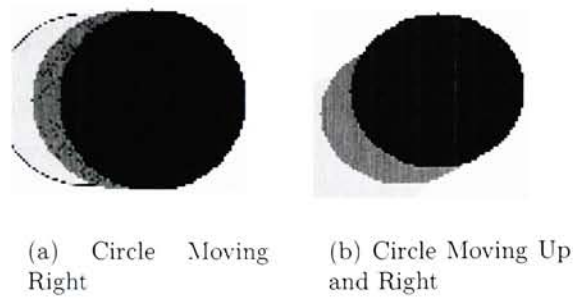


Figure 5.8: Unlike 5.7 this experiment was performed on DS-LISSOM after it had been prenatally trained on random ellipsoids. Although learning again occurs, it is important to realize that the relative amount of change in the maps is significantly reduced. Learning still must occur since the system has never seen horizontal and vertical lines presented in this way.



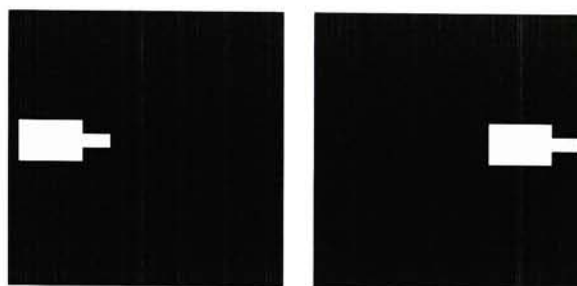
(c) Plot of Weight Changes

Figure 5.9: In this example, no pretraining occurred. In this way, the system became oriented to seeing only a few specific orientations. The top row shows the type of input images that were sent to the system. The first 900 iterations were input of a circle moving from the left to the right. After that the circle changed direction, moving from the right to the left. With this change in direction came a change in the amount the inhibitory weights were being adjusted.



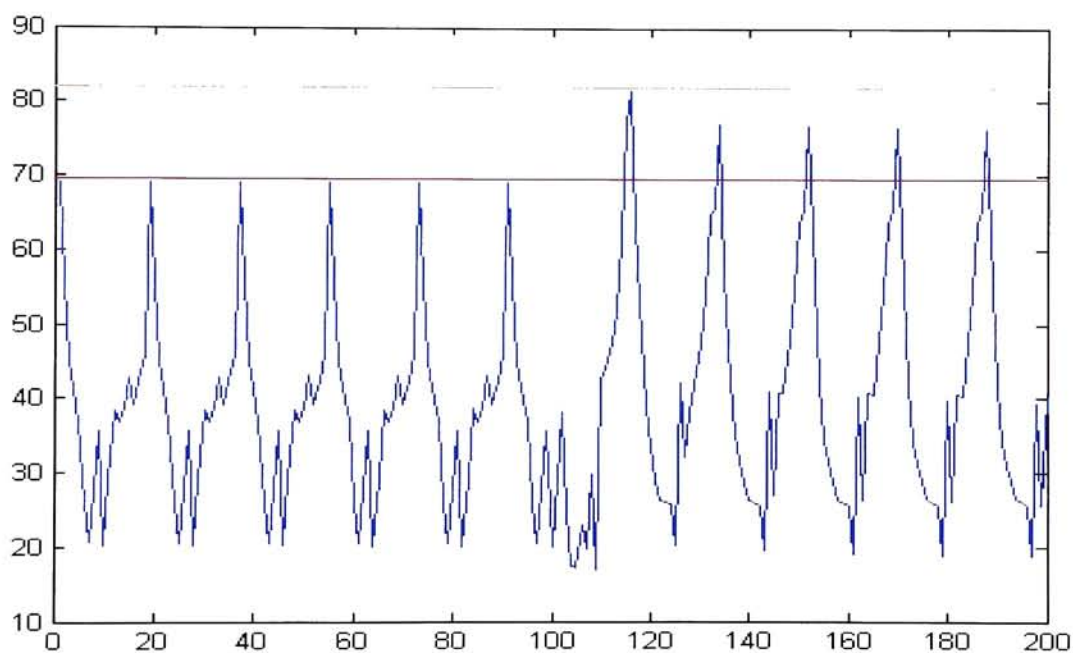
(c) Plot of Weight Changes

Figure 5.10: Like 5.9, this example was performed on DS-LISSOM with no pre-training. The top row shows the types of input images that were sent to the system. Images of a circle moving from the left to the right were displayed for the first 900 iterations. Next, images of a circle moving up and to the right were shown. The increase in weight change coincides with the change in direction.



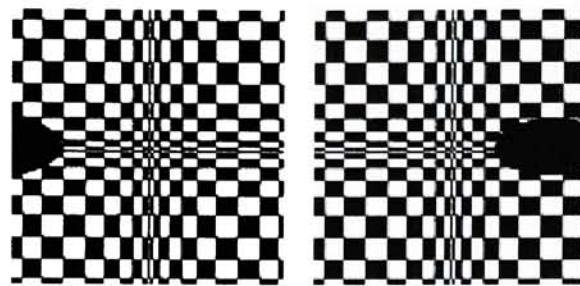
(a) Boxes Moving Right

(b) Boxes Moving Left

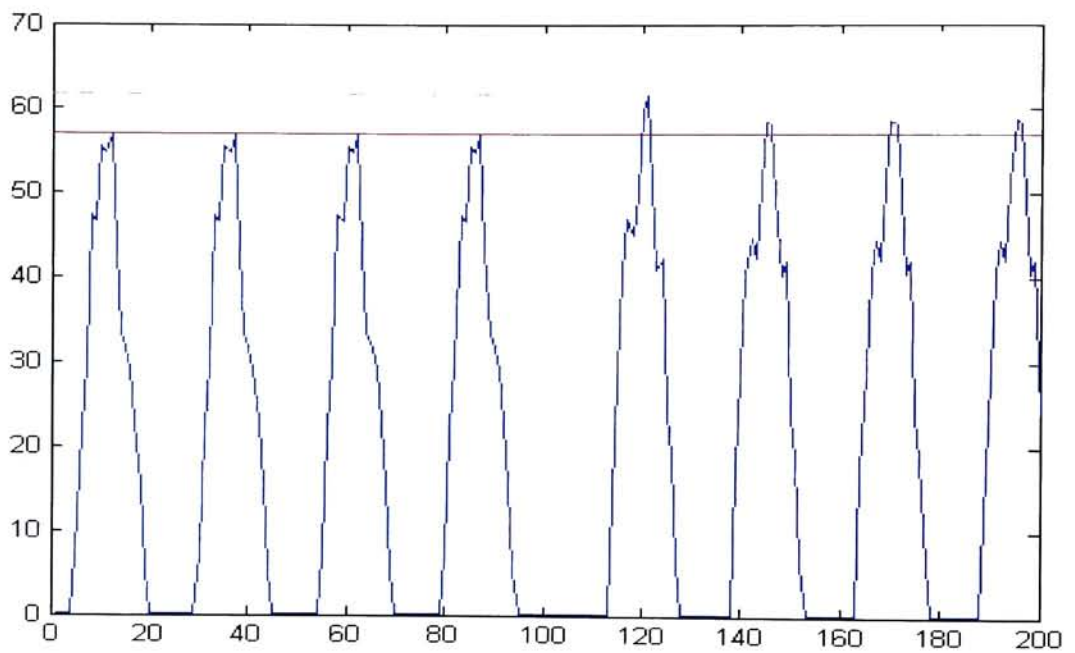


(c) Plot of Weight Changes

Figure 5.11: The detection of movement occurs not only with circles, but in the plot, with boxes as well.



(a) Circle Moving Right (b) Circle Moving Left



(c) Plot of Weight Changes

Figure 5.12: DS-LISSOM is also able to distinguish complex backgrounds from the moving objects. The above plot shows the detection of an ellipse's change of direction, even when a complex background exists.

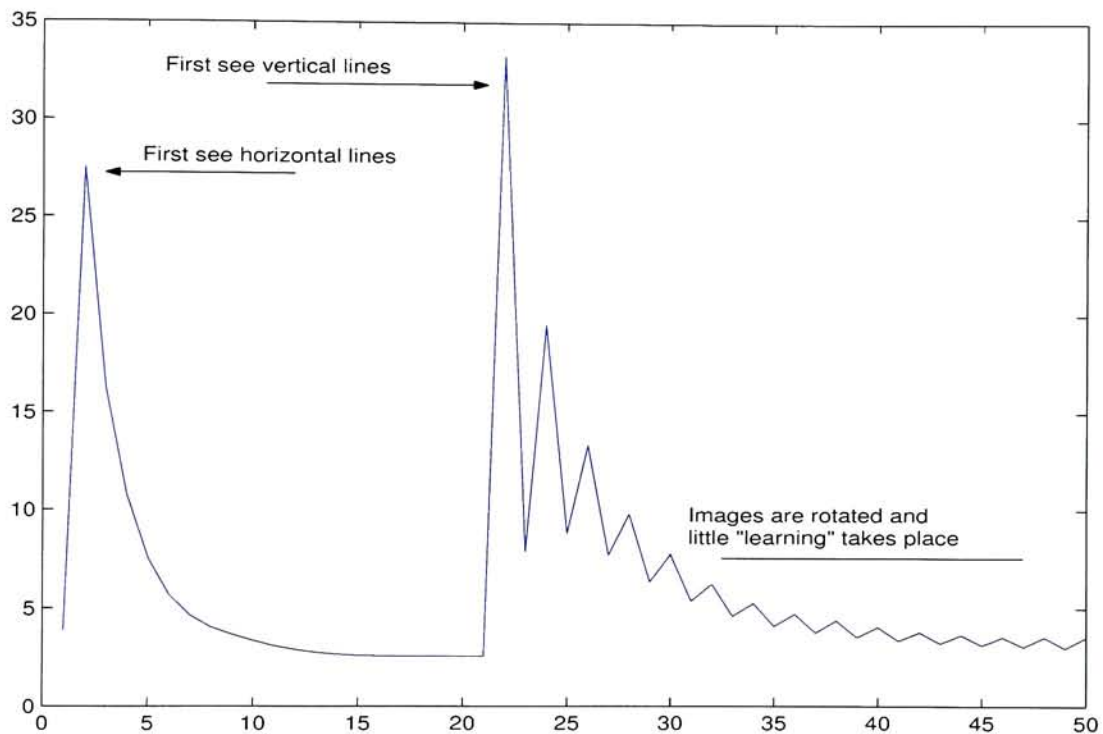


Figure 5.13: Once DS-LISSOM has seen an image, it is capable of retaining that knowledge. In the above sequence DS-LISSOM was shown horizontal lines 20 times in a row, followed by vertical and horizontal lines being displayed one after the other. As the plot shows DS-LISSOM reacts less strongly.

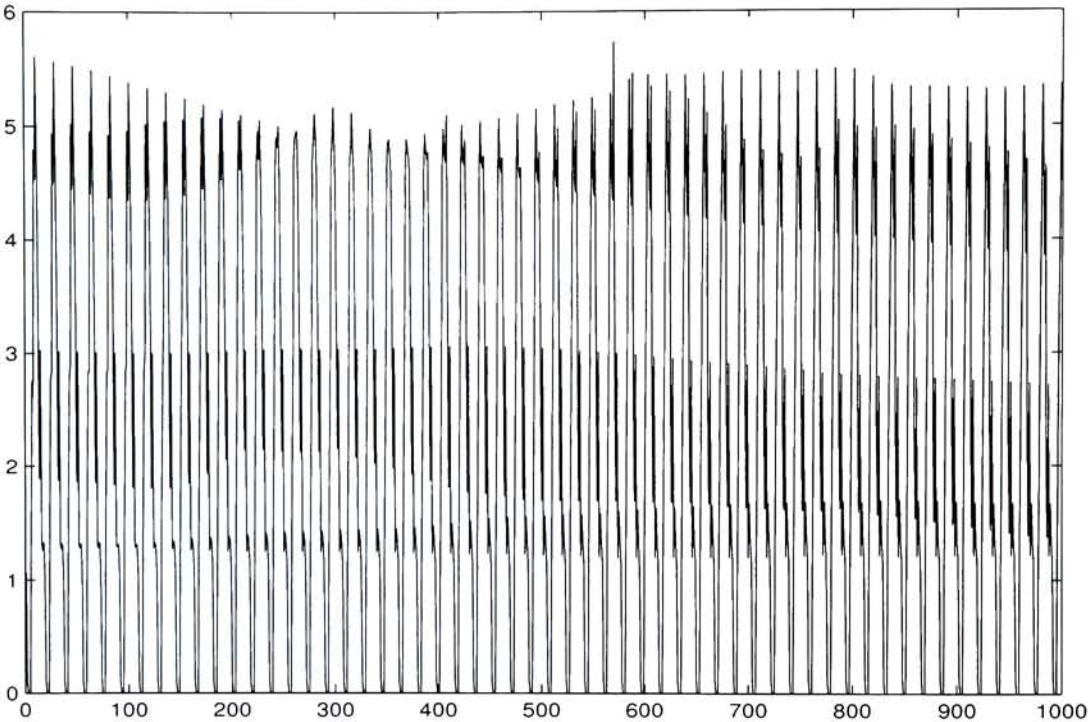


Figure 5.14: The above plot shows that once DS-LISSOM is trained it is already capable of perceiving a number of different directional motions. The amount of weight change is minimal, since many parts of the map are already tuned to this directional motion.

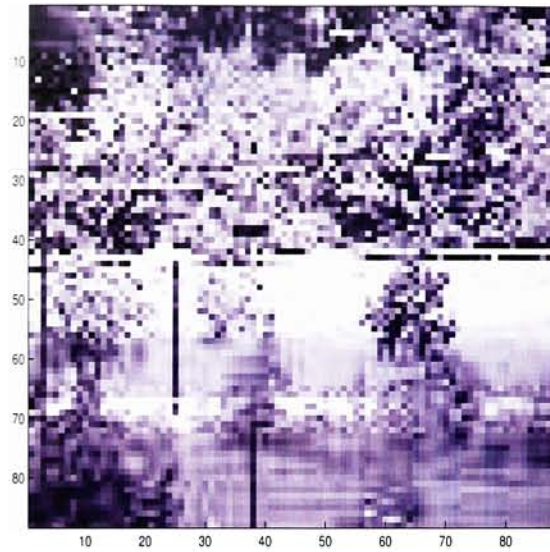
5.2.4 Working with Natural Images

The following experiment was conducted as follows:

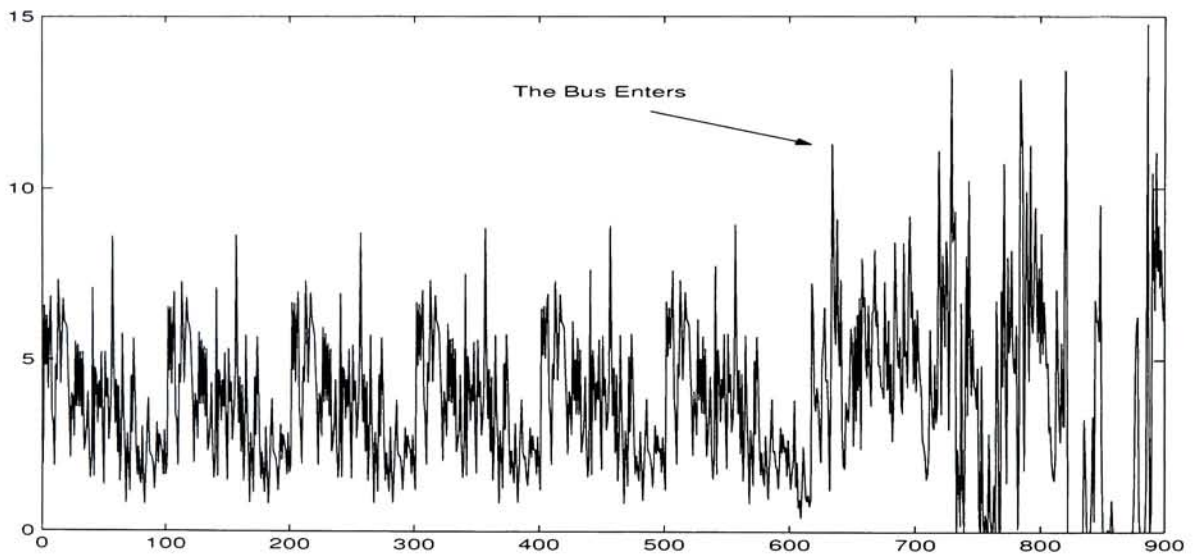
1. Train the system on random ellipsoid patterns (10,000 iterations).
2. Place the system in an environment where it will only see cars moving from the right to the left (2,000 iterations).
3. Change the environment by showing a bus which moves from the left to the right of the image.

The results show that it is possible for the system to recognize the difference. What is important to note is the fact that the system was trained on a large number of random ellipsoids initially. This meant that the typical motion of objects in the background were already learned. Large movements, such as that of the cars, were learned over time. Finally, when the environment changed and a bus moved in the opposite direction, the map reorganized to compensate, and thus the amount of weight change increased. Figure 5.15 shows some of the results from this experiment.

The type of training has the completely opposite effect when working with simple images. Figure 5.14 shows that when a box changes direction after training on random ellipsoids, there is little change in weight. Most likely this is because the directional motion is very simple and is already built into the system through prenatal development. Recall that the same result was seen when looking at the change in V1 weights when working with horizontal and vertical lines displayed both with training and without training (Figures 5.7 and 5.8).



(a) Input Image



(b) Weight Plot

Figure 5.15: The input image is of two roads. The top road is the only one where motion from cars occurs. At first, cars will only pass from the right to the left. After some time a bus moves from the left to the right. The plot shows the change in learning that occurs when the bus enters. Because the system was first trained on random elipsoids, much of the other movement, such as the movement in the trees, does not effect the results.

One problem with the system as it is set up now are limitations with memory. The above examples required over 400 megabytes of memory to run. If the size of the input image is increased, the amount of memory required increases exponentially. Matlab 6.5 running under Windows XP is not capable of using more than 1 Gigabyte of memory. As a result, natural images need to be small, and those images which are larger have a poor resolution. Therefore, as it is currently implemented, the ability for DS-LISSOM to work with natural images is limited.

5.3 Conclusion

DS-LISSOM is a general purpose visual learning system that is capable of learning both orientation and direction information. The proceeding experiments have shown that DS-LISSOM is capable of forming simple cells like those found in the primary visual cortex, and of producing cells that are directionally selective like those found in the MT area. Finally, experiments show that it is possible to exploit the learning process of DS-LISSOM in order to detect inconsistencies that occur within a specific environmental setting.

Chapter 6

DS-LISSOM: A Users Guide

During the development and testing of DS-LISSOM, a graphical environment was developed and is described in this chapter. In general the system allows for a user to train the system on random ellipsoids for a specified amount of time, after which it will be trained on a specific environment. The user can also ask for the system to be placed into a second environment which may, or may not, be inconsistent.

6.1 Explanation of the GUI

In 6.2 each of the parts of the GUI are labeled, and their function is detailed here.

1. The input image is the image as it is input into the system.
2. LGN Response is the response that the LGN sees once the input image passes through the Retinal Ganglion Cells.
3. The Orientation Response is the response of V1. This image shows the activity that is occurring within the V1 layer.

4. The Motion response represents pixels in V1 only if their activity has changed since the last period in time.
5. The MT Response is the activity that occurs in the MT layer.
6. The MT+ Response represents activity changes between two time periods in MT. It is currently my belief that such information can be useful in finding more complex motion such as contractions and expansions, and may be used to look for self-motion.
7. The V1 Responses plot will show up to the last 300 weight changes. The horizontal axis is the time when the weight measure was taken. The vertical axis represents the amount of change that occurred throughout the entire V1 map.
8. The MT Responses plot is similar to that of the V1 Responses plot, except that it measures changes that occur within the MT layer.
9. The slide bar allows a user to select the number of training iterations. Each training iteration is made up of one image of random ellipsoids. Typically it takes about 10,000 training iterations to fully prepare the system for a wide range of orientations and directional motions.
10. The number of control iterations allows the user to place the system in one environment for a while, and then switch it to a second experimental environment.
11. The control environment in which the system will first be placed.
12. The experimental environment.

13. Allows the user to load a previously run experiment. This is extremely useful since DS-LISSOM can start running from a previously saved training set, saving a great deal of time.
14. This button allows the user to save the correct state of DS-LISSOM, to be loaded at a later time.
15. This button will start DS-LISSOM.
16. This button will stop DS-LISSOM from running. Pressing the Start Training button will then start DS-LISSOM from this point.
17. This button will clear all of the current data from DS-LISSOM so that a new experiment can be run.
18. This button allows the user to quit.

6.2 A simple example

This section describes a simple example of running DS-LISSOM given that a trained version of DS-LISSOM is already available.

1. Start DS-LISSOM by running VisionSystem from the command window of Matlab.
2. Click on "Load Trained Set". This will pop up a file browser and will allow you to select a previously saved dataset. One provided in the DS-LISSOM distribution is 10000.mat.
3. Select the number of training iterations that you would like to take place. Since a trained set was already loaded this can be set to 0.

4. Select the number of training iterations to take place. Lets select 20 for example.
5. Select the control group. A number of them are listed in the pull down box.
6. Select the experimental group. Again, a number of them are already provided.
7. Press the "Start Training" button. This will start DS-LISSOM.
8. If you want to save data at any point in time, press the "Save Current State" button.
9. To quit press the "Quit" button.

Matlab does not allow for multithreading so it is often the case that the GUI seems unresponsive. For this reason there is a 2 second delay between each iteration, in which the user is able to press any button they desire.

6.3 Using Different Data

DS-LISSOM's GUI currently does not explicitly allow for a user to select their own control and experimental data sets. It is possible to overwrite the files in a particular data set in order to achieve this goal. Image file names are specified by number in order of the time that they appear. If you want to use a video sequence it must be in AVI format.

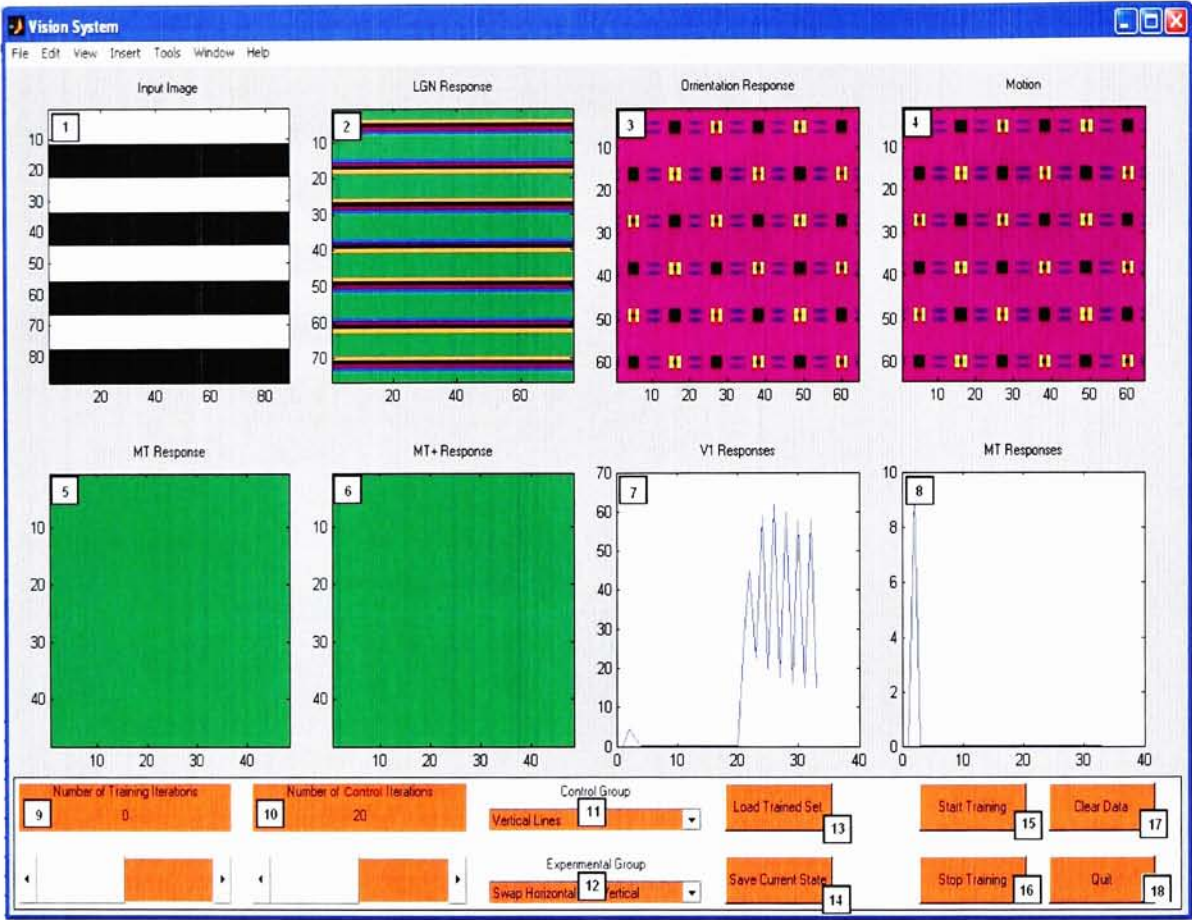


Figure 6.1: A screenshot of DS-LISSOM's graphical user interface

Chapter 7

Conclusion and Future Work

This thesis has investigated the possibility of creating a system whose components are based on biological equivalences. It has been shown that DS-LISSOM is biologically consistent not only in construction but function. Results have also shown that the way in which DS-LISSOM acquires information can be exploited to find inconsistencies within images. These results have been shown to work not only with the most simple of images but DS-LISSOM is also capable of finding inconsistencies within natural images.

Future work aims at both expanding upon the current system and using the system in a number of applications, as described in the following sections.

7.1 Modeling More of the Visual System

This thesis has developed a system that can describe the formation of specific cell structures within the visual system, and has focused on the V1 and MT layers. Even though DS-LISSOM has accomplished its goals, we still desire to produce a more extensive model of the visual system.

7.1.1 More about V1

Some research has shown that V1 is directionally selective, and work has begun on modeling this behavior (Bednar & Miikkulainen, 2003). Adding this behavior to V1 could potentially affect how well higher cortical areas are capable of learning the appropriate information. DS-LISSOM at the moment estimates this effect this has by only passing information to higher levels if some change in activation has occurred.

7.1.2 Modeling MT

MT is the first layer that is both selective of direction and velocity. This thesis has looked at the MT layer only in terms of its directional selectivity but future experiments should be performed to show that the MT layer, as implemented in DS-LISSOM, is selective of speed. There are a few questions that need to be considered when looking at speed. For example, DS-LISSOM uses discrete time steps that never change. It may be that such a simple approach is not adequate enough when looking at velocity. It may also be the case that using information from only four points in time is insufficient for learning velocity.

7.1.3 Modeling MST

Information passes through MT and into MST and a number of other smaller regions which do further motion processing. These areas can process more complex motions and also fuse information about overall motion (such as eye movements and optic flow) into the system. It would be a natural extension to attempt to model the MST area.

7.2 Finding Inconsistent Events

As implemented, DS-LISSOM only gives the user information about the amount change in weights. The next step in this direction is to actually label images that have been found to be inconsistent. Not only would it be useful to label the image, but it would also be useful to label the parts of the image which are thought to be inconsistent. This could be accomplished using the following:

1. Process an image or a series of images.
2. If an image is found to be inconsistent then do the following recursively.
 - Break the image at this time step and the two previous time steps into 4 regions.
 - Check for the relative amount of weight change in each region from one time step to the next.
 - Continue to recursively check those regions which are inconsistent until no one region is more inconsistent than the others. These 4 regions now make up the inconsistent part of the overall image.

Appendix A

Source Code

The following sections are the source of DS-LISSOM implemented in matlab.

A.1 Vision System

```
1
2
3 %Declare All Global Variables
4 global original_h;
5 global lgn_h;
6 global orrientation_h;
7 global color_h;
8
9 global training_pathname;
10 global detect_pathname;
11 global training_filename;
12 global detect_filename;
13
14
15 %Create and run the GUI interface
16 CreateGUI
```

A.2 GUI Creation

```
1 clear;
2
3 % This file will initialize and run our vision system from start to finish.
```

```
4 % This GUI will provide a user to train a system from scratch, view different
5 % outputs from the system, and will allow a previously trained network be loaded
6 % and run.
7 %
8 % For better efficiency it may be necessary for training to take place as a
9 % separate step. However, this GUI should make it easy for someone new to the
10 % system to get started.
11 %
12
13 %Declare All Global Variables
14
15 % GUI Variables
16 global Input_h;
17 global LGN_h;
18 global V1_h;
19 global difference_V1_h;
20 global MT_h;
21 global difference_MT_h;
22 global up_h;
23 global down_h;
24 global right_h;
25 global left_h;
26 global MTGraph_h;
27 global V1Graph_h;
28
29 % Files
30 global training_pathname;
31 global detect_pathname;
32 global training_filename;
33 global detect_filename;
34
35
36 % Image Sets
37 global controlSet;
38 global expSet;
39
40 % Used for movement through-out
41 global training;
42 global stopEverything;
43 global trainingIterations;
44 global controlIterations;
45 global saveFile;
46 global loadFile;
47 global startOver;
48 global start;
49
50
51 %
```

```

52 % Initialize needed variables
53 %
54
55 controlSet = 1;           % Set the default control set
56 expSet = 1;              % Set the default experimental set
57 training = 0;            % Don't train yet
58 stopEverything = 0;      % Set on quit
59 trainingIterations = 100; % How long to train
60 controlIterations = 100; % How long should the control image(s) be shown
61 saveFile = 0;           % Save the file now
62 loadFile = 0;           % Load a saved file
63 startOver = 1;          % Clear everything
64 start = 0;              % Begin initializing and
65                          % load any data if needed
66
67
68 training_pathname = '';   % Default path is where the program is
69                          % started.
70 training_filename = 'training.mat'; % The save name will be training.mat
71                          % followed by the iteration number
72
73
74
75 %Create a Figure
76 figpos=[70 00 1100 700];
77 fig = figure('Name','Vision System','NumberTitle','off', ...
78             'Pos',figpos,'Units','pixels');
79
80
81 %Create a frame for any options we may have!
82 uicontrol('Style','frame','Pos',[5 5 figpos(3)-10 110]);
83
84
85 %*****
86 %
87 % Create and display the axes for each of the displayed results
88 %
89 %*****
90
91 %Create Axes for the original image
92 uicontrol('Style','text','String','Input Image', 'Pos', [40 670 225 20], ...
93           'BackgroundColor', get( fig, 'color' ) );
94 Input_h = axes('Units','pixels','Pos',[40 440 225 225],'Box','off', ...
95              'Tag','Original_image');
96
97
98 %Create Axes for the LGN Response
99 uicontrol('Style','text','String','LGN Response', ...

```

```

100         'Pos', [305 670 225 20], ...
101         'BackgroundColor', get( fig, 'color' ) );
102     LGN_h = axes('Units','pixels','Pos',[305 440 225 225],'Box','off', ...
103             'Tag','LGN_Response');
104
105
106     %Create Axes for the Orientation Response
107     uicontrol('Style','text','String','Orientation Response', ...
108             'Pos', [570 670 225 20], ...
109             'BackgroundColor', get( fig, 'color' ) );
110     V1_h = axes('Units','pixels','Pos',[570 440 225 225],'Box','off', ...
111             'Tag','Orientation_Response');
112
113
114     %Create Axes for the Orientation Response
115     uicontrol('Style','text','String','Motion', 'Pos', [835 670 225 20], ...
116             'BackgroundColor', get( fig, 'color' ) );
117     difference_V1_h = axes('Units','pixels','Pos',[835 440 225 225], ...
118             'Box','off', ...
119             'Tag','Orientation_Response');
120
121
122     %Create Axes for the Color Response
123     uicontrol('Style','text','String','MT Response', 'Pos', [40 370 225 20], ...
124             'BackgroundColor', get( fig, 'color' ) );
125     MT_h = axes('Units','pixels','Pos',[40 140 225 225],'Box','off', ...
126             'Tag','Color_Response');
127
128
129     %Create Axes for the Color Response
130     uicontrol('Style','text','String','MT+ Response', ...
131             'Pos', [305 370 225 20], ...
132             'BackgroundColor', get( fig, 'color' ) );
133     difference_MT_h = axes('Units','pixels','Pos',[305 140 225 225], ...
134             'Box','off', ...
135             'Tag','Color_Response');
136
137
138     %Create Axes for the Color Response
139     uicontrol('Style','text','String','V1 Responses', ...
140             'Pos', [570 370 225 20], ...
141             'BackgroundColor', get( fig, 'color' ) );
142     V1Graph_h = axes('Units','pixels','Pos',[570 140 225 225],'Box','off', ...
143             'Tag','Color_Response');
144
145
146     %Create Axes for the Color Response
147     uicontrol('Style','text','String','MT Responses', ...

```



```

148         'Pos', [835 370 225 20], ...
149         'BackgroundColor', get( fig, 'color' ) );
150 MTGraph_h = axes('Units','pixels','Pos',[835 140 225 225],'Box','off', ...
151         'Tag','Color_Response');
152
153
154 %
155 % Set the colormap. For the system's images the best is rainbow. For
156 % input images the best would be gray. I have not figured out how
157 % to use multiple colormaps in a single figure.
158 %
159 colormap( 'rainbow' );
160 %colormap( HSV );
161
162 %*****
163 %
164 % Create Buttons, Lists etc. for human interaction
165 %
166 %*****
167
168 %Create Buttons for User Interaction
169 uicontrol('Style','push','String','Quit', ...
170         'Pos',[970 10 100 40],'Callback',[' training = 0;','...
171         ' stopEverything = 1;','...
172         ' pause(5);','...
173         ' close(gcf);'], ...
174         'BackgroundColor',[1 0.5 0],'ForegroundColor',[0 0 0]);
175
176 uicontrol('Style','push','String','Clear Data', ...
177         'Pos',[970 70 100 40],'Callback','startOver = 1;',' ...
178         'BackgroundColor',[1 0.5 0],'ForegroundColor',[0 0 0]);
179
180 uicontrol('Style','push','String','Start Training', ...
181         'Pos',[850 70 100 40],'Callback','training = 1; start = 1;',' ...
182         'BackgroundColor',[1 0.5 0],'ForegroundColor',[0 0 0]);
183
184 uicontrol('Style','push','String','Stop Training', ...
185         'Pos',[850 10 100 40],'Callback','training = 0; start = 1;',' ...
186         'BackgroundColor',[1 0.5 0],'ForegroundColor',[0 0 0]);
187
188
189 %This is the slider for setting the training iterations
190 slider.l = uicontrol('Style','text','Pos',[10 90 200 20], ...
191         'String','Number of Training Iterations', ...
192         'BackgroundColor',[1 0.5 0],'ForegroundColor',[0 0 0]);
193
194 slider.n = uicontrol('Style','text','Pos',[10 70 200 20], ...
195         'String',num2str(trainingIterations),...

```

```

196         'BackgroundColor',[1 0.5 0], 'Foreground',[0 0 0]);
197
198     slider.s = uicontrol('Style','slider','Pos',[10 10 200 40], 'Min',0,...
199         'Max',10000, 'Value',trainingIterations,...
200         'SliderStep',[.01 1], 'BackgroundColor',[1 0.5 0],...
201         'Foreground', [0 0 0],...
202         'CallBack', ['trainingIterations=get(slider.s, 'value');', ...
203             'set(slider.n, 'String'', trainingIterations);'] );
204
205
206
207     %This is the slider for setting the control iterations
208     slider2.l = uicontrol('Style','text','Pos',[230 90 200 20], ...
209         'String','Number of Training Iterations', ...
210         'BackgroundColor',[1 0.5 0], 'Foreground',[0 0 0]);
211
212     slider2.n = uicontrol('Style','text','Pos',[230 70 200 20], ...
213         'String',num2str(trainingIterations),...
214         'BackgroundColor',[1 0.5 0], 'Foreground',[0 0 0]);
215
216     slider2.s = uicontrol('Style','slider','Pos',[230 10 200 40], 'Min',0,...
217         'Max',10000, 'Value',trainingIterations,...
218         'SliderStep',[.01 1], 'BackgroundColor',[1 0.5 0],...
219         'Foreground', [0 0 0],...
220         'CallBack', ['controlIterations=get(slider2.s, 'value');', ...
221             'set(slider2.n, 'String'', controlIterations);'] );
222
223
224
225     %Allow a user to select what images to train on postnatally and
226     %what environment to subsequently place DS-LISSOM into
227
228     control.l = uicontrol('Style','text','Pos',[450 90 200 20], ...
229         'String','Control Group' );
230     control.p = uicontrol('Style','popupmenu','String',...
231         ['Box moving left to right|',...
232         'Box moving right to left|',...
233         'Cars|',...
234         'Bus|',...
235         'Horizontal Lines|',...
236         'Vertical Lines|',...
237         'Circle'],...
238         'CallBack', ['controlSet=get(control.p, 'value');'], ...
239         'Pos',[450 70 200 20], ...
240         'BackgroundColor',[1 0.5 0], 'Foreground',[0 0 0]);
241
242     exp.l = uicontrol('Style','text','Pos',[450 30 200 20], ...
243         'String','Experimental Group' );

```

```

244     exp.p = uicontrol('Style','popupmenu','String',...
245                     ['Box moving left to right|',...
246                     'Box moving right to left|',...
247                     'Cars|',...
248                     'Bus|',...
249                     'Horizontal Lines|',...
250                     'Vertical Lines|',...
251                     'Swap Horizontal and Vertical'],...
252                     'Callback', ['expSet=get(exp.p, 'value');'], ...
253                     'Pos',[450 10 200 20], ...
254                     'BackgroundColor',[1 0.5 0], 'ForegroundColor',[0 0 0]);
255
256
257     uicontrol('Style','push','String','Load Trained Set', ...
258             'Pos',[670 70 100 40], ...
259             'Callback',['[pathname,filename] = LoadData, ', ...
260             ' copyfile( strcat(pathname,filename), ',...
261             ' strcat(training_pathname,training_filename) );', ...
262             ' start = 0; loadFile = 1; startOver = 1;'], ...
263             'BackgroundColor',[1 0.5 0], 'ForegroundColor',[0 0 0]);
264
265     uicontrol('Style','push','String','Save Current State', ...
266             'Pos',[670 10 100 40], ...
267             'Callback', ['[pathname,filename] = SaveData, saveFile = 1'], ...
268             'BackgroundColor',[1 0.5 0], 'ForegroundColor',[0 0 0]);
269
270
271     %
272     % Start DS-LISSOM. I don't know how to spawn a seperate thread so this
273     % will run in an infinite loop and callbacks will set global variables
274     % that can change the execution path.
275     %
276     StartTraining( start, training_pathname, training_filename );

```

A.3 DS-LISSOM

```

1  %
2  % This is the main program. It consists of a number of large loops that
3  % will look at variables set by the gui to determine how it should run.
4  % This follows the system described in my thesis.
5  %
6
7  function StartTraining( first_time, pathname, filename )
8
9      % GUI Variables

```

```

10     global Input_h;
11     global LGN_h;
12     global V1_h;
13     global difference_V1_h;
14     global MT_h;
15     global difference_MT_h;
16     global up_h;
17     global down_h;
18     global right_h;
19     global left_h;
20     global MTGraph_h;
21     global V1Graph_h;
22
23     % Files
24     global training_pathname;
25     global training_filename;
26
27     % Image Sets
28     global controlSet;
29     global expSet;
30
31     % Used for movement through-out
32     global training;
33     global stopEverything;
34     global trainingIterations;
35     global controllIterations;
36     global saveFile;
37     global loadFile;
38     global startOver;
39     global start;
40
41
42     %
43     % Continue as long as the EXIT button has not been pressed. This is
44     % caught by watching the stopEverything variable.
45     %
46
47     while( stopEverything == 0 )
48
49         % If start is false then pause for 2 seconds and go back to the
50         % top of the while loop.
51         if( start == 0 )
52             pause(2);
53             continue;
54         end;
55
56         %
57

```

```

58      % Start the system
59      %
60
61      disp( 'Starting DS-LISSOM' )
62
63
64
65      %*****
66      % Initialize Data - Only if we are starting over
67      %
68
69      if( startOver == 1 )
70
71          %
72          % Start from scratch unless a file to start from was loaded
73          %
74
75          if( loadFile == 0 )
76              MT_NOT_SET = true;
77              this_rounds_image = 1;
78
79              % The following must be uncommented to make use of an USB camera
80              % vcapg2;
81
82
83              % All of this is taken from the appendix and from
84              % chapter 4 and 5 of Bednars PhD Thesis. He references a
85              % number of other papers that describe a large set of tests
86              % that were performed to determine the optimal values and
87              % describes how to scale these values.
88              %
89              % Basically, if something is a "subscript", it's marked with
90              % an underscore. For example,  $r_{A}$  for the afferent
91              % radius is marked by  $r_A$ . However, be aware that SOME
92              % VALUES DO INDEED CHANGE IN THE COURSE OF DS-LISSOM
93              % especially the gamma values and the  $r_A$  from receptors to LGN.
94
95              s_a = 2;                                % Scaling factor
96              r_A_o = 6.5;                             % Original radius
97              r_A = 6.5;                               % radius V1
98              r_MT = 8.5;                             % MINE: radius MT
99              r_E_o = 19/2;                          % radius E weights
100             r_I_o = 47/2;                          % radius I weights
101             MT_d = s_a * 24;                        % MINE: Size of MT
102             N_d = s_a * 24;                        % Bednars V1 size
103             N_d = MT_d + 2 * ( r_MT - 0.5 );        % MINE: Size of V1
104             LGN_d = N_d + 2 * ( r_A_o - 0.5 );      % Size of LGN
105             R_d = LGN_d + 2 * ( r_A - 0.5 );        %

```



```

106         r_E_i = floor( N_d / 10 ) + 0.5;    % radius E weights start
107         r_E_f = floor( max( 1.5, N_d/44 ) ) + 0.5; % E weights finish
108         r_E = r_E_i;                          % set E weights radius
109         r_I = floor( N_d / 10 ) + 0.5;        % set I weights radius
110         s_w = (r_A_o + 0.5)/r_A;              % scale weight radius
111         A = 7.5 / s_w;                        % Size of DoG
112         B = 1.5 / s_w;                        % Size of DoG
113
114         %
115         % Sigma and Gamma values for each set of weights
116         %
117         sigma_c = 0.5 / s_w;
118         sigma_s = 4 * sigma_c;
119         sigma_A = r_A / 1.3;
120         sigma_E = 0.78 * r_E;
121         sigma_I = 2.08 * r_I;
122         gamma_A = 1;
123         gamma_E = 0.9;
124         gamma_I = 0.9;
125         gamma_E_MT = 0.9;
126         gamma_I_MT = 0.9;
127         gamma_N = 0;
128         gamma_A_MT = gamma_A;
129         gamma_N_MT = gamma_N;
130
131         %
132         % Scaling factors
133         %
134         s_d = 1;
135         s_t = 1 / s_d;
136         n_A = 1;
137
138         %
139         % Learning rates
140         %
141         alpha_A_i = 0.0070 / ( n_A * s_t * s_d );
142         alpha_E = (0.002 * r_E_o^2) / ( s_t * s_d * r_E^2 );
143         alpha_I = (0.00025 * r_I_o^2) / ( s_t * s_d * r_I^2 );
144
145
146
147         %%%%%%%%%%%%%%%%%%%%%%%%%%%%%%%%%%%%%%%%%%%%%%%%%%%%%%%%%%%%%%%%%%%%%%%%%%%
148         % The weights. Basically in the format weight( from, to ).
149         % The initial weights are RANDOMIZED for afferent radii from
150         % LGN to V1. All other weights are done by GAUSSIAN.
151         %%%%%%%%%%%%%%%%%%%%%%%%%%%%%%%%%%%%%%%%%%%%%%%%%%%%%%%%%%%%%%%%%%%%%%%%%%%
152
153         % Weights from retina to LGN    ie: LGN's afferent weight

```

```

154 % mu_aff_LGN_OFF is simply a negative of mu_aff_LGN_ON.
155 mu_aff_LGN = zeros( r_A*2, r_A*2, LGN_d*LGN_d );
156
157 % Weights from LGN to V1. There are 2 channels: on and off
158 % which Bednar was able to show makes a difference
159 mu_aff_ON_V1 = rand( r_A_o*2, r_A_o*2, N_d*N_d );
160 mu_aff_OFF_V1 = rand( r_A_o*2, r_A_o*2, N_d*N_d );
161
162 % Weights from V1 to MT. Temporal effect start taking place
163 % here so I keep 4 "frames" of information alive at a time
164 mu_aff_1_MT = rand( r_MT*2, r_MT*2, MT_d*MT_d );
165 mu_aff_2_MT = rand( r_MT*2, r_MT*2, MT_d*MT_d );
166 mu_aff_3_MT = rand( r_MT*2, r_MT*2, MT_d*MT_d );
167 mu_aff_4_MT = rand( r_MT*2, r_MT*2, MT_d*MT_d );
168
169
170 % These are the weights for Face Processesing which
171 % I am not going to do
172 % mu_aff_FSA = rand( N*N, r_A*2, r_A*2 );
173
174
175 % Excitatory/Inhibitory lateral connections
176 % in V1
177 E_V1 = zeros( N_d*N_d, r_E*2, r_E*2 );
178 I_V1 = zeros( N_d*N_d, r_I*2, r_I*2 );
179
180
181 % Excitatory/Inhibitory lateral connections in MT
182 E_MT = zeros( MT_d*MT_d, r_E*2, r_E*2 );
183 I_MT = zeros( MT_d*MT_d, r_I*2, r_I*2 );
184
185
186 % Excitatory/Inhibitory lateral connections
187 % in Face Processing. They are only here to
188 % be complete in terms of Bednars model
189 %E_FSA = zeros( N*N, r_E, r_E );
190 %I_FSA = zeros( N*N, r_I, r_I );
191
192
193 % Binary circle masks. It may be possible to get better results
194 % if the receptive fields are circular.
195 V1_circle = draw_circle( r_A_o );
196 for ( x=1:(N_d^2) )
197     mu_aff_ON_V1( :, :, x ) = mu_aff_ON_V1(:, :, x) .* V1_circle;
198     mu_aff_OFF_V1( :, :, x ) = mu_aff_OFF_V1(:, :, x) .* V1_circle;
199 end;
200 clear x;
201 LGN_circle = draw_circle( r_A );

```

```

202
203 MT_circle = draw_circle( r_MT );
204 for ( x=1:(MT_d^2) )
205     mu_aff_1_MT( :, :, x ) = mu_aff_1_MT(:, :, x) .* MT_circle;
206     mu_aff_2_MT( :, :, x ) = mu_aff_2_MT(:, :, x) .* MT_circle;
207     mu_aff_3_MT( :, :, x ) = mu_aff_3_MT(:, :, x) .* MT_circle;
208     mu_aff_4_MT( :, :, x ) = mu_aff_4_MT(:, :, x) * MT_circle;
209 end;
210
211
212 %
213 % Initialize FIXED weights for LGN connections.
214 %
215 % num = the receptive field that it being looked at
216 %
217
218 a = 1;
219 b = 1;
220
221 sum_cent = 0;
222 sum_surr = 0;
223 num = ( (a-1)*LGN_d + b );
224
225 startx = a - ( r_A - 0.5 );
226 endx   = a + ( r_A - 0.5 );
227 starty = b - ( r_A - 0.5 );
228 endy   = b + ( r_A - 0.5 );
229
230 %
231 % Get totals for normalization. I can't think of a better
232 % way to do this and Matlab 6.5 seems to vectorize loops
233 % pretty well.
234 %
235     for ( x=startx:endx )
236         for ( y=starty:endy )
237             if ( LGN_circle( x-startx+1, y-starty+1 ) )
238                 sum_cent = sum_cent + normgaus( a,x,b,y, sigma_c );
239                 sum_surr = sum_surr + normgaus( a,x,b,y, sigma_s );
240             end;
241         end;
242     end;
243
244 %
245 % since the afferent weights for on/off are just opposites we
246 % can get away with just computing one. Later we will
247 % multiply this by negative one.
248 %
249 % temp_cent determines the width of the central Gaussian

```

```

250 % temp_surr determines the width of the surround Gaussian
251 %
252 % I believe there was an error in Bednars work here - the
253 % top equations top equations should be added
254 % ie: (x-x_o)^2 + (y-y_o)^2 not (x-x_o)^2 - (y-y_o)^2
255 %
256         for ( x=startx:endx )
257     for ( y=starty:endy )
258         if ( LGN_circle( x-startx+1, y-starty+1 ) )
259             temp_cent = normgaus( a,x,b,y, sigma_c ) / sum_cent;
260             temp_surr = normgaus( a,x,b,y, sigma_s ) / sum_surr;
261             mu_aff_LGN( x-startx+1, y-starty+1, num ) = ...
262                 temp_cent - temp_surr;
263         end;
264     end;
265     end;
266
267     for ( x = 1:(LGN_d*LGN_d) )
268 mu_aff_LGN( :, :, x ) = mu_aff_LGN( :, :, 1 );
269     end;
270
271     clear sum_cent sum_surr temp_cent temp_surr a b x y ...
272     tenth num startx endx starty endy;
273     disp( 'done - LGN Fixed weights are now initialized' );
274
275     tenth = round( N_d^2/10 );
276
277     E_circle = draw_circle(r_E);
278     I_circle = draw_circle(r_I);
279
280
281
282 % Initialize Gaussian starting weights for the
283 % excitatory/inhibitory lateral connections.
284
285     a = 1;
286     b = 1;
287
288     sum_E = 0;
289     sum_I = 0;
290     num = ( (a-1)*N_d + b );
291
292     startx = a - ( r_E - 0.5 );
293     endx    = a + ( r_E - 0.5 );
294     starty = b - ( r_E - 0.5 );
295     endy    = b + ( r_E - 0.5 );
296
297     for ( x=startx:endx )

```

```

298         for ( y=starty:end )
299             if ( E_circle(x-startx+1,y-starty+1 ) )
300                 sum_E = sum_E + normgaus( x, a, y, b, sigma_E );
301             end;
302         end;
303     end;
304
305     for ( x=startx:endx )
306         for ( y=starty:end )
307             if ( E_circle(x-startx+1,y-starty+1 ) )
308                 E_V1( num, x-startx+1, y-starty+1 ) = ...
309                     normgaus( x, a, y, b, sigma_E ) / sum_E;
310             end;
311         end;
312     end;
313
314     for ( x=1:(N_d*N_d) )
315         E_V1(x, :, :) = E_V1(1, :, :);
316     end;
317
318     startx = a - ( r_I - 0.5 );
319     endx   = a + ( r_I - 0.5 );
320     starty = b - ( r_I - 0.5 );
321     endy   = b + ( r_I - 0.5 );
322
323     for ( x=startx:endx )
324         for ( y=starty:end )
325             if ( I_circle(x-startx+1,y-starty+1 ) )
326                 sum_I = sum_I + normgaus( x, a, y, b, sigma_I );
327             end;
328         end;
329     end;
330
331     for ( x=startx:endx )
332         for ( y=starty:end )
333             if ( I_circle(x-startx+1,y-starty+1 ) )
334                 I_V1( num, x-startx+1, y-starty+1 ) = ...
335                     normgaus( x, a, y, b, sigma_I ) / sum_I;
336             end;
337         end;
338     end;
339
340     for ( x=1:(N_d*N_d) )
341         I_V1(x, :, :) = I_V1(1, :, :);
342     end;
343
344
345

```



```

346 %
347 % MT E/I weights
348 a = 1;
349 b = 1;
350
351 sum_E = 0;
352 sum_I = 0;
353 num = ( (a-1)*MT_d + b );
354
355 startx = a - ( r_E - 0.5 );
356 endx   = a + ( r_E - 0.5 );
357 starty = b - ( r_E - 0.5 );
358 endy   = b + ( r_E - 0.5 );
359
360 for ( x=startx:endx )
361     for ( y=starty:endy )
362         if ( E_circle(x-startx+1,y-starty+1 ) )
363             sum_E = sum_E + normgaus( x, a, y, b, sigma_E ); ;
364         end;
365     end;
366 end;
367
368 for ( x=startx:endx )
369     for ( y=starty:endy )
370         if ( E_circle(x-startx+1,y-starty+1 ) )
371             E_MT( num, x-startx+1, y-starty+1 ) =
372                 normgaus( x, a, y, b, sigma_E ) / sum_E;
373         end;
374     end;
375 end;
376
377 for ( x=1:(MT_d*MT_d) )
378     E_MT(x, :, :) = E_MT(1, :, :);
379 end;
380
381 startx = a - ( r_I - 0.5 );
382 endx   = a + ( r_I - 0.5 );
383 starty = b - ( r_I - 0.5 );
384 endy   = b + ( r_I - 0.5 );
385
386 for ( x=startx:endx )
387     for ( y=starty:endy )
388         if ( I_circle(x-startx+1,y-starty+1 ) )
389             sum_I = sum_I + normgaus( x, a, y, b, sigma_I );
390         end;
391     end;
392 end;
393

```

```

394     for ( x=startx:endx )
395         for ( y=starty:end )
396             if ( I_circle(x-startx+1,y-starty+1) )
397                 I_MT( num, x-startx+1, y-starty+1 ) =
398                     normgaus( x, a, y, b, sigma_I ) / sum_I;
399             end;
400         end;
401     end;
402
403     for ( x=1:(MT_d*MT_d) )
404         I_MT(x, :, :) = I_MT(1, :, :);
405     end;
406
407
408
409
410
411     %
412     % Again, I am not going to perform face processing so ignore
413     % these connections
414     %E_FSA = E_V1;
415     %I_FSA = I_V1;
416
417     clear sum_I sum_E a b x y tenth num startx endx starty endy;
418     disp( 'Done Initializing' );
419
420
421     %Statistical variables
422     testerV1 = zeros( N_d, N_d, 1 );
423     testerMT = zeros( N_d, N_d, 1 );
424     sum_V1 = 0;
425     sum_MT = 0;
426
427
428     %
429     %
430     % Train Once
431     %
432     %
433
434
435     % Taken from appendix of Bednar's thesis
436     % gamma_N works well if you set it to 0 for gaussian (training)
437     % ellipses (which have only one "1" in the center of each
438     % ellipsoid) it works well--but if you have a binary image
439     % (e.g., solid line) then gamma_N=1 works well.
440
441     delta_i = 0.1;

```

```

442         beta_i = delta_i + 0.55;
443         beta = beta_i;
444         delta = delta_i;
445         alpha_A = alpha_A_i;
446         alpha_E_i = alpha_E;
447         t_si = 9;
448         t_s = t_si;
449         gamma_N = 0.0;
450         t = 1;
451
452
453     else
454
455         %
456         % We were asked to load a file instead.
457         %
458         load(strcat(training_pathname, training_filename));
459         loadFile = 0;
460         disp( 'File Loaded' )
461
462     end;
463     pack;
464     startOver = 0;
465
466 end;
467 %
468 % End Initialization
469 %*****
470
471
472
473
474
475 %*****
476 % Start running training loops
477 %
478
479 % Do for t training iterations... ( 10000-20000 ideally )
480 while ( training == 1 )
481
482     % This allows for the user to press a button. In general these
483     % computations take a very long time so responses from the user
484     % seem to be difficult to get. I am not aware of a better way of
485     % doing this however.
486     pause( 5 );
487     if( training == 0 )
488         continue;
489     end;

```

```

490
491
492     %increment gamma_N
493     gamma_N = t / 10000;
494     if ( gamma_N > 1 )
495         gamma_N = 1;
496     end;
497
498
499
500     % initialize receptor, LGN reactions to zero.
501     xi_REC = zeros( R_d );
502     eta_LGN_ON = zeros( LGN_d );
503     eta_LGN_OFF = zeros( LGN_d );
504
505     if ( mod( t, 5 ) == 0 )
506         disp( [ num2str( t ), ' reached' ] );
507     end;
508
509
510     % Update parameters if necessary (again, taken from the appendix).
511     switch ( t )
512     case 0
513         r_E = max( r_E_f, r_E_i );
514         delta = delta_i;
515         beta = beta_i;
516         alpha_A = alpha_A_i;
517         r_E = floor( r_E ) + 0.5;
518         E_circle = draw_circle( r_E );
519     case 200
520         r_E = max( r_E_f, 0.6 * r_E_i );
521         delta = delta_i + 0.01;
522         beta = beta_i + 0.01;
523         r_E = floor( r_E ) + 0.5;
524         E_circle = draw_circle( r_E );
525     case 500
526         r_E = max( r_E_f, 0.42 * r_E_i );
527         delta = delta_i + 0.02;
528         beta = beta_i + 0.02;
529         alpha_A = 50/70 * alpha_A_i;
530         alpha_E = 0.5 * alpha_E_i;
531         r_E = floor( r_E ) + 0.5;
532         E_circle = draw_circle( r_E );
533     case 1000
534         r_E = max( r_E_f, 0.336*r_E_i );
535         delta = delta_i + 0.05;
536         beta = beta_i + 0.02;
537         r_E = floor( r_E ) + 0.5;

```

```

548         E_circle = draw_circle( r_E );
539     case 2000
540         r_E = max( r_E_f, 0.269*r_E_i );
541         delta = delta_i + 0.08;
542         beta = beta_i + 0.05;
543         t_s = t_s + 1;
544         r_E = floor( r_E ) + 0.5;
545         alpha_A = 40/70 * alpha_A_i;
546         E_circle = draw_circle( r_E );
547     case 3000
548         r_E = max( r_E_f, 0.215*r_E_i );
549         delta = delta_i + 0.10;
550         beta = beta_i + 0.08;
551         r_E = floor( r_E ) + 0.5;
552         E_circle = draw_circle( r_E );
553     case 4000
554         r_E = max( r_E_f, 0.129*r_E_i );
555         delta = delta_i + 0.10;
556         beta = beta_i + 0.11;
557         r_E = floor( r_E ) + 0.5;
558         alpha_A = alpha_A_i * 30/70;
559         E_circle = draw_circle( r_E );
560     case 5000
561         r_E = max( r_E_f, 0.077*r_E_i );
562         delta = delta_i + 0.11;
563         beta = beta_i + 0.14;
564         t_s = t_s + 1;
565         r_E = floor( r_E ) + 0.5;
566         E_circle = draw_circle( r_E );
567     case 6500
568         r_E = max( r_E_f, 0.046*r_E_i );
569         delta = delta_i + 0.12;
570         beta = beta_i + 0.17;
571         t_s = t_s + 1;
572         r_E = floor( r_E ) + 0.5;
573         E_circle = draw_circle( r_E );
574     case 8000
575         r_E = max( r_E_f, 0.028*r_E_i );
576         delta = delta_i + 0.13;
577         beta = beta_i + 0.20;
578         r_E = floor( r_E ) + 0.5;
579         E_circle = draw_circle( r_E );
580     end;
581
582
583     % If necessary, trim V1-r_E afferent weights.
584     old_r_E = (sum( size( E_V1( 1, 1, : ) ) ) - 2) / 2;
585     while ( old_r_E > r_E )

```



```

586         E_V1 = E_V1( :, 2:2*old_r_E-1, 2:2*old_r_E-1 );
587         old_r_E = (sum( size( E_V1( 1, 1, : ) ) )-2) / 2;
588     end;
589
590     clear old_r_E;
591
592
593     %
594     % For the first 100 iterations the system needs to be pretrained.
595     % Therefore we create random ellipsoids and feed these into the
596     % system.
597     %
598
599     if( t < trainingIterations )
600         % Create ellipsoids ( activation for LGN ).
601         for ( i = 1:4 )
602             x_o = round( rand(1) * N_d + r_A_o );
603             y_o = round( rand(1) * N_d + r_A_o );
604             %theta = deg2rad( rand(1) * 180 );
605             theta = rand(1) * pi;
606             for ( x = 1:R_d )
607                 for ( y = 1:R_d )
608                     temp = -1 * (((x-x_o) * cos(theta) - (y-y_o) * ...
609                                 sin(theta))^2 / A^2);
610                     temp = temp - (((x-x_o) * sin(theta) + ...
611                                 (y-y_o) * cos(theta))^2 / B^2);
612                     temp = exp( temp );
613                     xi_REC( x, y ) = xi_REC( x, y ) + temp;
614                 end;
615             end;
616         end;
617         clear x_o y_o theta x y i temp;
618     else
619         if( t < (controlIterations + trainingIterations) )
620
621             if( controlSet == 1 )
622                 xi_REC = imresize( double( imread( ...
623                                     strcat( 'images/images1/', ...
624                                     num2str( this_rounds_image ), ...
625                                     '.bmp' ) ) ) / 255, [R_d R_d] );
626                 this_rounds_image = this_rounds_image + 1;
627                 if( this_rounds_image > 18 )
628                     this_rounds_image = 1;
629                 end
630             elseif( controlSet == 2 )
631                 xi_REC = imresize( double( imread( strcat( ...
632                                     'images/images1/', num2str( ...
633                                     this_rounds_image ), '.bmp' ) ) ) ...

```

```

634         / 255, [R_d R_d] );
635     this_rounds_image = this_rounds_image + 1;
636     if( this_rounds_image < 0 )
637         this_rounds_image = 18;
638     end
639 elseif( controlSet == 3 )
640     mov = aviread( 'images/newShortCars.AVI', 74 + ...
641                 this_rounds_image );
642     whole_image = zeros( R_d, R_d, size( mov, 2 ) );
643
644     for( i=1:size( mov, 2 ) )
645         whole_image(:,:,i) = rgb2gray( imresize( ...
646             mov( 1, i ).cdata, [R_d R_d] ) );
647     end;
648     whole_image = whole_image ./ 255;
649     xi_REC = whole_image( :, :, 1 );
650
651     this_rounds_image = this_rounds_image + 1;
652     if( this_rounds_image > 100 )
653         this_round_image = 1;
654     end;
655 elseif( controlSet == 4 )
656     mov = aviread( 'images/newShortCars.AVI', 174 + ...
657                 this_rounds_image );
658     whole_image = zeros( R_d, R_d, size( mov, 2 ) );
659
660     for( i=1:size( mov, 2 ) )
661         whole_image(:,:,i) = rgb2gray( imresize( ...
662             mov( 1, i ).cdata, [R_d R_d] ) );
663     end;
664     whole_image = whole_image ./ 255;
665     xi_REC = whole_image( :, :, 1 );
666
667     this_rounds_image = this_rounds_image + 1;
668     if( this_rounds_image > 100 )
669         this_round_image = 1;
670     end;
671 elseif( controlSet == 5 )
672     xi_REC = imresize( double( imread( ...
673         'images/horizontal.bmp' ) ) / 255, [R_d R_d] );
674 elseif( controlSet == 6 )
675     xi_REC = imresize( double( imread( ...
676         'images/vertical.bmp' ) ) / 255, [R_d R_d] );
677 elseif( controlSet == 7 )
678     xi_REC = imresize( double( imread( 'images/circle.bmp' ) ) / 255, [R_d R_d] );
679 else
680     xi_REC = imresize( double( imread( strcat( ...
681         'images/images', num2str( controlSet ), ...

```

```

682         '/', num2str( this_rounds_image ) , ...
683         '.bmp' ) ) ) / 255, [R_d R_d] );
684     this_rounds_image = this_rounds_image + 1;
685     if( this_rounds_image > 18 )
686         this_rounds_image = 1;
687     end
688 end
689
690 else
691
692     if( t == ( controlIterations + trainingIterations ) )
693         this_rounds_image = 1;
694     end;
695
696     if( expSet == 1 )
697         xi_REC = imresize( double( imread( strcat( ...
698             'images/images1/', num2str( ...
699             this_rounds_image ) , '.bmp' ) ) ) / ...
700             255, [R_d R_d] );
701         this_rounds_image = this_rounds_image + 1;
702         if( this_rounds_image > 18 )
703             this_rounds_image = 1;
704         end
705     elseif( expSet == 2 )
706         xi_REC = imresize( double( imread( strcat( ...
707             'images/images1/', num2str( ...
708             this_rounds_image ) , '.bmp' ) ) ) / ...
709             255, [R_d R_d] );
710         this_rounds_image = this_rounds_image + 1;
711         if( this_rounds_image < 0 )
712             this_rounds_image = 18;
713         end
714     elseif( expSet == 3 )
715         mov = aviread( 'images/newShortCars.AVI', 74 + ...
716             this_rounds_image );
717         whole_image = zeros( R_d, R_d, size( mov, 2 ) );
718
719         for( i=1:size( mov, 2 ) )
720             whole_image(:, :, i) = rgb2gray( imresize( ...
721                 mov( 1, i ).cdata, [R_d R_d] ) );
722         end;
723         whole_image = whole_image ./ 255;
724         xi_REC = whole_image( :, :, 1 );
725
726         this_rounds_image = this_rounds_image + 1;
727         if( this_rounds_image > 100 )
728             this_round_image = 1;
729     end;

```

```

730         elseif( expSet == 4 )
731             mov = aviread( 'images/newShortCars.AVI', 174 + ...
732                             this_rounds_image );
733             whole_image = zeros( R_d, R_d, size( mov, 2 ) );
734
735             for( i=1:size( mov, 2 ) )
736                 whole_image(:,:,i) = rgb2gray( imresize( ...
737                     mov( 1, i ).cdata, [R_d R_d] ) );
738             end;
739             whole_image = whole_image ./ 255;
740             xi_REC = whole_image( :, :, 1 );
741
742             this_rounds_image = this_rounds_image + 1;
743             if( this_rounds_image > 100 )
744                 this_round_image = 1;
745             end;
746         elseif( expSet == 5 )
747             xi_REC = imresize( double( imread( ...
748                 'images/horizontal.bmp' ) ) / 255, [R_d R_d] );
749         elseif( expSet == 6 )
750             xi_REC = imresize( double( imread( ...
751                 'images/vertical.bmp' ) ) / 255, [R_d R_d] );
752         elseif( expSet == 7 )
753             if( mod( this_rounds_image, 2 ) == 0 )
754                 xi_REC = imresize( double( imread( ...
755                     'images/vertical.bmp' ) ) / 255, [R_d R_d] );
756             else
757                 xi_REC = imresize( double( imread( ...
758                     'images/horizontal.bmp' ) ) / 255, [R_d R_d] );
759             end;
760             this_rounds_image = this_rounds_image + 1;
761         else
762             xi_REC = imresize( double( imread( strcat( ...
763                 'images/images', num2str( expSet ), '/', ...
764                 num2str( this_rounds_image ), '.bmp' ...
765                 ) ) ) / 255, [R_d R_d] );
766             this_rounds_image = this_rounds_image + 1;
767             if( this_rounds_image > 18 )
768                 this_rounds_image = 1;
769             end;
770         end;
771     end;
772 end;
773
774
775
776 % Debug purposes only.
777 % xi_REC = image;

```

```

778
779 % Threshold to 1 or below.
780 xi_REC = (xi_REC > 1) + ((xi_REC <= 1) .* xi_REC);
781
782
783
784 % start calculating xi and eta for LGN
785 xi_LGN_ON = zeros( LGN_d );
786 xi_LGN_OFF = zeros( LGN_d );
787
788 for ( a = 1:LGN_d )
789     for ( b = 1:LGN_d )
790
791         num = (a-1)*LGN_d+b;
792         startx = a;
793         endx = a + ( r_A - 0.5 )*2;
794         starty = b;
795         endy = b + ( r_A - 0.5 )*2;
796
797
798         for ( x = startx:endx )
799             for ( y = starty:endy )
800                 if ( LGN_circle(x-startx+1,y-starty+1) )
801                     xi_LGN_ON( a, b ) = xi_LGN_ON( a, b ) + ...
802                         xi_REC( x, y ) * (-1 * ...
803                             mu_aff_LGN( x-startx+1 ...
804                                 , y-starty+1, num ));
805                     xi_LGN_OFF( a, b ) = xi_LGN_OFF( a, b ) + ...
806                         xi_REC( x, y ) * ...
807                             mu_aff_LGN( x-startx+1 ...
808                                 , y-starty+1, num );
809
810                 end;
811             end;
812         end;
813     end;
814 end;
815
816 clear a b x y nm startx endx starty endy;
817 pack;
818
819 div = max(max(xi_LGN_ON));
820 if( div == 0 )
821     div = 1;
822 end;
823
824 gamma_A = 1 / div;
825

```



```

826
827 %Sigma Function - this is repeated so that Matlab 6.5 can better
828 %optimize the code are runtime.
829 x = gamma_A .* xi_LGN_ON;
830 temp_size = size( x );
831 temp_delta = zeros( temp_size(1) ) + delta;
832 temp_beta = zeros( temp_size(1) ) + beta;
833 clear temp_size;
834
835 eta_LGN_ON = ( x > temp_delta );
836 eta_LGN_ON = eta_LGN_ON .* ( x < temp_beta );
837 clear temp_delta;
838 clear temp_beta;
839
840 eta_LGN_ON = eta_LGN_ON .* ( ( x - delta ) / ( beta - delta ) );
841 eta_LGN_ON = eta_LGN_ON + ( x >= beta );
842
843
844 div = max(max(xi_LGN_OFF));
845 if( div == 0 )
846     div = 1;
847 end;
848
849 gamma_A = 1 / div;
850
851
852
853 %Sigma Function
854 x = gamma_A .* xi_LGN_OFF;
855 temp_size = size( x );
856 temp_delta = zeros( temp_size(1) ) + delta;
857 temp_beta = zeros( temp_size(1) ) + beta;
858 clear temp_size;
859
860 eta_LGN_OFF = ( x > temp_delta );
861 eta_LGN_OFF = eta_LGN_OFF .* ( x < temp_beta );
862 clear temp_delta;
863 clear temp_beta;
864
865 eta_LGN_OFF = eta_LGN_OFF .* ( ( x - delta ) / ( beta - delta ) );
866 eta_LGN_OFF = eta_LGN_OFF + ( x >= beta );
867 % end calculating eta (reaction) for both LGN channels
868
869
870
871
872 %
873 % This is where LGN moves to V1

```

```
%
zeta_V1 = zeros( N_d );

% start calculating zeta (activation) for V1
for ( i=1:N_d )
    for ( j=1:N_d )

        num = (i-1)*N_d+j;

        starta = i;
        enda   = i + ( r_A_o - 0.5 ) * 2;
        startb = j;
        endb    = j + ( r_A_o - 0.5 ) * 2;
        sum_zeta_V1 = 0;

        for ( a = starta:enda )
            for ( b = startb:endb )
                if ( V1_circle(a-starta+1,b-startb+1 ) )
                    %
                    % The original thought was to take the strongest
                    % response and feed it to V1. However,
                    % experiments have shown that this is not
                    % accurate.
                    %
                    % if ( xi_LGN_ON( a, b ) * mu_aff_ON_V1( a-starta+1, b-startb+1 ) > xi
                    %     zeta_V1( i, j ) = zeta_V1( i, j ) + xi_LGN_ON( a, b ) * mu_aff_0
                    %     sum_zeta_V1 = sum_zeta_V1 + xi_LGN_ON( a, b );
                    % else
                    %     zeta_V1( i, j ) = zeta_V1( i, j ) + xi_LGN_OFF( a, b ) * mu_aff_
                    %     sum_zeta_V1 = sum_zeta_V1 + xi_LGN_OFF( a, b );
                    % end;
                    %
                    % Instead of taking the larger of the two lets
                    % try and sum everything up. This seems to
                    % work better - but the actual mechanism for
                    % this is still unknown. Therefore more work
                    % could be done to find the optimal way of
                    % combining the on/off channels when feeding
                    % them into V1
                    %
                    zeta_V1( i, j ) = zeta_V1( i, j ) + ...
                        eta_LGN_ON( a, b ) * ...
                        mu_aff_ON_V1( a-starta+1, ...
                        b-startb+1, num );
                    sum_zeta_V1 = sum_zeta_V1 + ...
                        eta_LGN_ON( a, b ) + ...
                        eta_LGN_OFF( a, b );
                end
            end
        end
    end
end
```

```

922         zeta_V1( i, j ) = zeta_V1( i, j ) + ...
923             eta_LGN_OFF( a, b ) * ...
924             mu_aff_OFF_V1( a-starta+1, ...
925                 b-startb+1, num );
926     end;
927 end;
928 end;
929
930     zeta_V1( i, j ) = ( gamma_A .* zeta_V1( i, j ) ) / ...
931         ( 1 + gamma_N * sum_zeta_V1 );
932
933     end;
934 end;
935
936 % Set the maximum to 1
937
938 div = max(max(zeta_V1));
939 if( div == 0 )
940     div = 1;
941 end;
942
943 gamma_A = 1/div;
944 zeta_V1 = zeta_V1 .* gamma_A;
945 clear num centera centerb starta enda startb endb sum_zeta_V1 ...
946     i j a b;
947
948 % end calculating zeta for V1.
949
950 clear i j k l num startk endk startl endl;
951
952
953
954
955 % Start settling iterations. (eta V1)
956 if( t > 1 )
957     last_eta_V1 = eta_V1;
958 end;
959
960 for ( blah = 0:t_s );
961
962 % Calculate eta (reaction) for V1. If this is the first settling
963 % iteration this is basically the sigma function implemented on V1.
964 % Else, the reaction is "tweaked" based on the weights.
965
966 if ( blah==0 )
967     %eta_V1 = sigma_function( zeta_V1, delta, beta );
968
969     %Sigma Function

```

```

970         x = zeta_V1;
971         temp_size = size( x );
972         temp_delta = zeros( temp_size(1) ) + delta;
973         temp_beta = zeros( temp_size(1) ) + beta;
974         clear temp_size;
975
976         eta_V1 = ( x > temp_delta );
977         eta_V1 = eta_V1 .* ( x < temp_beta );
978         clear temp_delta;
979         clear temp_beta;
980
981         eta_V1 = eta_V1 .* ( ( x - delta ) / ( beta - delta ) );
982         eta_V1 = eta_V1 + ( x >= beta );
983
984         if( t == 1 )
985             last_eta_V1 = eta_V1;
986         end;
987
988     else
989         old_eta_V1 = eta_V1;
990         for ( i=1:N_d )
991             for ( j=1:N_d )
992
993                 num = (i-1)*N_d+j;
994
995                 sum_E = 0;
996                 sum_I = 0;
997
998                 startk = max( 1, i - ( r_E-0.5 ) );
999                 endk = min( N_d, i + ( r_E-0.5 ) );
1000                 startl = max( 1, j - ( r_E-0.5 ) );
1001                 endl = min( N_d, j + ( r_E-0.5 ) );
1002
1003                 for ( k = startk:endk )
1004                     for ( l = startl:endl )
1005                         if ( E_circle(k-startk+1,l-startl+1) )
1006                             sum_E = sum_E + E_V1( num, k-startk+1, ...
1007                                 l-startl+1 ) * old_eta_V1( k, l );
1008                         end;
1009                     end;
1010                 end;
1011
1012                 startk = max( 1, i - ( r_I-0.5 ) );
1013                 endk = min( N_d, i + ( r_I-0.5 ) );
1014                 startl = max( 1, j - ( r_I-0.5 ) );
1015                 endl = min( N_d, j + ( r_I-0.5 ) );
1016
1017                 for ( k = startk:endk )

```

```

1018         for ( l = startl:end1 )
1019             if ( I_circle(k-startk+1,l-startl+1) )
1020                 sum_I = sum_I + I_V1( num, k-startk+1, ...
1021                     l-startl+1 ) * old_eta_V1( k, l );
1022             end;
1023         end;
1024     end;
1025
1026     eta_V1( i, j ) = zeta_V1( i, j ) + gamma_E * ...
1027         sum_E    gamma_I * sum_I;
1028 end;
1029 end;
1030
1031 clear i j k l num sum_E sum_I startk endk startl endl;
1032 %eta_V1 = sigma_function( eta_V1, delta, beta );
1033
1034
1035 %Sigma Function
1036 x = eta_V1;
1037 temp_size = size( x );
1038 temp_delta = zeros( temp_size(1) ) + delta;
1039 temp_beta = zeros( temp_size(1) ) + beta;
1040 clear temp_size;
1041
1042 eta_V1 = ( x > temp_delta );
1043 eta_V1 = eta_V1 * ( x < temp_beta );
1044 clear temp_delta;
1045 clear temp_beta;
1046
1047 eta_V1 = eta_V1 .* ( ( x - delta ) / ( beta - delta ) );
1048 eta_V1 = eta_V1 + ( x >= beta );
1049
1050 end;
1051 % end calculating eta V1 (reaction).
1052
1053
1054
1055 % Now update weights based on V1 reactions. (This is the self
1056 % organization!!!) IT seems to work well but I am curious to
1057 % see if there are better ways to update these weights - or
1058 % perhaps faster ways by looking at approximations of regions.
1059 % If this is the case then it might be possible to distribute a
1060 % lot of these computations and would drastically speed things up.
1061 old_mu_aff_ON_V1 = mu_aff_ON_V1;
1062 old_mu_aff_OFF_V1 = mu_aff_OFF_V1;
1063 old_E_V1 = E_V1;
1064 old_I_V1 = I_V1;
1065

```



```

1066 % Update V1 afferent weights.
1067 for ( i=1:N_d )
1068     for ( j = 1:N_d )
1069
1070         num = ( i-1 ) * N_d + j;
1071         sum_mu_aff_ON_V1 = 0;
1072         sum_mu_aff_OFF_V1 = 0;
1073
1074         startm = i;
1075         endm   = i + ( r_A_o   0.5 ) * 2;
1076         startn = j;
1077         endn   = j + ( r_A_o   0.5 ) * 2;
1078
1079         for ( m=startm:endm )
1080             for ( n=startn:endn )
1081                 if ( V1_circle(m-startm+1,n-startn+1) )
1082                     sum_mu_aff_ON_V1 = sum_mu_aff_ON_V1 + ...
1083                         old_mu_aff_ON_V1( ...
1084                             m-startm+1, n-startn+1, ...
1085                             num ) + alpha_A * ...
1086                             eta_V1( i, j ) * ...
1087                             eta_LGN_ON( m, n );
1088                     sum_mu_aff_OFF_V1 = sum_mu_aff_OFF_V1 + ...
1089                         old_mu_aff_OFF_V1( ...
1090                             m-startm+1, n-startn+1, ...
1091                             num ) + alpha_A * ...
1092                             eta_V1( i, j ) * ...
1093                             eta_LGN_OFF( m, n );
1094                 end;
1095             end;
1096         end;
1097
1098         for ( m=startm:endm )
1099             for ( n = startn:endn )
1100                 if ( V1_circle(m-startm+1,n-startn+1) )
1101                     mu_aff_ON_V1( m-startm+1, n-startn+1, num ) ...
1102                         = ( old_mu_aff_ON_V1( m-startm+1, ...
1103                             n-startn+1, num ) + alpha_A * ...
1104                             eta_V1( i, j ) * ...
1105                             eta_LGN_ON( m, n ) ) / ...
1106                             sum_mu_aff_ON_V1;
1107                     mu_aff_OFF_V1( m-startm+1, n-startn+1, num ) ...
1108                         = ( old_mu_aff_OFF_V1( m-startm+1, ...
1109                             n-startn+1, num ) + alpha_A * ...
1110                             eta_V1( i, j ) * ...
1111                             eta_LGN_OFF( m, n ) ) / ...
1112                             sum_mu_aff_OFF_V1;
1113                 end;

```

```

1114         end;
1115     end;
1116 end;
1117 end;
1118
1119 clear i j num sum_mu_aff_ON_V1 sum_mu_aff_OFF_V1 startm ...
1120     endm startn endn old_mu_aff_ON_V1 old_mu_aff_OFF_V1;
1121
1122
1123
1124 % Update V1 lateral weights.
1125 for ( i = 1:N_d )
1126     for ( j = 1:N_d )
1127
1128         sum_E_V1 = 0;
1129         sum_I_V1 = 0;
1130         num = (i-1)*N_d+j;
1131
1132         startm = max( 1, i (r_E-0.5) );
1133         endm = min( N_d, i + (r_E-0.5) );
1134         startn = max( 1, j (r_E-0.5) );
1135         endn = min( N_d, j + (r_E-0.5) );
1136
1137         for ( m=startm:endm )
1138             for ( n = startn:endn )
1139                 if ( E_circle(m-startm+1,n-startn+1) )
1140                     sum_E_V1 = sum_E_V1 + old_E_V1( num, ...
1141                         m-startm+1, n-startn+1 ) + ...
1142                         alpha_E * eta_V1( i, j ) * ...
1143                         eta_V1( m, n );
1144                 end;
1145             end;
1146         end;
1147
1148         for ( m = startm:endm )
1149             for ( n = startn:endn )
1150                 if ( E_circle(m-startm+1,n-startn+1) )
1151                     E_V1( num, m-startm+1, n-startn+1 ) = ...
1152                         (old_E_V1( num, m-startm+1, ...
1153                             n-startn+1 ) + alpha_E * ...
1154                             eta_V1( i, j ) * eta_V1( m, n )) ...
1155                         / sum_E_V1;
1156                 else
1157                     E_V1(num,m-startm+1,n-startn+1) = 0;
1158                 end;
1159             end;
1160         end;
1161

```

```

1162         startm = max( 1, i - (r_I-0.5) );
1163         endm   = min( N_d, i + (r_I-0.5) );
1164         startn = max( 1, j - (r_I-0.5) );
1165         endn   = min( N_d, j + (r_I-0.5) );
1166
1167         for ( m=startm:endm )
1168             for ( n = startn:endn )
1169                 if ( I_circle(m-startm+1,n-startn+1) )
1170                     sum_I_V1 = sum_I_V1 + old_I_V1( num, ...
1171                         m-startm+1, n-startn+1 ) + ...
1172                         alpha_I * eta_V1( i, j ) * ...
1173                         eta_V1( m, n );
1174                 end;
1175             end;
1176         end;
1177
1178
1179
1180         for ( m = startm:endm )
1181             for ( n = startn:endn )
1182                 if ( I_circle(m-startm+1,n-startn+1) )
1183                     I_V1( num, m-startm+1, n-startn+1 ) = ...
1184                         (old_I_V1( num, m-startm+1, ...
1185                             n-startn+1 ) + alpha_I * ...
1186                             eta_V1( i, j ) * eta_V1( m, n )) / sum_I_V1;
1187                 end;
1188             end;
1189         end;
1190
1191
1192     end;
1193 end;
1194
1195 % Finish updating lateral weights (and all weights).
1196
1197 clear i j m n num old_E_V1 startm endm startn endn ...
1198       sum_I_V1 sum_E_V1;
1199 end; % End settling iterations.
1200
1201 clear blah;
1202
1203
1204
1205
1206
1207 %
1208 % This will test for inconsistencies between images
1209 % Images should be continuous for this to be meaningful because it

```

```

1210 % looks at the response between two iterations in order to cancel of
1211 % the effect of "seeing something out of the corner of your eye".
1212 % In other words, in human vision when we first see things our
1213 % attention is quickly focused not because we don't understand
1214 % what we are seeing but because something drastic in the image
1215 % has changed.
1216 %
1217 % What remains is what I call the unknown response. It is what the
1218 % system must learn about the system.
1219 %
1220 unknown_response = abs( eta_V1 - last_eta_V1 ) > 0;
1221 temp = (1-(eta_LGN_ON - eta_LGN_OFF));
1222 size1 = size( eta_LGN_ON );
1223 size2 = size( unknown_response );
1224 s1 = size1(1) - size2(1);
1225 s2 = s1 / 2;
1226
1227 unknown_response = unknown_response .* eta_V1;
1228 clear temp;
1229
1230 %
1231 % Now we must look at processing motion. For this we continue the
1232 % above process in the same fashion feeding information to two
1233 % different areas, MT and MST. Later, this information will need
1234 % to be feedback into themselves and/or the V1 layer. In order
1235 % to keep orientation processing my current feeling is that the
1236 % V1 layer should stay as it is and that MT and MST should be
1237 % designed to feed into one another.
1238 %
1239
1240 zeta_MT = zeros( MT_d );
1241
1242 if( MT_NOT_SET )
1243     %eta_V1_5 = eta_V1;
1244     %eta_V1_4 = eta_V1;
1245     %eta_V1_3 = eta_V1;
1246     %eta_V1_2 = eta_V1;
1247     %eta_V1_1 = eta_V1;
1248     eta_V1_5 = unknown_response;
1249     eta_V1_4 = unknown_response;
1250     eta_V1_3 = unknown_response;
1251     eta_V1_2 = unknown_response;
1252     eta_V1_1 = unknown_response;
1253
1254 end
1255
1256
1257 div = abs(min(min( unknown_response )));

```

[illegible]


```

1306             eta_V1_2( a, b ) * ...
1307             mu_aff_2_MT( a-starta+1, ...
1308             b-startb+1, num ) + ...
1309             eta_V1_3( a, b ) * ...
1310             mu_aff_3_MT( a-starta+1, ...
1311             b-startb+1, num ) + ...
1312             eta_V1_4( a, b ) * ...
1313             mu_aff_4_MT( a-starta+1, ...
1314             b-startb+1, num );
1315         sum_zeta_MT = sum_zeta_MT + ...
1316             eta_V1_1( a, b ) + ...
1317             eta_V1_2( a, b ) + ...
1318             eta_V1_3( a, b ) + ...
1319             eta_V1_4( a, b );
1320     end;
1321 end;
1322 end;
1323
1324     zeta_MT( i, j ) = ( gamma_A_MT .* zeta_MT( i, j ) ) / ...
1325         ( 1 + gamma_N_MT * sum_zeta_MT );
1326
1327 end;
1328 end;
1329
1330 % Set the maximum to 1
1331 div = max(max(sum_zeta_MT));
1332 %div = max(max(xi_V1));
1333 if( div == 0 )
1334     div = 1;
1335 end;
1336
1337 gamma_A_MT = 1/div;
1338 zeta_MT = zeta_MT .* gamma_A_MT;
1339 clear num centera centerb starta enda startb endb sum_zeta_MT ...
1340     i j a b;
1341 % end calculating zeta for MT.
1342
1343 clear i j k l num startk endk startl endl;
1344
1345
1346
1347 % Start settling iterations. (eta MT)
1348 for ( blah = 0:t_s );
1349
1350 % Calculate eta (reaction) for MT. If this is the first settling
1351 % iteration this is basically the sigma function implemented on MT.
1352 % Else, the reaction is "tweaked" based on the weights.
1353

```

```

1354     if ( blah==0 )
1355         %eta_MT = sigma_function( zeta_MT, delta, beta );
1356
1357         %Sigma Function
1358         x = zeta_MT;
1359         temp_size = size( x );
1360         temp_delta = zeros( temp_size(1) ) + delta;
1361         temp_beta = zeros( temp_size(1) ) + beta;
1362         clear temp_size;
1363
1364         eta_MT = ( x > temp_delta );
1365         eta_MT = eta_MT .* ( x < temp_beta );
1366         clear temp_delta;
1367         clear temp_beta;
1368
1369         eta_MT = eta_MT .* ( ( x - delta ) / ( beta - delta ) );
1370         eta_MT = eta_MT + ( x >= beta );
1371
1372     else
1373         old_eta_MT = eta_MT;
1374         for ( i=1:MT_d )
1375             for ( j=1:MT_d )
1376
1377                 num = (i-1)*MT_d+j;
1378
1379                 sum_E = 0;
1380                 sum_I = 0;
1381
1382                 startk = max( 1, i - ( r_E-0.5 ) );
1383                 endk = min( MT_d, i + ( r_E-0.5 ) );
1384                 startl = max( 1, j - ( r_E-0.5 ) );
1385                 endl = min( MT_d, j + ( r_E-0.5 ) );
1386
1387                 for ( k = startk:endk )
1388                     for ( l = startl:endl )
1389                         if ( E_circle(k-startk+1,l-startl+1) )
1390                             sum_E = sum_E + E_MT( num, k-startk+1, ...
1391                                 l-startl+1 ) * old_eta_MT( k, l );
1392                         end;
1393                     end;
1394                 end;
1395
1396                 startk = max( 1, i - ( r_I-0.5 ) );
1397                 endk = min( MT_d, i + ( r_I-0.5 ) );
1398                 startl = max( 1, j - ( r_I-0.5 ) );
1399                 endl = min( MT_d, j + ( r_I-0.5 ) );
1400
1401                 for ( k = startk:endk )

```

```

1402         for ( l = startl:end1 )
1403             if ( I_circle(k-startk+1,l-startl+1) )
1404                 sum_I = sum_I + I_MT( num, k-startk+1, ...
1405                     l-startl+1 ) * old_eta_MT( k, l );
1406             end;
1407         end;
1408     end;
1409
1410     eta_MT( i, j ) = zeta_MT( i, j ) + gamma_E * ...
1411         sum_E - gamma_I * sum_I;
1412 end;
1413 end;
1414
1415 clear i j k l num sum_E sum_I startk endk startl endl;
1416 %eta_MT = sigma_function( eta_MT, delta, beta );
1417
1418
1419 %Sigma Function
1420 x = eta_MT;
1421 temp_size = size( x );
1422 temp_delta = zeros( temp_size(1) ) + delta;
1423 temp_beta = zeros( temp_size(1) ) + beta;
1424 clear temp_size;
1425
1426 eta_MT = ( x > temp_delta );
1427 eta_MT = eta_MT .* ( x < temp_beta );
1428 clear temp_delta;
1429 clear temp_beta;
1430
1431 eta_MT = eta_MT .* ( ( x - delta ) / ( beta - delta ) );
1432 eta_MT = eta_MT + ( x >= beta );
1433
1434 end;
1435 % end calculating eta MT (reaction).
1436
1437
1438 if( t > 1 )
1439     eta_MT_4 = eta_MT_3;
1440     eta_MT_3 = eta_MT_2;
1441     eta_MT_2 = eta_MT_1;
1442     eta_MT_1 = eta_MT;
1443 else
1444     eta_MT_4 = eta_MT;
1445     eta_MT_3 = eta_MT;
1446     eta_MT_2 = eta_MT;
1447     eta_MT_1 = eta_MT;
1448 end
1449

```



```

1498             eta_MT_4( i, j ) * eta_V1( m, n );
1499
1500         end;
1501     end;
1502 end;
1503
1504 for ( m=startm:endm )
1505     for ( n = startn:endn )
1506         if ( MT_circle(m-startm+1,n-startn+1) )
1507
1508             mu_aff_1_MT( m-startm+1, n-startn+1, num ) ...
1509                 = ( old_mu_aff_1_MT( m-startm+1, ...
1510                     n-startn+1, num ) + alpha_A * ...
1511                     eta_MT_1( i, j ) * eta_V1( m, n ) ) ...
1512                     / sum_mu_aff_1_MT;
1513             mu_aff_2_MT( m-startm+1, n-startn+1, num )
1514                 = ( old_mu_aff_2_MT( m-startm+1, ...
1515                     n-startn+1, num ) + alpha_A * ...
1516                     eta_MT_2( i, j ) * eta_V1( m, n ) ) ...
1517                     / sum_mu_aff_2_MT;
1518             mu_aff_3_MT( m-startm+1, n-startn+1, num ) ...
1519                 = ( old_mu_aff_3_MT( m-startm+1, ...
1520                     n-startn+1, num ) + alpha_A * ...
1521                     eta_MT_3( i, j ) * eta_V1( m, n ) ) ...
1522                     / sum_mu_aff_3_MT;
1523             mu_aff_4_MT( m-startm+1, n-startn+1, num ) ...
1524                 = ( old_mu_aff_4_MT( m-startm+1, ...
1525                     n-startn+1, num ) + alpha_A * ...
1526                     eta_MT_4( i, j ) * eta_V1( m, n ) ) ...
1527                     / sum_mu_aff_4_MT;
1528
1529         end;
1530     end;
1531 end;
1532 end;
1533 end;
1534
1535 clear i j num sum_mu_aff_ON_MT sum_mu_aff_OFF_MT startm endm ...
1536         startn endn old_mu_aff_ON_MT old_mu_aff_OFF_MT;
1537
1538 % Update MT lateral weights.
1539 for ( i = 1:MT_d )
1540     for ( j = 1:MT_d )
1541
1542         sum_E_MT = 0;
1543         sum_I_MT = 0;
1544         num = (i-1)*MT_d+j;
1545

```



```

1546         startm = max( 1, i - (r_E-0.5) );
1547         endm   = min( MT_d, i + (r_E-0.5) );
1548         startn = max( 1, j - (r_E-0.5) );
1549         endn   = min( MT_d, j + (r_E-0.5) );
1550
1551         %           if( endm > N_d ) endm = N_d; end
1552         %           if( endn > N_d ) endn = N_d; end
1553
1554         for ( m=startm:endm )
1555             for ( n = startn:endn )
1556                 if ( E_circle(m-startm+1,n-startn+1) )
1557                     sum_E_MT = sum_E_MT + old_E_MT( num, ...
1558                         m-startm+1, n-startn+1 ) + alpha_E * ...
1559                         eta_MT( i, j ) * eta_MT( m, n );
1560                 end;
1561             end;
1562         end;
1563
1564         for ( m = startm:endm )
1565             for ( n = startn:endn )
1566                 if ( E_circle(m-startm+1,n-startn+1) )
1567                     E_MT( num, m-startm+1, n-startn+1 ) = ...
1568                         (old_E_MT( num, m-startm+1, ...
1569                             n-startn+1 ) + alpha_E * ...
1570                             eta_MT( i, j ) * eta_MT( m, n )) ...
1571                         / sum_E_MT;
1572                 else
1573                     E_MT(num,m-startm+1,n-startn+1) = 0;
1574                 end;
1575             end;
1576         end;
1577
1578         startm = max( 1, i - (r_I-0.5) );
1579         endm   = min( MT_d, i + (r_I-0.5) );
1580         startn = max( 1, j - (r_I-0.5) );
1581         endn   = min( MT_d, j + (r_I-0.5) );
1582
1583         for ( m=startm:endm )
1584             for ( n = startn:endn )
1585                 if ( I_circle(m-startm+1,n-startn+1) )
1586                     sum_I_MT = sum_I_MT + old_I_MT( num, ...
1587                         m-startm+1, n-startn+1 ) + ...
1588                         alpha_I * eta_MT( i, j ) * ...
1589                         eta_MT( m, n );
1590                 end;
1591             end;
1592         end;
1593

```

```

1594
1595
1596         for ( m = startm:endm )
1597             for ( n = startn:endn )
1598                 if ( I_circle(m-startm+1,n-startn+1) )
1599                     I_MT( num, m-startm+1, n-startn+1 ) = ...
1600                         (old_I_MT( num, m-startm+1, ...
1601                             n-startn+1 ) + alpha_I * ...
1602                             eta_MT( i, j ) * eta_MT( m, n )) ...
1603                         / sum_I_MT;
1604                 end;
1605             end;
1606         end;
1607
1608     end;
1609 end;
1610
1611 % Finish updating lateral weights (and all weights).
1612
1613 clear i j m n num old_E_MT startm endm startn endn ...
1614         sum_I_MT sum_E_MT;
1615 end; % End settling iterations.
1616
1617 clear blah;
1618 pack;
1619
1620 unknown_response_MT = eta_MT - old_eta_MT;
1621
1622
1623
1624
1625 %
1626 % Display the results for this round to the user.
1627 %
1628 imagesc( 1-xi_REC , 'Tag','test','Parent', Input_h, ...
1629         'CDataMapping', 'scaled', [0 100] );
1630
1631 imagesc( 1-(eta_LGN_ON - eta_LGN_OFF) , 'Tag','test','Parent', ...
1632         LGN_h, 'CDataMapping', 'scaled', [0 100] );
1633
1634 imagesc( eta_V1 , 'Tag','test','Parent', V1_h, 'CDataMapping', ...
1635         'scaled', [0 100] );
1636
1637 imagesc( unknown_response, 'Tag', 'test', 'Parent', ...
1638         difference_V1_h, 'CDataMapping', 'scaled', [0 100] );
1639
1640 imagesc( eta_MT, 'Tag', 'test', 'Parent', MT_h, 'CDataMapping', ...
1641         'scaled', [0 100] );

```

```

1642
1643     imagesc( unknown_response_MT, 'Tag', 'test', 'Parent', ...
1644             difference_MT_h, 'CDataMapping', 'scaled', [0 100] );
1645
1646
1647
1648
1649
1650
1651     %FOR STATISTICAL ANALYSIS
1652         for ( i = 1:N_d )
1653             for ( j = 1:N_d )
1654                 num = (i-1)*N_d+j;
1655                 testerV1(i,j,1) = sum(sum(abs(old_I_V1( num, :, : ) ...
1656                                             I_V1( num, :, : ))));
1657             end;
1658         end;
1659     for ( i = 1:MT_d )
1660         for ( j = 1:MT_d )
1661             num = (i-1)*MT_d+j;
1662             testerMT(i,j,1) = sum(sum(abs(old_I_MT( num, :, : ) ...
1663                                         - I_MT( num, :, : ))));
1664         end;
1665     end;
1666     clear i j num old_I_V1;
1667     %END STATISTICAL ANALYSIS
1668
1669     sum_V1 = [sum_V1;sum( sum( testerV1(:, :, 1) ) )];
1670     sum_MT = [sum_MT;sum( sum( testerMT(:, :, 1) ) )];
1671
1672     if( t > 300 )
1673         show_sum_V1 = sum_V1(t-299:t);
1674         show_sum_MT = sum_MT(t-299:t);
1675     else
1676         show_sum_V1 = sum_V1;
1677         show_sum_MT = sum_MT;
1678     end;
1679
1680     plot( show_sum_V1, 'Parent', V1Graph_h );
1681     plot( show_sum_MT, 'Parent', MTGraph_h );
1682
1683     pause( 1 );
1684
1685     t = t + 1;
1686
1687     %
1688     % Save the file every 100 iterations, on the first iteration
1689     % and if the save button is pressed

```

```

1690         %
1691         if( mod( t, 100 ) == 0 )
1692             test_image = xi_REC;
1693             name = strcat( filename, ' ', num2str( t ), '.mat' );
1694             save( [pathname, name] );
1695         end;
1696
1697         if( training == 0 )
1698             disp( 'Saving data...' )
1699             test_image = xi_REC;
1700             name = strcat( filename, '_', num2str( t ), '.mat' );
1701             save( [pathname, name] );
1702             disp( 'Data Saved' )
1703         end;
1704
1705         if( saveFile == 1 )
1706             disp( 'Saving data...' )
1707             test_image = xi_REC;
1708             name = strcat( filename, '_', num2str( t ), '.mat' );
1709             save( [pathname, name] );
1710             disp( 'Data Saved' )
1711         end;
1712
1713         pack;
1714
1715         end;
1716
1717         if( training == 0 )
1718             pause( 2 );
1719         end;
1720
1721     end;
1722
1723 end;

```

A.4 Helper Functions

```

1 function [pathname,filename] = LoadData( )
2 %
3 % Holds the different method calls depending on the processing
4 % requested. X is the image chosen and Y is the method.
5 %
6
7 [filename,pathname] = uigetfile('*.mat','Select the MAT Data Set');
8 if isequal(filename,0)|isequal(pathname,0)

```

```

9      disp('File not found')
10 else
11     disp(['File ', pathname, filename, ' found...'])
12     disp('Loading Data...')
13 end
14

1 function [pathname,filename] = SaveData( )
2 %
3 % Holds the different method calls depending on the processing
4 % requested. X is the image chosen and Y is the method.
5 %
6
7 [filename,pathname] = uiputfile('*.mat','Select the VIS Data Set');
8 if isequal(filename,0) | isequal(pathname,0)
9     disp('No file specified')
10 else
11     disp(['File ', pathname, filename, ' created...'])
12     disp('Saving Data...')
13 end
14

1 % Calculates the obvious repeating portion of
2 % the formula 4.1 on page 37 of the Bednar thesis.
3
4 function ret=normgaus( X, X0, Y, Y0, SIGMA )
5
6
7 ret = ( X - X0 ) * ( X - X0 );
8 ret = ret + ( ( Y - Y0 ) .* ( Y - Y0 ) );
9 ret = ret / ( SIGMA * SIGMA );
10 ret = ret .* -1;
11 ret = exp( ret );

1 %
2 % Will simply return a circle mask given a radius
3 %
4
5 function ret=draw_circle( radius )
6
7
8 x = ones(1, (radius*2))' * [(radius):-1:0.5,1.5:1:radius];
9 y = x';
10 ret = (((x.^2+y.^2).^0.5)<=(radius+0.5));
11

```


A.5 Rainbow Colormaps

```

1 function [cmap] = rainbow(maplength);
2 % ColEdit function [cmap] = rainbow(maplength);
3 %
4 % colormap m-file written by ColEdit
5 % version 1.0 on 25-Apr-2003
6 %
7 % input :          [maplength]          [64]          - colormap length
8 %
9 % output :         cmap                  colormap RGB-value array
10
11 % set red points
12 r = [ [];...
13      [0 0];...
14      [0.11282 1];...
15      [0.24872 0.98936];...
16      [0.36923 0.98936];...
17      [0.5 0.12766];...
18      [0.62564 0.28723];...
19      [0.75385 0.021277];...
20      [0.88462 0.35106];...
21      [1 0.5];...
22      [] ];
23
24 % set green points
25 g = [ [];...
26      [0 0];...
27      [0.11795 0.010638];...
28      [0.24872 0.59574];...
29      [0.3641 0.97872];...
30      [0.5 0.60638];...
31      [0.61795 0.55319];...
32      [0.75128 0.32979];...
33      [0.87692 0.12766];...
34      [1 0.042553];...
35      [] ];
36
37 % set blue points
38 b = [ [];...
39      [0 0.010638];...
40      [0.11795 0.010638];...
41      [0.24872 0.010638];...
42      [0.37949 0.010638];...
43      [0.5 0.15957];...
44      [0.63333 0.48936];...
45      [0.74872 0.52128];...

```

```

46     [0.88205 0.57447];...
47     [1 0.48936];...
48     [] ];
49 % ColEditInfoEnd
50
51 % get colormap length
52 if nargin==1
53     if length(maplength)==1
54         if maplength<1
55             maplength = 64;
56         elseif maplength>256
57             maplength = 256;
58         elseif isinf(maplength)
59             maplength = 64;
60         elseif isnan(maplength)
61             maplength = 64;
62         end
63     end
64 else
65     maplength = 64;
66 end
67
68 % interpolate colormap
69 np = linspace(0,1,maplength);
70 rr = interp1(r(:,1),r(:,2),np,'linear');
71 gg = interp1(g(:,1),g(:,2),np,'linear');
72 bb = interp1(b(:,1),b(:,2),np,'linear');
73
74 % compose colormap
75 cmap = [rr(:),gg(:),bb(:)];

1 function [cmap] = rainbow2(maplength);
2 % ColEdit function [cmap] = rainbow2(maplength);
3 %
4 % colormap m-file written by ColEdit
5 % version 1.0 on 12-May-2003
6 %
7 % input :          [maplength]          [64]          colormap length
8 %
9 % output :          cmap                  - colormap RGB-value array
10
11 % set red points
12 r = [ [];...
13     [0 0];...
14     [0.012821 0.97872];...
15     [0.079487 0.97872];...
16     [0.13846 0.97872];...
17     [0.20513 0.97872];...

```

```

18     [0.25897 0.96809];...
19     [0.32051 0.95745];...
20     [0.4 0.97872];...
21     [0.48462 0.68085];...
22     [0.5359 0.5];...
23     [0.59744 0.12766];...
24     [0.66154 0.17021];...
25     [0.72308 0.18085];...
26     [0.79231 0.085106];...
27     [0.84615 0.26596];...
28     [0.92308 0.34043];...
29     [0.97436 0.51064];...
30     [1 0.97872];...
31     [] ];
32
33 % set green points
34 g = [ [];...
35     [0 0.074468];...
36     [0.012821 0.010638];...
37     [0.082051 0.24468];...
38     [0.14103 0.42553];...
39     [0.19487 0.48936];...
40     [0.25641 0.69149];...
41     [0.31795 0.85106];...
42     [0.41538 0.97872];...
43     [0.59231 0.98936];...
44     [0.65897 0.61702];...
45     [0.69744 0.38298];...
46     [0.79487 0.11702];...
47     [0.85385 0.12766];...
48     [0.90513 0.1383];...
49     [0.98205 0.074468];...
50     [1 0.96809];...
51     [] ];
52
53 % set blue points
54 b = [ [];...
55     [0 0.021277];...
56     [0.020513 0.021277];...
57     [0.076923 0.010638];...
58     [0.12564 0.021277];...
59     [0.18462 0.021277];...
60     [0.5 0.010638];...
61     [0.61538 0.042553];...
62     [0.67949 0.28723];...
63     [0.74359 0.54255];...
64     [0.79744 0.98936];...
65     [0.85385 0.7766];...

```

```
66     [0.90256 0.61702];...
67     [0.97692 0.5];...
68     [1 0.98936];...
69     [] ];
70 % ColEditInfoEnd
71
72 % get colormap length
73 if nargin==1
74     if length(maplength)==1
75         if maplength<1
76             maplength = 64;
77         elseif maplength>256
78             maplength = 256;
79         elseif isinf(maplength)
80             maplength = 64;
81         elseif isnan(maplength)
82             maplength = 64;
83         end
84     end
85 else
86     maplength = 64;
87 end
88
89 % interpolate colormap
90 np = linspace(0,1,maplength);
91 rr = interp1(r(:,1),r(:,2),np,'linear');
92 gg = interp1(g(:,1),g(:,2),np,'linear');
93 bb = interp1(b(:,1),b(:,2),np,'linear');
94
95 % compose colormap
96 cmap = [rr(:),gg(:),bb(:)];
```

List of Abbreviations

Abbreviation	Details
HLLISOM	Hierarchical LISSOM
LISSOM	Laterally Interconnected Synergetically Self-Organizing Map
PGO	ponto-geniculo-occipital
REM	rapid eye movement
RF-LISOM	the Receptive-Field LISSOM
SOM	Self Organizing Map
V1	Primary Visual Cortex

Bibliography

- Beardsley, S.A. & Vaina, L.M. (1998). Computational modelling of optic flow selectivity in mstd neurons. *Network: Computation in Neural Systems*, **9**, 467–493.
- Bednar, J. (2002). *Learning to See: Genetic and Environmental Influences on Visual Development*. Ph.D. thesis, University of Texas at Austin.
- Bednar, J.A. & Miikkulainen, R. (2003). Self-organization of spatiotemporal receptive fields and laterally connected direction and orientation maps. *Neurocomputing*, **52-54**, 473–480.
- Blake, R., Sekuler, R. & Grossman, E. (2003). *Motion Processing in Human Visual Cortex*. CRC Press, Boca Raton, Florida.
- Blakemore, C. & Cooper, G. (1970). Development of the brain depends on the visual environment. *Nature*, **228**, 477–478.
- Brazeau, J.D., Humphrey, J. & Gaborski, R. (2003). A biologically-based model of a visual learning system. In *2003 Western New York Image Processing Workshop*, 55–58.
- Chalupa, L.M. & Rhoades, R.W. (1988). Environmental influences upon the

- development of the golden hamster's visual system. *Neurophysiology and psychophysiology: Experimental and clinical applications*, 889–935.
- Chapman, B. (2000). Necessity for afferent activity to maintain eye-specific segregation in ferret lateral geniculate nucleus. *Science*, **287**, 2479–2483.
- Chapman, B. & Stryker, M.P. (1993). Development of orientation selectivity in ferret primary visual cortex and effects of deprivation. *Journal of Neuroscience*, **13**, 5251–5262.
- Coon, D. (2000). *Essentials of Psychology: Exploration and Application*. Wadsworth, Belmont, California, eighth edn.
- Crair, D.C., M. C. and Gillespie & Stryker, M.P. (1998). The role of visual experience in the development of columns in cat visual cortex. *Science*, **279**, 566–570.
- Gilbert, C.D., Hirsch, J. & Wiesel, T. (1990). Lateral interaction in visual cortex. *Cold Spring Harbor Symposia on Quantitative Biology*, **LV**, 663–677.
- Grossberg, S., Mingolla, E. & Viswanathan, L. (2001). Neural dynamics of motion integration and segmentation within and across apertures. *Vision Research*, **41**, 2521–2553.
- Grzywacz, N.M. & Merwine, D. (2002). *Motion Perception, Neural Basis of*. Macmillan Press, Cambridge.
- Hebb, D.O. (1949). *The Organization of Behavior*. John Wiley and Sons, New York.

- Kandel, E.R., Schwartz, J. & Jessell, T. (1991). *Principles of Neural Science*. McGraw-Hill, New York, 3rd edn.
- Kasamatsu, T., Kitano, M., Sutter, E. & Norcia, A. (1998). Lack of lateral inhibitory interaction in visual cortex of monocularly deprived cats. *Vision Research*, **38**, 1–12.
- Katz, L.C. & Shatz, C.J. (1996). Synaptic activity and the construction of cortical circuits. *Science*, **274**, 1133–1138.
- Kohonen, T. (1997). *Self-Organizing Maps*. Springer, 2nd edn.
- Linsker, R. (1986). From basic network principles to neural architecture: Emergence of orientation columns. *Proceedings of the National Academy of Sciences*, **83**, 8779–8783.
- Lowel, S. & Singer, W. (1992). Selection of intrinsic horizontal connections in the visual cortex by correlated neuronal activity. *Science*, **255**, 209–212.
- Marks, G.A., Shaffery, J.P., Oksenberg, A., Speciale, S.G. & Roffwarg, H.P. (1995). A functional role for rem sleep in brain maturation. *Behavioural Brain Research*, **69**, 1–11.
- Medler, D. (1998). A brief history of connectionism. Tech. rep., University of Alberta.
- Newsome, W.T. & Pare, E.B. (1998). A selective impairment of motion perception following lesions of the middle temporal visual area (mt). *Journal of Neuroscience*, **8**, 2201–2211.

- Piepenbrock, C., Ritter, H. & Obermayer, K. (1996). Cortical map development driven by spontaneous retinal activity waves. In *ICANN*, 427–432.
- Pomplum, M., Liu, Y., Martinez-Trujillo, J., Simine, E. & Tsotsos, J. (2002). A neurally-inspired model for detecting and localizing simple motion patterns in image sequences. In *4th Workshop Dynamic Perception*, 47–52.
- Rochester, N., Holland, J.H., Haibt, L.H. & Duda, W.L. (1956). Tests on a cell assembly theory of the action of the brain, using a large digital computer. *IRE Transactions on Information Theory*, **2**, 80–93.
- Rolls, E.T. & Deco, G. (2002). *Computational Neuroscience of Vision*. Oxford University Press, Oxford.
- Rosenzweig, Leiman & Breedlove (1999). *Biological Psychology: An Introduction to Behavioral, Cognitive, and Clinical Neuroscience*. Sinauer Associates, Inc, Sunderland, Massachusetts, 2nd edn.
- Simoncelli, E.P. & Heeger, D.J. (1998). A model of neuronal responses in visual area mt. *Vision Research*, **38**, 743–761.
- Sirosh, J. (1995). *A Self-Organizing Neural Network Model of the Primary Visual Cortex*. Ph.D. thesis, University of Texas at Austin.
- Stratton, G. (1897). Vision without inversion of the retinal image. *Psychological Review*, **4**, 341–360.
- Thiele, A., Dobkins, K.R. & Albright, T.D. (1999). The contribution of color to motion processing in macaque middle temporal area. *The Journal of Neuroscience*, **19**, 6571–6587.

- von der Malsburg, C. (1973). Self-organization of orientation-sensitive cells in the striate cortex. *Kybernetik*, **15**, 85–100.
- Wiesel, T.N. (1982). Postnatal development of the visual cortex and the influence of environment. *Nature*, **299**, 583–591.